The Jack Turbine Blade

Jack turbinbladet

Shaun Victor Jack

Norwegian University of Life Sciences

Department of Mathematical Sciences and Technology

Master Thesis 30 credits, May 2011

The Jack Turbine Blade

By

Shaun Victor Jack

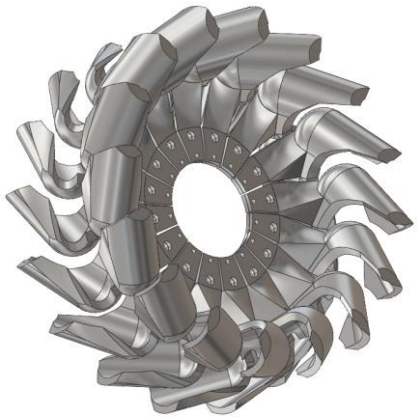

A master thesis, May 2011

Preface

The Pelton turbine is the most widely used impulse turbine today. It is the only impulse turbine used in large scale energy production and is the most trusted. Like all machinery, it has its weaknesses and its strengths. One of these weaknesses is that it is unable to manipulate a water jet in such a way that it makes a full 180 degrees turn. This is to avoid any unwanted collisions on its neighbouring blade. I wish to design an entirely different blade that can manipulate the water jet 180 degrees without colliding upon itself. If this is done the blade should gain more of the water jets energy from a purely vectors point of view. If an improved impulse turbine can be designed, this can have dramatic consequences for society in general, whereby more power is utilized from the same hydroelectric water flows. My motivation for this thesis is to simply discover an alternative design for impulse water turbines that could potentially have an improved efficiency.

The production of this thesis has been both exciting and demanding. I thoroughly enjoyed it.

I would like to thank: Associate Professor, Mr Jan Kåre Bøe for his supervising throughout the production of this thesis.

I would also like to thank others such as, Senior Engineer: Mr Egil Stemsrud for helping me with 3-D printing.

I would also like to thank Associate Professor; Mr Jarle Tommy Bjørkholdt for lending me his water turbine rig for testing as well as for his theoretical advice. Thanks must also be given to any others that may have helped or supported me throughout the adventures of this thesis.

Ås, 13 May 2011

_____

Shaun Victor Jack

Sammendrag

I teorien lærte jeg, at jeg trengte et blad design som kunne produsere en vannstråle med en absolutt hastighet på null under optimale operasjonsbetingelser. For å gjøre dette måtte vannet klare å snu 180 grader over selve blad. Under simuleringene viste det seg fort at designet ikke innfridde dette. Vannet snudde 360 grader istedenfor 180 grader. Dermed ble all energien i vannstrålen overført til bladene og vannet stoppet fullstendig.

I det nye designet jeg da utarbeidet, ble vannet løftet opp og retningen på vannet ble mer effektiv. Simulering viste at dette nye designet oppførte seg på en måte som stemte bra med våre delmål for enkelbladscenarioet. Dermed fortsatte jeg å simulere og forbedre dette designet i multibladsenarioet. Her var målet å oppnå god vannstrøm fra et blad til den neste, samtidig som væskebevegelsen på det enkelte bladet var optimal. Jeg forventet at den nye ”Jack Turbinen” skulle generere mer omdreiningsmoment enn Pelton Turbinen og dermed var det nye designet klart for konstruksjon og testing.

”The Jack Turbine Blade” ble konstruert med en 3-D printer. Maskinen skrev ut lag (pulver) av gips bundet sammen med et svakt lim. De printede bladene ble deretter dyppet i epoxy lim for å styrke bladene.

Testing av både ”Jack Turbinen” og ”Pelton Turbinen” ble gjort for å kunne sammenligne blant annet virkningsgrad. Test-riggen produserte en hydraulisk effekt på cirka 50 Watt. Dessverre var ikke test-riggen egnet til å måle omdreiningsmoment på grunn av et belte/talje system. Derfor var test-riggen bedre tilpasset Pelton Turbinen med sin høyere omdreiningshastighet. Resultatet viste at Pelton Turbinen produserte en maksimal virkningsgrad på 64 prosent, mens ”Jack turbinen” klarte en maksimal virkningsgrad på 54 prosent. Den gjennomsnittlige forskjellen i virkningsgrad av alle de målte verdier var 11.5 prosent mellom de to turbinene. Når man tar hensyn til feil i forhold til omdreiningsmoment og andre feilkilder er disse resultatene veldig positive for videre arbeid og undersøking.

Abstract

I theoretically understood that I needed a blade design that could produce a departing water jet with an absolute velocity of zero, during optimal operating conditions. To do this water had to make an effective turn of approximately180 degrees without colliding with any other blades in a multi-blade scenario.

I quickly discovered in simulations, that our original blade design failed this objective. This occurred because water was actually moving a total of 360 degrees instead of 180 degrees as required. Thus naturally, all energy in the water flow was deposited on the blade and the water flow made a complete stop.

I therefore moved on to a new blade design. Water would be scooped up and deflected more effectively. Simulating showed that this design was behaving itself according to our partial objectives for a single blade scenario. I then continued to simulate and improve this blade design in a multi-blade scenario. Here I were striving to accomplish good overflow from one blade to the next whilst retaining optimal flow over the blades. The final design was expected to create more torque and less angular momentum than The Pelton Turbine would. The New blade design proved to be suitable for construction and testing.

A suitable construction method was chosen. The construction of The Jack Turbine Blade was done by a 3-D printer machine. The Printer machine prints out in gips powder layers and is held together by a weak binder. This is then soaked in a glue infiltrate to give the blade its strength.

Testing of both The Jack Turbine and The Pelton Turbine was completed for comparisons. The test Rig managed hydraulic powers of approximately 50 Watts. Unfortunately it was apparent that The Test rig I was using did not record accurate torque readings because of its Belt/Pulley system. Thus the Test Rig favoured The Pelton Turbine, with its higher angular velocity. Results showed that The Pelton Turbine produced a maximum efficiency of 64 percent whilst The Jack Turbine Blade produced a maximum efficiency of 54 percent. The average efficiency difference for all the recorded readings was 11.5 percent. Taking into consideration the torque errors and other errors, The Jack Turbine shows positive results for future research and investigation.

Contents

		Page
1	**Background**	9
1.1	Background	9
1.2	Main Objectives	12
1.2.1	The main structural objectives	12
1.2.2	The main water flow objectives	12
1.3	Process levels	12
1.4	Working plan for thesis	13
1.5	Limitations	13
2	**Symbols and Notations**	15
2.1	Notations	15
2.2	Symbols	15
2.3	Subscripts	16
2.4	Acronyms	16
2.5	Terms	16
3	**Theory**	17
3.1	Concepts and equations	17
3.1.1	Bernoulli s equation	17
3.1.2	Continuity equation	17
3.1.3	Power in a water jet	18
3.1.4	Impulse water turbines	18
3.1.5	Euler`s equation and the ideal turbine	19
3.1.6	Efficiency	21
3.1.7	Angle of attack (Ø)	21
3.1.8	Pitch	22
3.2	Flow phenomena	22
3.3	The ideal theoretical efficiency of a hypothetical Jack turbine blade	24
3.4	An introduction to The Pelton Turbines blade design	27
3.4.1	The basic blade design of The Pelton Turbine	27
3.4.2	The ideal theoretical efficiency of The Pelton Turbine	30
3.5	Discussing Euler`s equation	34
4	**Ansys Workbench (CFX)**	36
4.1	Simulations	36
4.2	Free Surface Flows (F.S.F) vs Single Fluids (S.F)	36
4.3	Simulation remarks	39

		Page
5	**Physical boundary conditions**	40
5.1	The housing of The Pelton turbine test rig	40
5.2	The holder	42
5.3	Operating boundary conditions for water jet	42
6	**Blade design**	43
6.1	Discussions and partial objectives	43
6.2	Design Procedure	45
7	**Design category 1**	46
7.1	Single Blade Scenario	46
7.2	Multi Blade Scenario	49
8	**Design category 2**	50
8.1	Description of design category 2	50
8.2	Building and naming sections	51
9	**Single blade simulations of design category 2**	54
9.1	Simulations number 4	54
9.2	Simulations number 5	55
9.3	Simulations number 6	56
9.4	Simulations number 7	57
9.5	Simulations number 11	59
9.6	Simulations number 14	60
9.7	Simulations number 15	61
10	**Multi-blade design of design category 2**	63
10.1	Multi-blade challenges	63
10.2	Simulations number 16	66
10.3	Simulations number 20	67
10.4	Simulations number 23 and 24	68
10.5	Simulations number 29	69
10.6	Simulations number 30	70
10.7	The chosen flow and subsequent blade design (Simulation number 37) .	73
11	**Presentation of chosen 3-D solution**	75
11.1	Single blade Procedure	75
11.2	Multiple blade assembly	77
12	**Operating loads for The Jack Turbine Blades**	78
12.1	The “worst case scenario”	78
12.2	Estimate the maximum angular velocity	78
12.3	Maximum force due to water flow	79
12.4	Centrifugal forces at 2000rev/min	79
12.5	Structural stresses on blade during “worst case scenario”	80

		Page
12.6	Rod testing for minimum material stresses	81
12.7	Conclusions for testing and construction	82
13	**Constructions of the Jack turbine blades**	83
13.1	3-D printing	83
13.2	Quality control	84
13.3	Infiltration of glue	85
13.4	Drying and finishing touches	85
13.5	Installation	86
14	**Pre-testing background**	87
14.1	Goals and expectations for testing	87
14.2	Equipment and its function	87
14.2.1	The Hydraulic Bench	87
14.2.2	The Water Turbines Rig	88
14.2.3	The Tachometer	89
14.2.4	The Belt and Pulley	89
14.2.5	Springs and adjustable arm	90
14.2.6	Waters inlet to outlet	91
14.3	Preliminary checks	92
15	**Testing Procedure**	93
15.1	Testing procedure for single blade flow	93
15.2	Testing Procedure for The Multiple Blade Setup	94
16	**Testing Results**	96
16.1	Single Blade Results	96
16.1.1	Failed single force readings	96
16.1.2	The Jack Turbines single blade flow analysis	96
16.1.3	The Pelton Turbines single blade flow analysis	97
16.2	Equation used for results in multiple blade analysis	97
16.3	Multiple blade results, scenario 1	98
16.4	Multiple blade results, scenario 2	101
16.5	Error Analysis	104
16.5.1	Human error Analysis	104
16.5.2	Faulty Equipment Analysis	105
17	**Discussion**	106
18	**Conclusion**	108
19	**Further work**	109
20	**References**	111
Appendix		I-V

1.1 Background

The most relevant background for this master thesis was done in the course Machinery and Product Development (TMP301). The course involves a project whereby one designs a machine against fatigue, stress and other phenomena that is relevant for the design.

The project I chose during this course was an impulse water turbine. Through the study of impulse turbines in other courses, I had learnt that the main efficiency losses found in The Pelton Turbines blade design, was due to the turbines inability to fully manipulate an approaching water jet 180 degrees. The Pelton turbines blade design did this on purpose to avoid any unwanted collision with its adjacent blade. The Pelton Turbines blade design has therefore found a suitable compromise to the problem by manipulating its water jet no more than 165 degrees. Thus the Pelton turbine can never fully utilize all of the water jets energy from a vectors point of view.

My so called solution to the problem was inspired by the shape and geometry of natural sea waves. This was most likely a product of my surfing years as a child in my home country, South Africa.

I had managed to visualize a specific type of blade design whereby a flow movement would effectively move 180 degrees without colliding with the back of the adjacent blade or incoming water jet.

One major issue was that using ones imagination is great for coming up with ideas but it is not very convincing when trying to convey that information to someone else. In other words I could not prove anything because I had not made any water simulations or live tests on the blades. Simulations of multi-flow or so called Free Surface Flows (F.S.F) proved too complicated and time consuming to learn at the time.

Since I did not have any blade simulations I decided to avoid blade designing as much as possible. Instead I decided to design a power transmission system that could convey a certain amount of power. To make things even more interesting I introduced a practical scenario from the farm in South Africa. I gathered information from my brother at home regarding water fall height and water flow from a nearby stream on the mountain. The stream had very little flow but a very high fall height of around 200m. This made it ideal for a small scale impulse turbine or micro-power setup. I used the data in a series of calculations that were based on Euler's equation. From here I could calculate the expected forces involved from the water jet. I took a worst case scenario whereby the turbines blades were blasted by the water jet whilst remaining stationary. The blades were assumed to absorb all of the provided force for both stationary, worst case scenarios and dynamic worst case scenarios.

The blades were designed in such a way that the ejected water could gain maximum clearance when leaving the turbine blades. In addition to this, the design only allowed the water jet to hit the top half of the blades curvature. This prevented unwanted counteracting flows where water travelling down cancels out with water travelling up.

The blades were rather small, only about 15 cm wide and totalling about 3 cm in height. They were designed for a water jet diameter of 1cm or less. From here with the help of Associate Professor , Mr Jan Kåre Bøe, I designed a suitable design for the given conditions.

They were as follows:

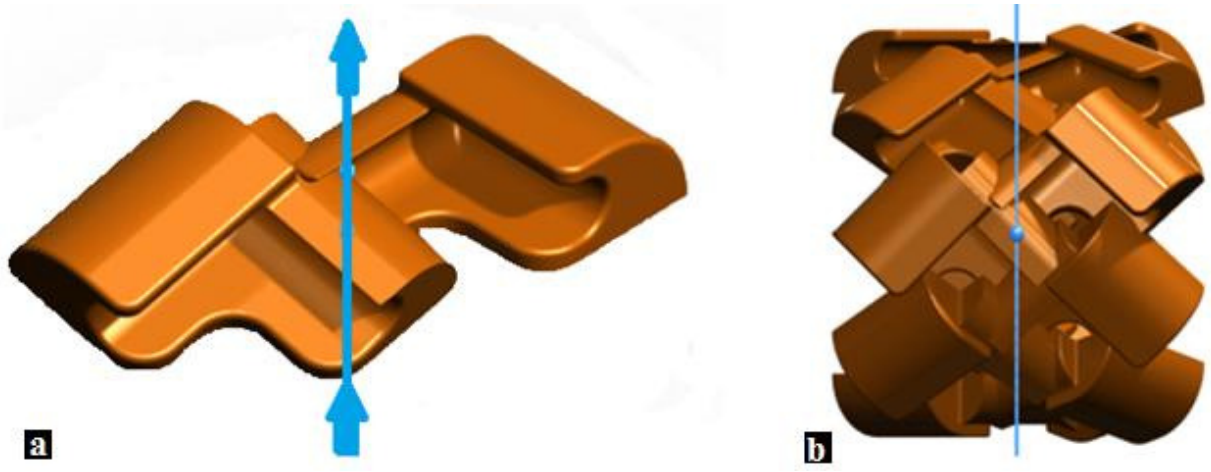

Figure 1.1. **a.)** Two of the blades used in TMP301. The blue line represents the plane in which the water jet will strike the turbine. **b.)** On the right we can see all of the blades gathered around the axis of rotation.

On the left hand side of figure 1.1 above we have a part of the blade setup used in the course TMP301. It consists of two blades that mirror one another but are positioned a given distance around its axis of rotation. The line in blue represents the plane in which the blades would be hit by a water jet. The water jet would strike the top half of the blade. This would keep the entire water jet on the turbine but also maximize torque (T) on the turbine.

In figure 1.2 below we have an exploded view of the main parts used in the power transmission system. The blades section in orange was designed to be cast as one part.

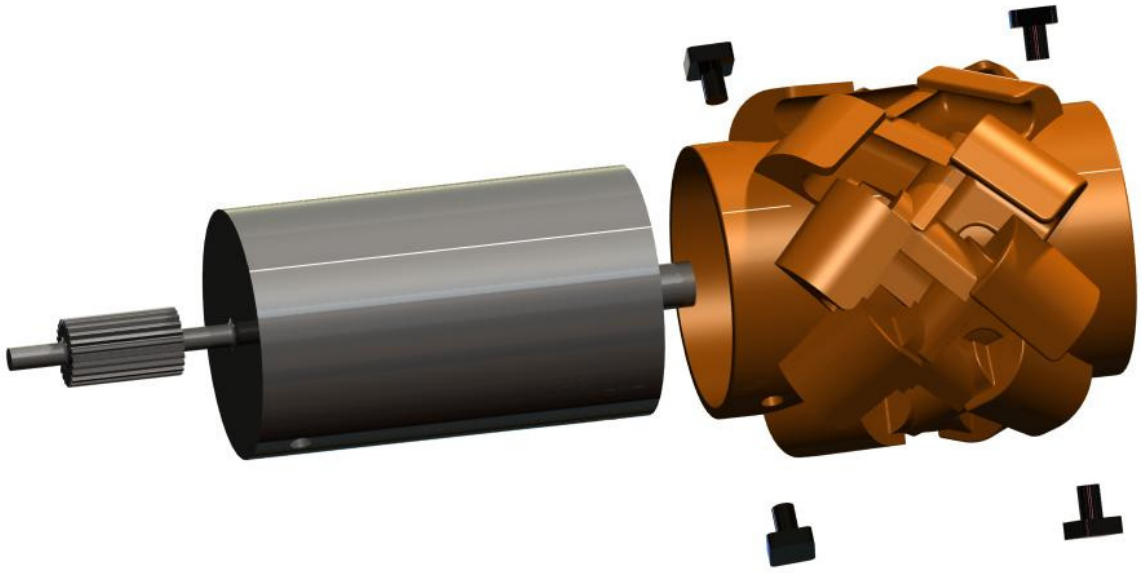

Figure 1.2. Shows an exploded view of all the parts used in the design. The interior shaft and barrel part is shown in black on the left. The Drum with all its blades is shown in orange on the right. Screws and sockets are found around the drum.

The inner drum was designed to be robust and survive the test of time. The outer drum could be easily replaced as shown in the completed assembly below, figure 1.3.

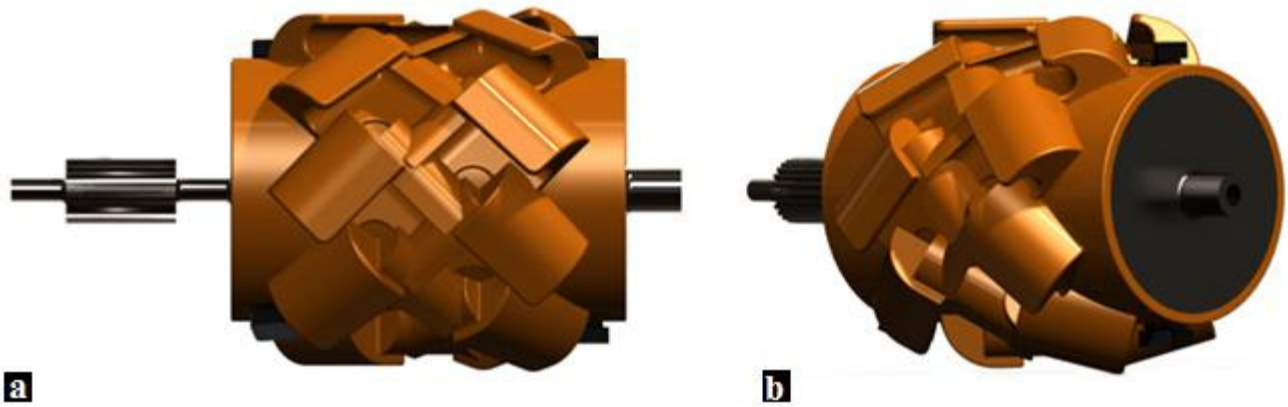

Figure 1.3. **a.)** Front view of the assembled turbine. **b.)** Slightly rotated view of the assembled turbine.

The water flow over the blades can be mentally visualized with the help of some paper and a pencil, shown in figure 1.4 below. If we place two semi-circular cylinders (or gutters) perpendicularly to each other, we can duplicate the fundamental structure of the blades used in figure 1.1 to 1.3. We first place a pencil on the right top gutter (figure 1.4a) and gently push the pencil at 45 degrees to the perpendicular as shown in figure 1.4a. We do the same thing on the other side (outgoing) of figure 1.4a. After several attempts the general conclusion once we roll the paper out is a flow behaviour outlined in figure 1.4b below. A supposed water jet would first move down the blade and to the left until it was at the bottom of the blade. This directional flow behaviour is then mirrored on the adjacent blade except that the water flow now starts from the base of the blade and exits at the top. Repeated attempts shows that the supposed water jet should move pi (3.141) times the diameter of the gutter used as shown in figure 1.4b.

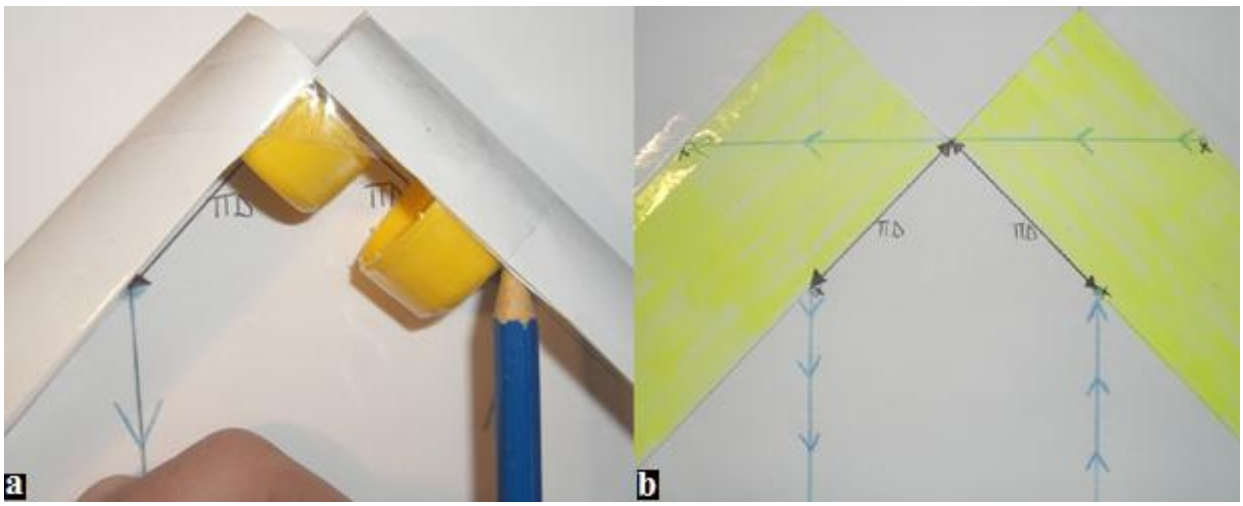

Figur 1.4. **a.)** The two semi-cylinders or gutters at 90 degrees to one another. The yellow objects are bottle tops to help support the structure. The blue pencil is used to create a mark on the page when it is gently nudged along the paper. **b.)** Shows the path of the hypothetical water jet when the paper gutters are rolled out afterwards. The yellow markings represent the blades surface and the white represents the free space.

1.2. Main objectives

Our main objectives can be placed in two main categories; structural and flow objectives.

1.2.1. The structural main objective

- The blades must not make any contact with one another or any of the parts in its proposed housing. This excludes the axel holding the water and the water itself.

1.2.2. The water flows main objectives

- For a **single blade scenario** where water only hits one blade; the blades design must absorb the oncoming water jets energy as efficiently as possible for operational conditions.

- For a **multiple blade scenario** where water hits more than one blade at a time, the blade design must allow easy flow of water from one blade to the next and conserve the single blades main objective.

1.3. Process levels

This thesis will undergo a 10-level process. Each level must be fulfilled before we can move to the next level.

1. We will first become familiar with some fundamental theory to better understand how impulse turbines operate.

2. I will then document our main objectives, boundary conditions[1] (chapter 5) and specific specifications[2] (chapter 6).

3. Whilst acknowledging points 1 and 2 we will consider some potential designs and digitally construct them in the Engineering program Solid Works.

4. I will then digital test our constructions in The Engineering Program Ansys Workbench (CFX).

5. I will then analyse these simulations, look for improvements and change our construction. Thus moving back to point 4. If other unexpected phenomena proves the intended flow design a complete failure, then we will start from the beginning in point 3.

6. After finally discovering a solution that fulfils point 2, we can analyse our blade for operating loads.

7. Choose a method of construction and roughly check that the chosen material can withstand operating loads.

8. Construct blades through chosen method and install.

[1] Boundary conditions are the physical limitations for the blade design. This is presented in chapter 5.
[2] Specific specifications will be presented later in section 6.1 because one needs to understand some theory to fully understand why I have chosen these specifications.

9. Test flow behaviour for both The Jack turbine blades and The Pelton turbine blades under the same operating conditions.

10. Analyse results and conclude.

1.4. Working plans for thesis

The amount of time available is not much and therefore it must be planned out in order to achieve maximum effectiveness. Table 1.1 below will provide an action plan for now but unexpected events will most likely occur and disrupt table 1.1.

Table 1.1. A table representing the working plan of action for this master thesis.

Date	Information gathering and research	Theoretical research	Designing, Solidworks and AnsysCFX	Boulding and testing	General report writing	General improvments and printing
Jan 15-31	active		active		active	
Feb 1-15	active	active	active		active	
Feb 15-28		active	active		active	
Mar 1-15			active		active	
Mar 15-30			active		active	
Apr 1-15				active	active	
Apr 15-30					active	
May 1-15					active	active
Total Time						900 hours

1.5. Limitations

Computation fluid Dynamics (CPD) and its limitations

- Computational fluid Dynamics is something I have not attempted before. I will be learning Ansys Workbench (CFX) for the very first time whilst I perform this Master Thesis. This creates obvious restrictions on what I am able to accomplish in the given time at hand. As we will see in chapter 4, there are also limitations of the size and type of simulations I can run. This is both dependent on the computer running the simulation and the amount of time I have available. It would have been ideal if I could do simulations of Fluid Structure Interaction (F.S.I) but I lack expertise and time.

Flow phenomenal limitations

- This master thesis does not allow for adequate time to analyse all of the strange and wonderful flow phenomena that occurs in nature. I have attempted to highlight some of the most important when designing a blade in chapter 3. It is impossible to always anticipate what a particular flow is going to do before actual tests and experiments are done.

Testing limitations

- Our blade design will be tested in the laboratory on an existing Pelton turbine. We are therefore restricted to the physical amount of space within that turbines housing. This could create unwanted design alterations.

Constructional limitations

- I am limited to the available recourses at UMB, we do not have a plastic 3-D printer but a powder based 3-D printer. A solution to this situation must be resolved such that testing can occur.

Structural limitations

- I will not concern myself with long term operating conditions and problems such as sand abrasion and corrosion.

- I will not be concerned with structural phenomena such as fatigue and harmonic frequency (or specific angular rotational velocity) on the blades due to limited time.

- If any unknown material is constructed I cannot know its properties. I can therefore not accurately predict how it will behave in a dynamic load scenario during testing.

2. Symbols and notations

Table 2.1. Notations.

Symbol	Description	SI Units
A	Cross-sectional area	[m^2]
c	Neutral axis length	[m]
C_v	Velocity co-efficient factor	[-]
d	Diameter	[m^2]
e	Specific energy	[J]
E	Power	[W]
F	Force	[N]
g	Gravity	[m/s^2]
h	Water height	[m]
I	Moment of Inertia	[m^4]
k	Surface friction factor	[-]
L	Length	[m]
m	Mass	[kg]
M	Moment	[N.m]
n	Angular velocity	[rev/min]
p	Specific pressure	[Pa]
P	Pressure	[Pa]
Q	Flow	[m^3/s]
r	Radius	[m]
s	Displacement	[m]
T	Torque	[N.m]
u	Tangential velocity of blade	[m/s]
V	Volume	[m^3]
z	Number of blades	[-]
v	Velocity of fluid	[m/s]

Table 2.2. Symbols.

Symbol	Description	SI Units
α	Alpha angle of attack	[°]
ŋ	Efficiency	[-]
∅	Phi angle of attack	[°]
θ	Theta angle of exit	[°]
$\dot{m}$	Mass flow rate	[kg/s]
ω	Angular velocity	[rad/s]
σ	Stress	[N/m^2]

Table 2.3. Subscripts.

Subscript	Explanation
1	In
2	Out
mec	Mechanical
rel	Relative
tan	Tangent
v	Velocity

Table 2.4. Acronyms.

C.F.D	Computational Fluid Dynamics
F.S.F	Free Surface Flow
S.F	Surface flow
F.S.I	Fluid Solid Interaction

Terms:

- **Absolute velocity** refers to the velocity of the fluid relative to a stationary object in the room. The symbol used here will be: $|v|$.
- **Bars.** One bar is equivalent to 100 000 N/m^2

3. Theory

3.1. Concepts and equations

Before I can start the blade design process, it is important that the reader is aware of a few fundamental fluid mechanics concepts and equations.

3.1.1. Bernoulli's equation:

The total specific energy (J) of a particular incompressible fluid can be defined as the sum of that substances kinetic, potential and internal specific energies (J). The value of this specific energy is constant at various positions such that:

$$mgh_1 + \frac{1}{2}mv_1^2 + \mathrm{p}_1 V = mgh_2 + \frac{1}{2}mv_2^2 + \mathrm{p}_2 V = constant \tag{3.1}$$

We know that mass (m) is equal to the product of its respective density (ρ) and volume (V). The volume of the substance in question is constant and is usually the volume of the fluid found in the reservoir or tank. If we now divide equation 3.1 with its volume we find Bernoulli´s equation:

$$\rho g H_1 + \frac{1}{2}\rho v_1^2 + \mathrm{p}_1 = \rho g H_2 + \frac{1}{2}\rho v_2^2 + \mathrm{p}_2 = constant \tag{3.2}$$

3.1.2. Continuity Equation:

Consider a continuous system such as a pipe with a varying diameter shown in figure 3.1 below.

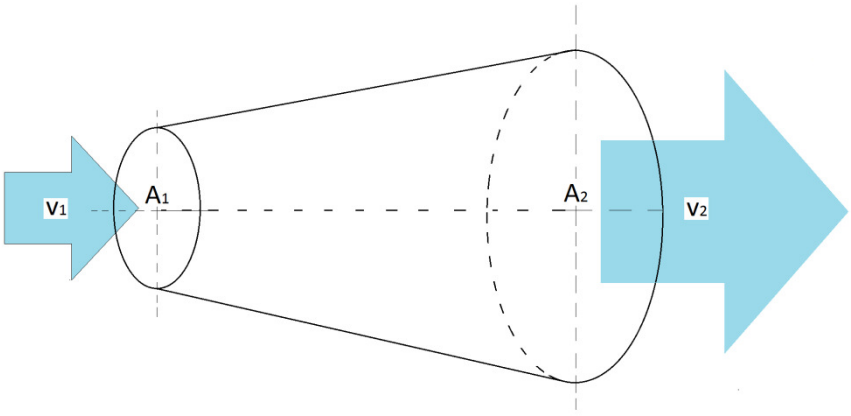

Figure 3.1. A cylindrical pipe of varying diameter. Inlet is on the left whilst outlet is on the right.

We know from the conservation of mass that the rate of mass entering the system is equal to the rate of mass leaving the system. Thus

$$\frac{d}{dt}m_1 = \frac{d}{dt}m_2 = \dot{m}_1 = \dot{m}_2$$

$$\Rightarrow \frac{d}{dt}\rho V_1 = \frac{d}{dt}\rho V_2 \tag{3.3}$$

If we divide equation 3.3 by its density (ρ) and consider the fact that a given volume entering and exiting the pipe is the same. Volume is the product of its area and displacement (s) such that:

$$\frac{d}{dt}A_1 s_1 = \frac{d}{dt}A_2 s_2 \tag{3.4}$$

The areas at points one and two in figure 3.1 are constant. The derivative of the area is zero. The derivative of displacement (s) becomes a velocity (v). Thus by utilizing the chain rule we find:

$$A_1 v_1 = A_2 v_2 \tag{3.5}$$

An abbreviated symbol for equation 3.5 is known as the flow (Q) such that equation 3.5 becomes:

$$Q_1 = Q_2 \tag{3.6}$$

3.1.3. Power in a water jet

For a given constant volume (V) of fluid (shown in figure 3.2 below) there exists a hydrostatic pressure (P) at a certain depth.

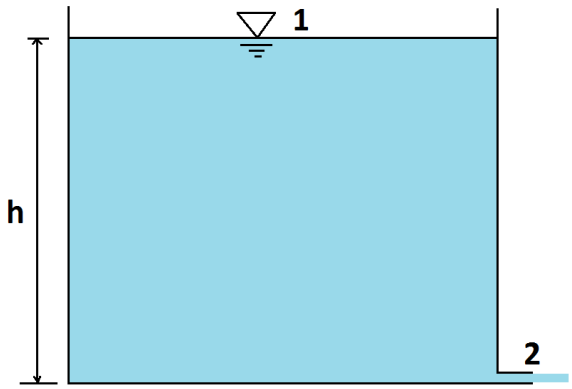

Figure 3.2. A tank of water with depth h. The surface area of point one is infinitely large. Both point one and two are in contact with the atmosphere. At point 2 water is discharged to form a fast moving water jet.

Hydrostatic Pressure is dependent on Bernoulli's equation (eq 3.2). The available specific energy (measured in Joules) of the fluid is the summation of its kinetic, potential and internal energy. The power (E) obtained from this fluid is the rate at which this specific energy is moving and can be found by differentiating the fluids specific energy (eq 3.1). We find:

$$E = \frac{d}{dt}\left(mgh + \frac{1}{2}mv^2 + \mathrm{p}V\right) = \frac{d}{dt}\left(\rho gh + \frac{1}{2}\rho v^2 + \mathrm{p}\right)V = 0 + \left(\rho gh + \frac{1}{2}\rho v^2 + \mathrm{p}\right)Q = PQ \tag{3.7}$$

Looking at figure 3.2 above we see that at point one the velocity (v) of the surface of an infinitely large reservoir approaches zero. The surrounding pressure is atmospheric pressure which is very small in comparison to the hydrostatic pressure formed by the fluids own weight. Utilizing Bernoulli´s equation (eq 3.2) and equation 3.7, we gather an expression for the exiting power at point 2 of figure 3.2 above.

$$E_1 = PQ = (\rho gh + 0 + 0)Q = \rho ghQ \tag{3.8}$$

Since energy and therefore power is conserved, the power at point two is the same as point one. Therefore the power delivered in the water jet at point two is:

$$E_2 = E_1 = \rho ghQ = \frac{1}{2}\rho v_2^2 Q \tag{3.9}$$

3.1.4. Impulse water turbines

Impulse turbines utilize the energy transmitted by a free moving water jet. By free moving, water flows through the atmosphere and is not encapsulated within a pipe. The main objective for an impulse turbine setup (as shown in figure 3.2 above) is to conserve the water jets flow and transform potential energy stored in the reservoir into kinetic energy. The result is a very fast moving water jet. Utilizing the conservation of energy (equation 3.9) at point one and two of figure 3.2 we find:

$$E_1 = E_2$$

$$\Rightarrow \rho g h_1 + \frac{1}{2}\rho v_1^2 + \mathrm{p}_1 = \rho g h_2 + \frac{1}{2}\rho v_2^2 + \mathrm{p}_2$$

$$\Rightarrow \cancel{\rho} g h_1 + 0 + \cancel{1\ \mathrm{atm}} = 0 + \frac{1}{2}\cancel{\rho} v_2^2 + \cancel{1\ \mathrm{atm}}$$

$$\Rightarrow v_2 = \sqrt{2gh_1} \tag{3.10}$$

The velocity obtained here is a theoretical solution and does not take into consideration various losses caused by the piping and nozzle leading to the outlet. We therefore must multiply equation 3.10 with a velocity co-efficient factor, (C_v). Under optimal conditions this factor is usually between 0.97 and 0.99.

The velocity coefficient (C_v) is dependent on the nozzles opening area. Figure 3.9 shows this relationship in detail.

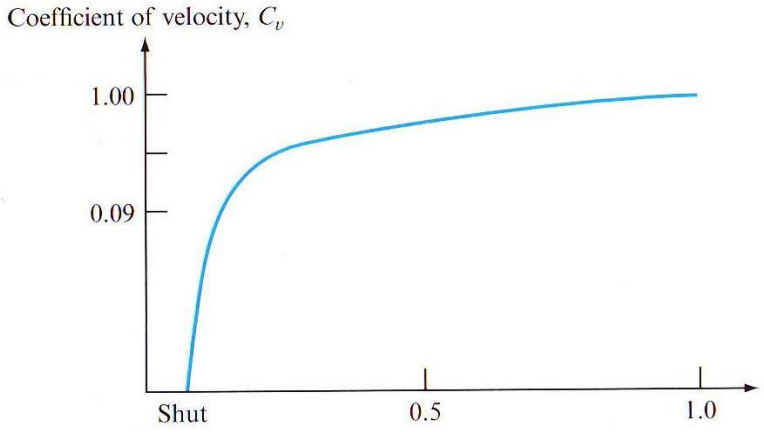

Figure 3.3. Shows the varying velocity coefficient factor ($\boldsymbol{C_v}$) has when the nozzle is fully shut and when it is fully opened. Picture scanned, **Ref: [1]**

Substituting the velocity co-efficient into equation 3.10 and we have:

$$v_2 = C_v\sqrt{2gh_1} \tag{3.11}$$

3.1.5. Euler's equation and the ideal turbine

Euler´s equation is an extension of Sir Isaac Newton´s basic laws of physics.

This equation is central to the study for all roto-dynamic machines that involve a moving fluid. The Pelton turbines roto-dynamic theory is heavily based on this equation too.

The equation makes a connection between the incoming and outgoing water flows into and from a moving object. From here, an expression for the amount of mechanical energy a typical turbine can extract from the water jet is derived. If we consider figure 3.4.

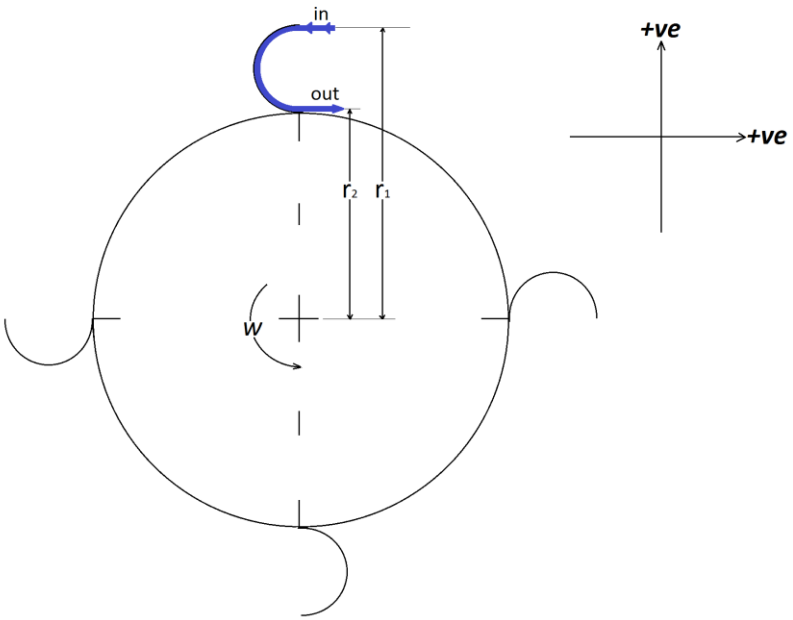

Figure 3.4. A two-dimensional cross section of a hypothetical turbine. There are four blades rotating anti-clockwise. Water making contact with one of the blades is shown in blue. Two different radiuses occur at inlet and outlet points shown as r_1 and r_2.

For a 2-dimentional cross-section of a system shown in figure 3.4, the torque a water jet imposes on a turbine is equal to the rate of change of angular momentum:

$$T = \frac{d}{dt}[m(v_{in}r_1 \ - v_{out}r_2)] = \frac{d}{dt}[m\Delta(vr)] = \dot{m}\Delta(vr) + 0 = \rho Q(v_{in}r_1 - v_{out}r_2) \qquad (3.11)$$

In equation 3.11 above v_{in} and v_{out} are water velocities. The radiuses at which these velocities enter or exit are indicated as r_1 and r_2.

An ideal turbine would produce an outgoing absolute velocity $|v_{out}|$ of zero. In so doing all of the energy from the water jet will be absorbed into the rotating turbine. It is therefore important that gravity can move this stationary liquid away from the turbine so that no unnecessary collisions are made.

The turbine itself will react to the oncoming water by creating a torque that is dependent on the amount of counter resistance or load the axel is given.

Note that if we were working with a linear system for example a jet hitting a single blade with no ration, then equation 3.11 would become a force value with no radius values in it, such that:

$$F = \rho Q(v_{in} - v_{out}) \qquad (3.12)$$

The total mechanical power the turbine (figure 3.4) can extract from the moving fluid is equal to the product of the torque (T) and angular velocity (ω).

Thus multiplying the angular velocity with the torque in equation (3.11) we find the mechanical power for the blade of figure 3.4.

$$E_{mec} = \ \rho Q(v_{in}\omega r_1 - v_{out}\omega r_2) \qquad (3.13)$$

At any given point on the rotating turbine the absolute tangential velocity (u) is equal to the product of the angular velocity (ω) and the radius such that:

$$u = \omega r \tag{3.14}$$

Thus substituting equation 3.14 into equation 3.13 above, we have Euler's equation.

$$E_{mec} = \rho Q(v_{in}u_1 - v_{out}u_2) \tag{3.15}$$

During calculations it is easier to calculate velocities relative to another body. Thus:

$$v_{in} = v_{rel\ in} \quad \text{and} \quad v_{out} = v_{\text{rel out}}$$

Therefore equation 3.15 becomes:

$$E_{mec} = \rho Q(v_{rel\ in} \cdot u_1 - v_{\text{rel out}} \cdot u_2) \tag{3.16}$$

3.1.6. Efficiency

If we consider a water turbine that is subjected to a jet of water; we`ll find that no real turbine is able to convert all the hydraulic energy into mechanical energy. The losses we will be considering in this thesis are flow losses. These flow losses are caused by varying surface areas, surface finishes, turbulence, directional losses and other phenomena. On a general scale, we know that the total efficiency any given water turbine can extract from a water jet is simply the mechanical energy obtained divided by the hydraulic energy in the water jet such that:

$$\eta = \frac{energy\ out}{energy\ in} = \frac{E_{mec}}{E_{in}} = \frac{T\omega}{PQ} \tag{3.17}$$

If we look at figure 3.2 again, we can consider that the flow at point 2 (outlet) has reached equilibrium[3] and by substituting equation 3.16 and 3.8 into equation 3.17 we find:

$$\eta = \frac{\rho Q(v_{rel\ in} \cdot u_1 - v_{\text{rel out}} \cdot u_2)}{\rho g H Q} = \frac{(v_{rel\ in}u_1 - v_{rel\ out}u_2)}{gH} \tag{3.18}$$

Equation 3.18 is the maximum theoretical efficiency that is possible for any impulse turbine setup. It is by all means impossible to reach in a real system.

3.1.7. Angle of attack (Ø)

The water jet can vary its angle of attack on the blade, see figure 3.5 below. In the schematic diagrams that follow the water jets centre line will be in blue.

[3] Equilibrium refers to the state of balance whereby very little or zero acceleration occurs.

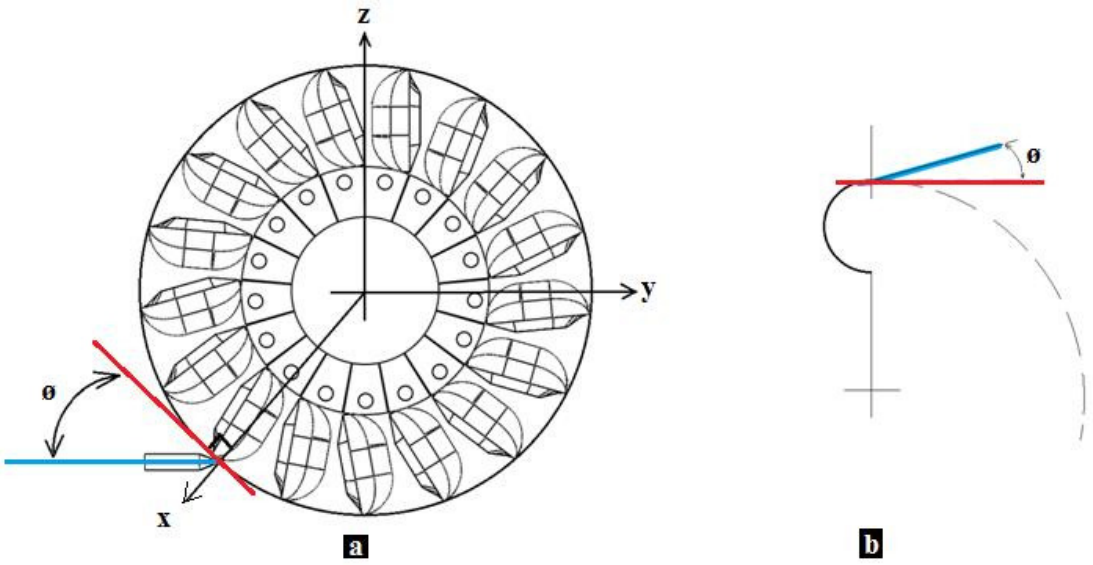

Figure 3.5. **a.** A side view of The Pelton Turbine rotating in the yz-plane. The blue line represents the direction of the water jet hitting the blades and the red line represents the tangent of the circumference of the turbine. The phi angle of attack is the angle between these two lines. **b.** Shows a better configuration of the same setup in a.

If we consider a turbine (in this case a Pelton turbine) rotating about the x-axis in the yz-plane shown above in figure 3.5. Then the phi angle of attack (Ø) is found between the incoming water jet centre line (in blue) and the turbine circumference (in red).

3.1.8. Pitch

Pitch is the angle between two blades in relation to its axis of rotation. For example a turbine with 20 blades will have a pitch of 18 degrees. There is therefore a direct relationship between the number of blades (z) and it´s pitch. If there are too few blades, then water is lost and not utilized. One wants to introduce as many blades as possible in order to distribute the load from the water jet. Although if there are too many blades then the blades behave more like a wall for the water jet, rather than absorbing it´s flow. A balance is in order and through years of experimenting a typical Pelton turbine can have any number of blades between 16 and 24 [ref]. For small micro-power systems this can be reduced rather significantly to for example 12 blades.

3.2. Flow phenomena

Free surface flows (F.S.F):

Impulse turbines only utilize free surface flows (F.S.F). These flows refer to any water flow that is exposed to the atmosphere.

Surface tension:

Surface tension has a tendency to hold the flow intact, within a certain speed and cross-sectional thickness. If the flow over the blade retains some thickness, then surface tension can actually benefit the flow by retaining cohesiveness. This helps avoid too much spreading of the water jet whilst it travels over the blade.

Gravity:

Free surface flows are very much affected by gravity. This is especially true for long distance water flows that have adequate time. We will utilize gravity as a mechanism for removing water from our water turbine without contributing any extra energy.

Cavitation:

Cavitation is an extremely damaging phenomenon. It occurs because a liquid begins to vaporise or boil. A boiling behaviour of the fluid eats away on materials and can create permanent damage.

How commen is cavitation in F.S.F`s? To answer this we need to do some more explaining.

Well we know that for a relatively thin water flow the pressure in the fluid must be equal to its surroundings, which is atmospheric pressure. The pressure in the moving fluid is dependent on Bernoulli's equation (eq 3.2) such that:

Pressure in fluid = pressure in surroundings

$$\rho g\mathrm{h} + \frac{1}{2}\rho v^2 + \mathrm{p} = 1\ atm$$

$$0 + \frac{1}{2}\rho \mathrm{v}^2 + \mathrm{p} = 1\ atm \tag{3.19}$$

If we consider a water jet travelling at 1m/s and substitute this into equation 3.19 we will notice that the specific pressure (p) is nearly the same as 1 atm.

As the moving fluid increases its velocity more of the specific pressure (p) changes in the form of kinetic energy. This occurs because energy is conserved and thus one could say that pressure energy is converted into kinetic energy when a free surface flow increases in velocity. When all of the pressure energy is converted to kinetic energy the pressure in the fluid becomes zero and it begins to boil. Note that the left hand side of equation 3.19 is still constant although the velocity increases and the specific pressure (p) decreases respectively.

The critical velocity at which cavitation can occur, can be found by rearranging equation 3.19 and setting the specific pressure (p) to zero.

$$0 + \frac{1}{2}\rho \mathrm{v}^2 + 0 = 1.1023 \times 10^5 N/m^2$$

$$0 + \frac{1}{2}\rho \mathrm{v}^2 + 0 = 1.1023 \times 10^5 \left(\frac{kg.m}{s^2}\right)/m^2$$

$$v = \left(\frac{2 \times 1.1023 \times 10^5 \left(\frac{kg.m}{s^2}\right)/m^2}{997 kg/m^3}\right)^{\frac{1}{2}} = 14.87 m/s$$

Thus one could say that all liquid on the blade must travel under the velocity of 14.87 m/s to avoid Cavitation from occurring. Well this is not the case thanks to the continuity equation

As the water flow approaches a velocity of 14.87 m/s it increases in area effectively decreasing the velocity of the moving water.

Thus we can say that although cavitation does occur in F.S.F it`s less of a threat than in closed pipes setups such as the Francis Turbine. This does not mean that water never travels faster than 14.87

m/s because it often does. It just means that if enough time is given, then fast moving water travelling over a blade will expand such that cavitation is avoided.

Counter flow losses:

Just as Newton's third law states, "that every action has an opposite and equal reaction", so too does two water flows travelling towards each other. The easiest way to create an opposing water flow is to direct a water jet perpendicularly to a smooth solid wall. It may appear as though the water is distributing itself evenly around the impact area. Thus according to Euler`s equation the water jet has effectively deposited a quarter (90 deg turn) of the water jets energy onto the wall.

This is entirely wrong because many water particles are rebounded back towards the water jet and cancel out much of its energy before the water actually touches the wall.

The described analogy is a very chaotic[4] system. What we do know from previous experimentation (of The Pelton Turbine) is that in order to capture a water flows energy we need to make the water turn as gradually as possible. This helps avoid counter flows and improve energy capture.

Flow standstill:

If we consider the following situation:

- A thin water jet
- Travelling along a frictionless wall
- Water travelling on a single plane
- The water follows the wall and effectively turns 360 degrees
- A free surface flow (FSF) environment
- No gravity

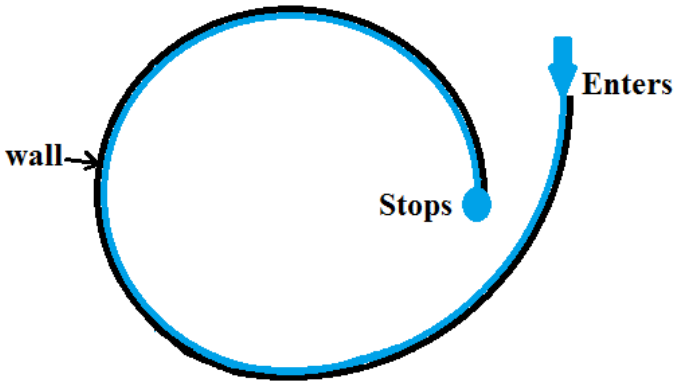

Figure 3.7. Water in blue enters a F.S.F environment along a frictionless wall (in black). The water follows the wall and will stop after 360 degrees.

The conclusion of one such situation would create a complete standstill of the entering water jet (shown in figure 3.7 above). This will occur despite the velocity of the entering water jet.

This is important to keep in mind when designing a blade because we want to extract half of the flows energy (entails a movement of ideally180 degrees) on impact such that during operational conditions all of its energy is extracted.

This is better understood if we have a look at Euler`s equation and how it is used in sections 3.4 and 3.5 below.

[4] Chaotic refers to a non-linear system of unpredictable behaviors. A good example would be the weather system of our planet. It can never be perfectly predicted.

3.3. The ideal theoretical efficiency of a hypothetical Jack turbine.

Let us consider a hypothetical blade setup shown below in figure 3.8.

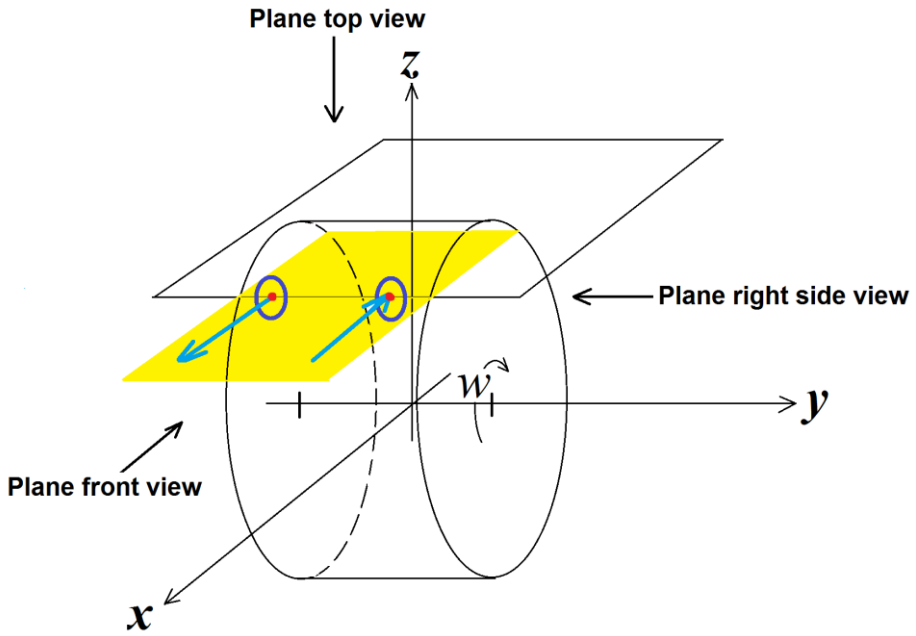

Figure 3.8. The figure shows a 3-D system of a rotating water turbine. A cross-section plane of the water jet lies parallel to the xy-plane, shown in yellow. Three viewing angles are present. A top, front and right side view shown in figure 3.9 below.

The figure above shows three viewing angles as well as the inlet and outlet water jets on the plane shown in yellow.

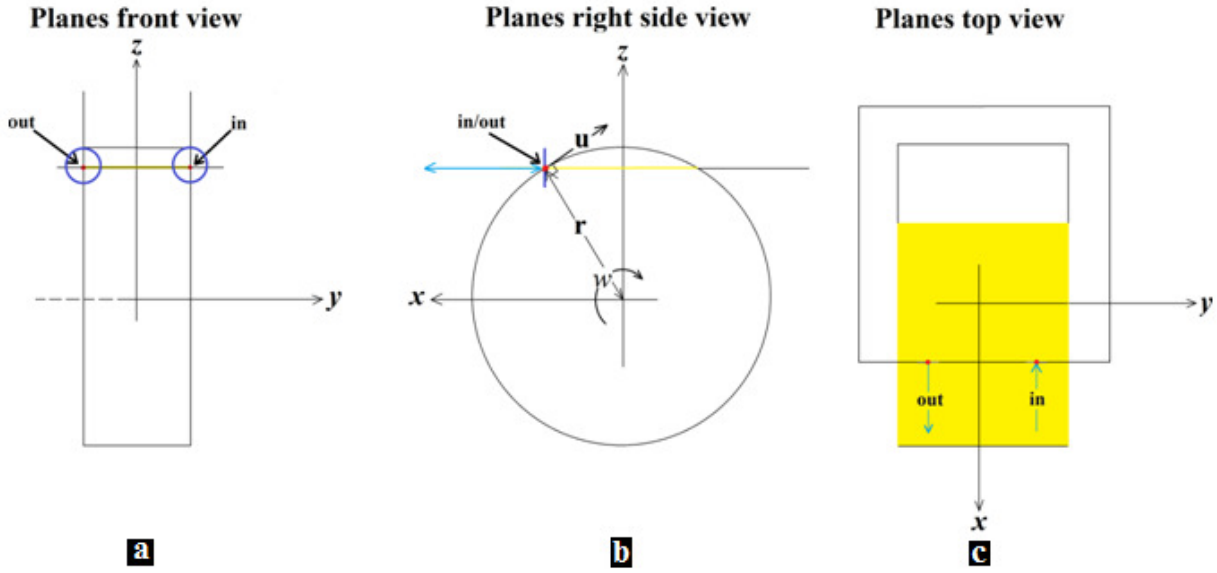

Figure 3.9. **a.)** The front view of figure 3.8, the yz-plane. **b.)** The planes right side view, shows the rotation of the turbine and the tangential velocity (u) of the blade. **c.)** The top view, showing the inlet and outlet of the water jet on the cross-section in yellow.

The centre line of the incoming water jet (light blue line of figure 3.8 and 3.9), would strike a hypothetical blade in a direction that was perpendicularly to the yz-plane of figure 3.9 a.

This would hit the turbine at a point on the turbine ("red dot **in**" in figure 3.8 and 3.9). This red point of contact would be directly on the zy-plane **if** the water jet was infinitely thin.

In the case of figure 3.8 and figure 3.9 we have used a real scenario where the water jets have a cross-sectional area. In a real scenario like this the outer diameter of the water jet touches the circumference of the turbine shown as a dark blue ring on figure 3.8 and 3.9a. The light blue line represents the centre line of a real water jet.

From this inlet position of the water jet in figure 3.8 the water flow would make a 180 degrees turn.

This 180 degrees turn is not shown in figure 3.8 or 3.9 because it is not necessary. All that matters when using Euler`s equation is the velocity and trajectory of the incoming and outgoing water.

If we now look at Euler`s equation from section 3.2 we have:

$$\mathrm{E} = \rho Q(v_{rel\,in} \cdot u_1 - v_{rel\,out} \cdot u_2)$$

The tangential velocity (u) of the turbine (red dot in figure 3.8b) is the same at the water jets inlet point and exit point because they have the same radius. Thus:

$$u_1 = u_2 = u_{tan}$$

Thus Euler's equation becomes:

$$\mathrm{E} = \rho Q u(v_{rel\,in} - v_{rel\,out}) \tag{3.20}$$

The water velocity relative to the moving blade at entry is equal to the incoming water jets tangential velocity (v_{in}) minus the turbines tangential velocity (u_{tan}) at the point in question. Thus:

$$v_{rel\,in} = v_{in} - u_{tan} \tag{3.21}$$

As the water moves over the blade it slows down because of friction. It is therefore necessary to include a frictional factor (k). Thus the following is true:

$$v_{rel\,out} = -k(v_{rel\,in}) = -k(v_{in} - u_{tan}) \tag{3.22}$$

The negative sign refers to the direction which is opposite to the direction of inflow.

Substituting equation 3.21 and 3.22 into 3.20 we find:

$$\mathrm{E} = \rho Q u_{tan}(1+k)(v_{in} - u_{tan})$$

$$E = \rho Q(1+k)(v_{in}u_{tan} - (u_{tan})^2) \tag{3.23}$$

Equation 3.23 expresses the power in Watts at any given moment.

To find the maximum possible efficiency that is available for the Jack turbine we need to differentiate equation 3.23 with respect to the tangential velocity (u_{tan}) of the blade. We then make this expression equal to zero and resolve.

Thus:

$$\frac{\mathrm{dE}}{\mathrm{d}u_{tan}} = \rho Q(1+k)(v_{in} - 2u_{tan}) = 0$$

$$u_{tan} = \frac{1}{2} \cdot v_{in} \tag{3.24}$$

Thus for maximum efficiency the outgoing velocity will be half the incoming velocity (travelled 180 degrees), only in opposite directions. This means the absolute velocity of the outgoing water jet would effectively become zero and be subjected to gravity:

$$|v_{out}| = 0$$

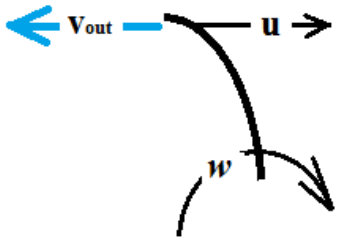

Figure 3.10. The figure shows a rotating blade in black with an angular rotational velocity of $\boldsymbol{\omega}$. The velocity out (v_{out}) is equal in magnitude to the tangential velocity (u) of the blade under max efficiency conditions. The absolute velocity of the outgoing water jet ($|\boldsymbol{v_{out}}|$) becomes zero under these conditions.

Substituting equation 3.24 into 3.23 and we find:

$$E_{max} = \left(\frac{1}{4}\right)(1+k)\rho Q \cdot v_{tan}^2 \tag{3.25}$$

In equation 3.25 we have found the maximum possible power.
From equation 3.8 we have the jets power to the turbine:

$$E_{in} = \rho g h Q = \rho g Q \left(\frac{v_{tan}^2}{2g}\right) = \left(\frac{1}{2}\right)\rho Q (v_{tan}^2) \tag{3.26}$$

The maximum efficiency of the turbine is acquired if we substitute equations 3.25 and 3.26 into equation 3.17 for efficiency such that:

$$\eta_{max} = \frac{energy\ out}{energy\ in} = \frac{E_{mec}}{E_{in}} = \frac{1+k}{2} \tag{3.27}$$

Here we have found the maximum theoretical efficiency for our ideal, hypothetical Jack Turbine blade. This blade has water entering and exiting at the same radius although it turns its water flow 180 degrees. Thus if we design a different blade with varying inlet and outlet radiuses we will have an entirely different expression than that found in equation 3.17 above.

3.4. An introduction to the Pelton Turbines blade design

3.4.1. The basic blade design of the Pelton turbine

The basic structure of the Pelton Turbine blade is shown in figure 3.11.

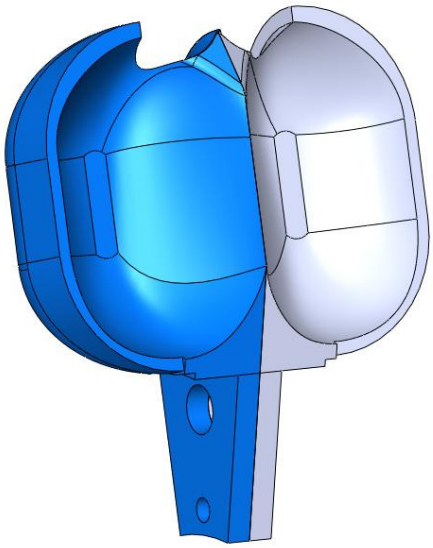

Figure 3.11. Shows a single Pelton turbine blade. The blade is perfectly symmetrical about its centre axis. The two halves are shown in blue and grey. Image drawn in Solid Works.

The blade (shown in figure 3.11) consists of two spoon-like configurations placed next to each other. The top of the blade has a pointed like configuration for easy flow passage from one blade to the next. The blade is perfectly symmetrical (shown in blue and grey) and is designed to split the water jet hitting it. The assembled version of figure 3.11 is shown below in figure 3.12.

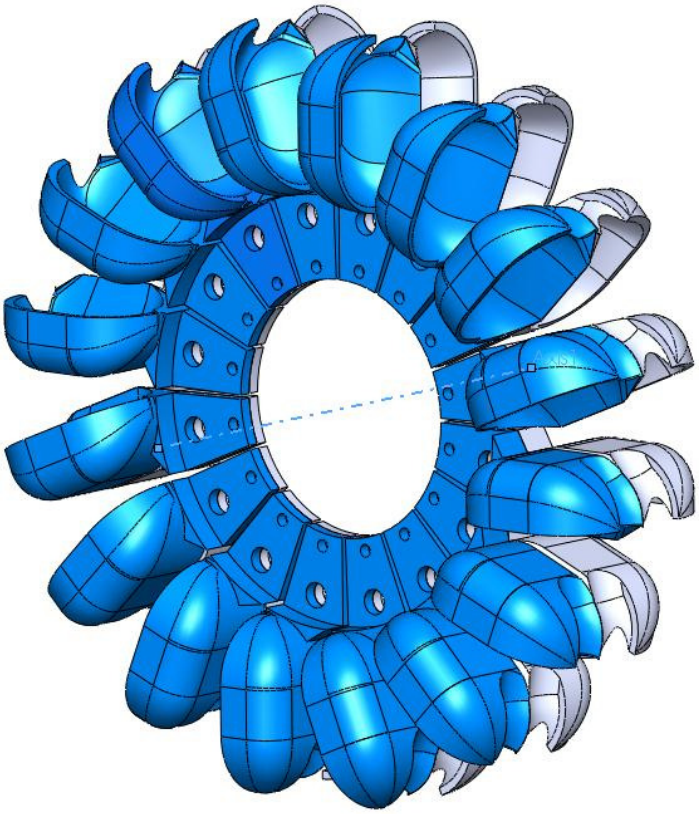

Figure 3.12. The complete assembly of The Pelton Turbine with 16 Blades. Image drawn in Solid Works.

Most Pelton Turbine blades are bolted onto a shaft and therefore have two holes underneath for bolted attachment. For micro-power applications, where smaller forces are involved , there various alternatives as to how the blades are connected to the shaft.

Smaller setups of The Pelton Wheel are usually positioned vertically as in figure 3.13 below. Larger Pelton Turbines have their axis of rotation pointing up from the ground which is more stable. The most effective Pelton turbines have six inlet nozzles which are evenly distributed around the turbine to create a stabilized configuration.

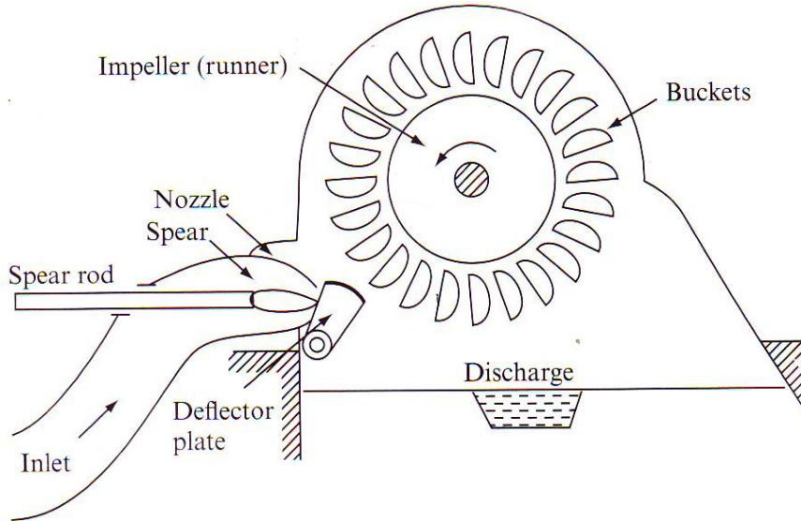

Figure 3.13. A typical Pelton turbine setup. The turbine is in a vertical position whereby gravity is used to remove static water away from the rotating turbine. Scanned image from ref: **[1]**

Figure 3.13 above is an example of a Pelton turbine in the vertical position with gravity down the page. The next question is how water moves over the blade in a Pelton turbine? To better understand this we can have a look at figure 3.14 below.

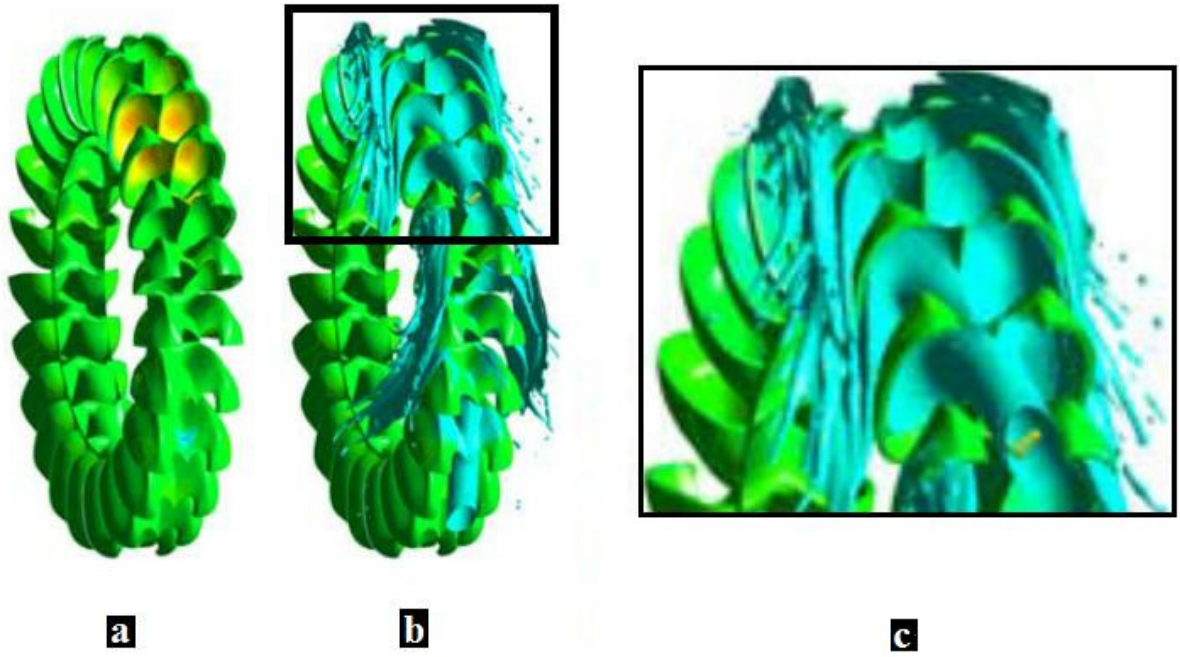

Figure 3.14. **a.)** Shows the pressure distribution over the blades. **b.)** The Pelton turbine with a water jet impacting the blade. The black box is the cut area for figure 3.14 c. **c.)** An exploded view of the cut area in figure 3.14 b. Water is deflected and passes over its adjacent blade just enough to miss it. A great deal of spreading is evident. Scanned image from; **[2]**.

3.5.2. The ideal theoretical efficiency of The Pelton Turbine

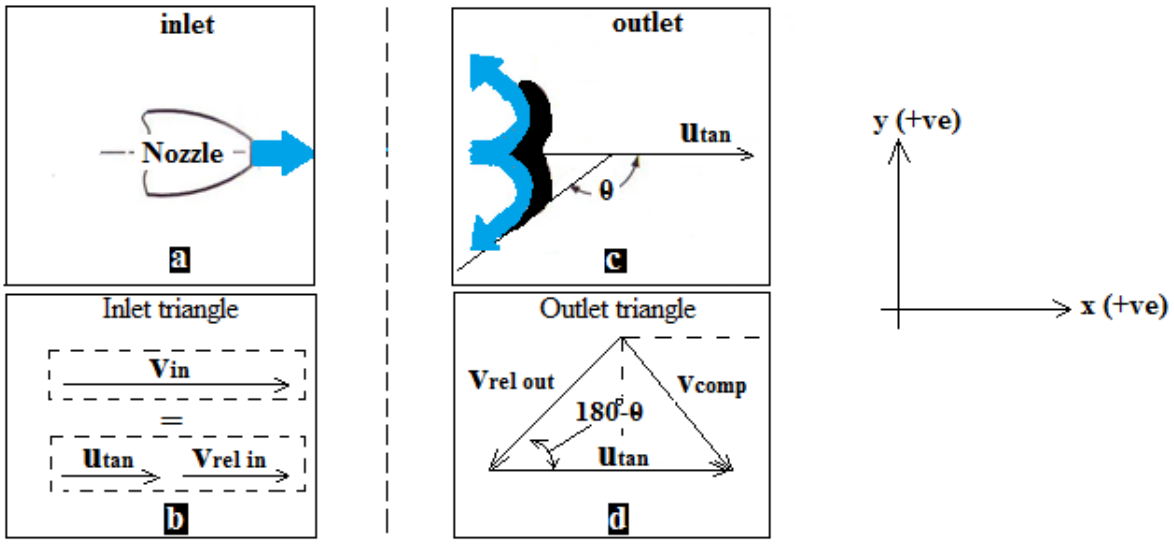

Figure 3.15. **a.)** The inlet nozzle with the exiting water jet in blue. **b.)** The inlet water triangle, a vector representation of the inlet nozzle scenario in a. **c.)** The outlet flow with a blade in black and water flow in blue. **d.)** A vector representation of c. The outlet triangle shows a water velocity ($v_{rel\ out}$) relative to the turbines tangential velocity (u_{tan}).

We know that the total energy transferred to the wheel is provided by Eulers equation (eq 3.16)

$$E_{mec} = \rho Q(v_{rel\ in} \cdot u_1 - v_{\text{rel out}} \cdot u_2)$$

We know that the velocity on either side of the turbine blade (tangential velocity) is the same because there is no change in radius between inlet and outlet, such that:

$$u_{in} = u_{out} = u_{tan}$$

Thus Euler's Equation becomes;

$$E_{mec} = \rho Q u_{tan}(v_{rel\ in} - v_{\text{rel out}}) \tag{3.28}$$

If we look at figure 3.15 a and b, we can see that the inlet velocity can be defined as the sum of the tangential velocity (u_{tan}) of the Pelton turbines rotating blade and the relative velocity ($v_{rel\ in}$), such that:

$$v_{rel\ in} = v_{in} - u_{tan} \tag{3.29}$$

Note that equation 3.29 is in the positive x direction.

We know that surface friction (k) will slow the water flow down by a factor of k. The relative velocity out ($v_{rel\ out}$) of the turbines blade would be equal to the relative velocity in ($v_{rel\ in}$) multiplied by this frictional factor (k) such that:

$$v_{rel\ out} = k v_{rel\ in} = k(v_{in} - u_{tan}) \tag{3.30}$$

As we can see in equation 3.30 above, there is no inclusion of the fact that the outlet water jet is not travelling in a purely x-direction.

Extracting information from figure 3.14 c and vector triangle 3.14 d, we can include a componential factor ($\cos(180 - \theta)$) . Thus equation 3.30 becomes:

$$v_{rel\ out} = -k \cdot (v_{in} - u_{tan}) \cdot \cos(180 - \theta)$$

$$v_{rel\ out} = k(v_{in} - u_{\text{tan}})cos\theta \tag{3.31}$$

If we now substitute equations 3.30 and 3.31 into Eulers equation 3.28 we find:

$$E_{mec} = \rho Q u_{tan}[(v_{in} - u_{tan}) - k(v_{in} - u_{\tan})cos\theta]$$

$$\Rightarrow E_{mec} = \rho Q u_{tan}[(v_{in} - u_{tan})(1 - kcos\theta)]$$

$$\Rightarrow E_{mec} = \rho Q[(u_{tan}v_{in} - u^2{}_{tan})(1 - kcos\theta)] \quad (3.32)$$

At any given time the mechanical power a Pelton turbine can extract from the water jet for an ideal situation can be calculated using equation 3.32.

The next question is when is the mechanical power at a maximum? To find out when this occurs we need to differentiate equation 3.32 with respect to the tangential velocity (u). We then make this equal to zero and resolve. Such that:

$$\frac{dE}{du} = \frac{d}{du}\rho Q[(u_{tan}v_{in} - u^2{}_{tan})(1 - kcos\theta)] = 0$$

$$v_{in} - 2u_{tan} = 0$$

$$u_{tan} = \frac{1}{2}v_{in}$$

As expected the resulting conclusion is the same as equation 3.24 found previously in section 3.4. If we now substitute this value in equation 3.32 we find the following maximum power:

$$E_{max} = \left(\tfrac{1}{4}\rho Q v_{tan}^2\right)(1 - k\cos\ \theta) \quad (3.33)$$

Utilizing equation 3.26 for the incoming water jet we have:

$$E_{in} = \rho g h Q = \rho g Q\left(\frac{v_{tan}^2}{2g}\right) = (\frac{1}{2})\rho Q(v_{tan}^2)$$

We can therefore calculate the maximum theoretical efficiency for the Pelton turbine by substituting eq 3.33 and eq 3.26 into equation 3.17. This produces the following:

$$\eta_{max} = \frac{E_{max}}{E_{in}}$$

$$\eta_{max} = \tfrac{1}{2}\cdot(1 - k\cos\theta) \quad (3.34)$$

Thus equation 3.34 shows that the maximum efficiency for The Pelton Turbine is only dependent on friction and the angle of the deflector buckets. Let us now make a graph of equation 3.34 with varying frictional factor (k). the Pelton Turbine has an angle of 165 degrees and the Jack turbine has an angle of 180 deg. Equation 3.34 becomes the same as 3.27 when 180 degrees is used.

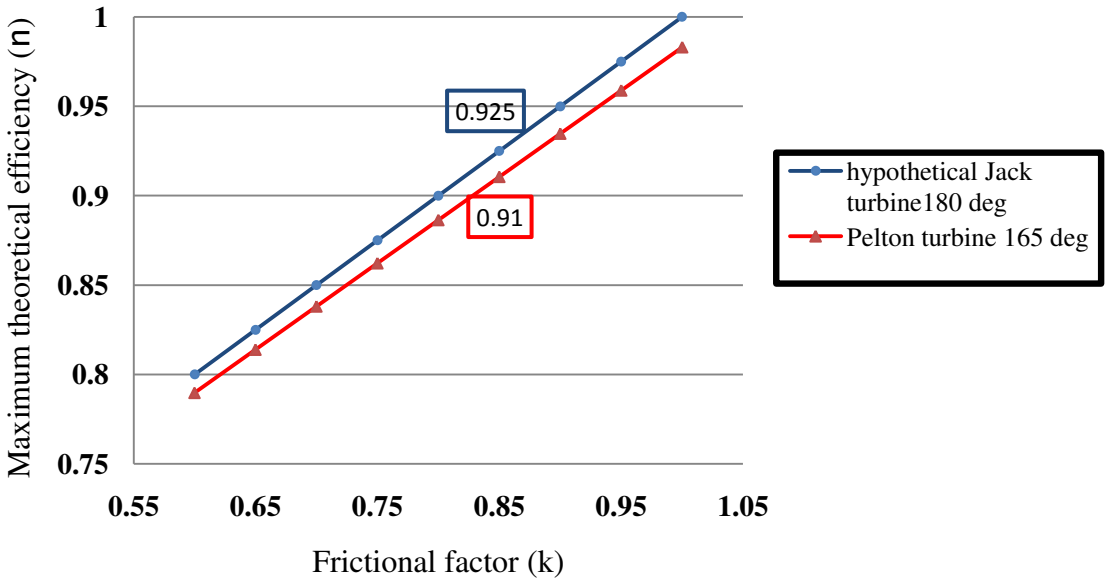

Figure 3.16. **Maximum theoretical efficiency (η) vs variable frictional factor (k).** A hypothetical Jack turbine can turn the incoming water 180 degrees and eject the water at the same radius as the incoming water jet. The Pelton turbine does the same as the Jack turbine, except it turns the incoming water jet 165 degrees instead. Both blade scenarios have used equation 3.34 with varying frictional factor k.

The efficiency at any given time can similarly be found:

$$\eta = \frac{E_{mec}}{E_{in}} = \frac{\cancel{\rho Q}[(u_{tan}v_{in} - u^2{}_{tan})(1-kcos\theta)]}{\cancel{\rho g h Q}} \tag{3.35}$$

We will assume a perfectly working nozzle with a flow co-efficient of 1 (usually approx 0.97). Substituting equation 3.11 into the denominator of equation 3.35 we find the following equation:

$$\eta = \frac{[(u_{tan}v_{in} - u^2{}_{tan})(1-kcos\theta)]}{\frac{1}{2}v^2} \tag{3.36}$$

The next graph shows the efficiency of The Pelton turbine when subjected to:

- Constant velocity from the incoming water jet.
- Starts at a zero load situation on the turbines axial and gradually increases it until the turbine reaches a maximum angular velocity.
- Ignore energy losses caused by the flow from one blade to the next.
- Assume a very thin water jet.
- Assume that The Jack Turbine can behave exactly the same as The Pelton Turbine except that it can turn its water jet 180 deg instead of 165 degrees. Thus like The Pelton turbine, The Jack turbine has the same radius when water enters and exits the blade and we can use equation 3.36 for both turbines.
- Wait for the turbine to stabilize at its chosen load.
- Water jets diameter remains relatively constant

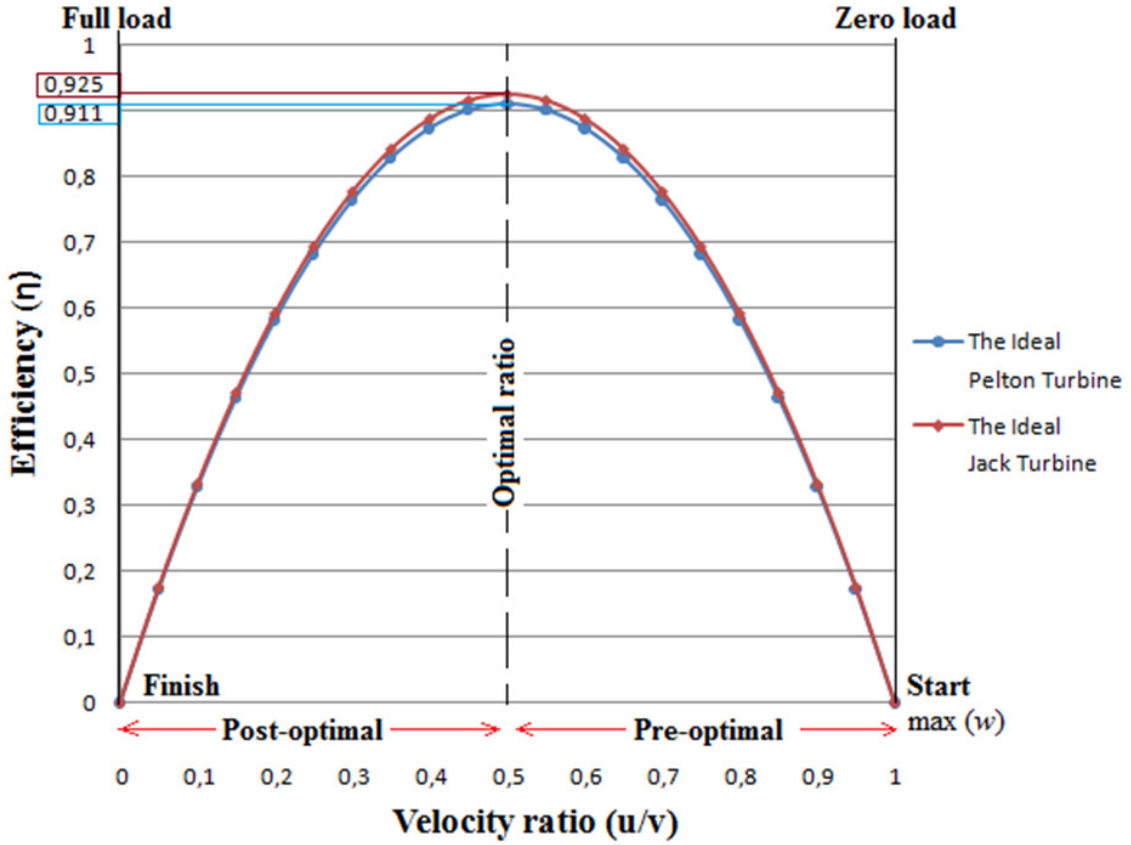

Figure 3.17. **Efficiency vs Velocity ratio (u/v).** The turbine starts at a zero load scenario on the right bottom corner. Here the turbine reaches its maximum angular velocity. During pre-optimal conditions the turbine rotates too quickly for water to exit the blades properly. During optimal conditions water exiting the blade is at the same velocity as the tangential velocity of the blade. The waters absolute velocity is zero and water looses all of its energy. During post-optimal conditions the turbine is rotating too slowly. The water jet is deposits no more than half its energy. Although here the exiting water flow has a positive absolute velocity. Energy is wasted because the turbine is rotating too slowly.

Experiments have shown that the reality of the curve above is that The Pelton Turbine reaches its optimal ratio at about 0.47, [1]. How The Jack turbine behaves is yet to be discovered. We know that its characteristic curve will not look like the one above in red, although similar.

Pre-optimal:

Due to the blades design (irrespective of the water velocity), the blade will slow the water down to no more than half the inlet water velocity (v_{in}) depending on its turning angle. Such that:

$$v_{out} < \frac{1}{2} v_{in}$$

This means that before optimal conditions, the tangential velocity (v_{out}) of the water leaving the turbines blades will be less than the tangential velocity ($u_{tan\ out}$) of the blade at the radius of water exit.

$$v_{out} < u_{tan}$$

Optimal conditions:

During optimal conditions the water flows velocity (v_{out}) leaving the turbines blades will be the same as the tangential velocity (u_{tan}) of the blade, at the radius at which water exits the blade.

$$v_{out} = u_{tan}$$

The blade will be working to its full potential and slowing the water down as best as its blade design can. The ideal Jack Turbine (100% efficiency) would turn the water 180 degrees and have a frictional factor (k) of 1. Here the Ideal Jack turbine would slow the incoming water jet to exactly half its exiting velocity. The Pelton turbine can never accomplish this even ideally because its blade design has to turn its water jet no more than 165 degrees. Both turbines will have some surface friction and thus during optimal conditions the following is true:

$$v_{out} \approx \frac{1}{2} v_{in}$$

Thus: $|v_{out}| \approx |0|$ (for hyperthetical Jack Turbine)

Post-optimal:

During post-optimal conditions the turbine is slowing down from optimal conditions (max efficiency) to a standstill. Here, even at a standstill the water entering the blade is behaving the same as during optimal conditions.

$$v_{out} \approx \frac{1}{2} v_{in}$$

The difference here is that there is so too much load on the axial. The turbine cannot rotate any faster and thus the water exiting the blade will always travel faster than the Tangential velocity (u) of the blade at the point of water exit. Such that:

$$v_{out} > u_{tan}$$

3.5. Discussing Euler's equation

There are several enormous discrepancy`s when using Euler`s equation.

- The first assumption Euler`s equation makes is that it refers the water jet as a line trajectory. A line trajectory of a water jet does not exist and the reality of a real water jet (has a cross sectional area) is far more complicated. Since Euler`s equation utilizes an infinitely thin water jet it is true to say that if this water jet were to turn 180 degrees it would deposit all of its energy onto a optimally operating blade. The reality is that no water jet in existence can turn 180 degrees and deposit exactly half its energy on a stationary blade or all its energy for that matter on an optimally operating blade. Thus if there is anything we can learn from Euliers equation is that deflecting the water jet from 165 degrees (used on the Pelton turbine) to 180 degrees will improve the probability of a better blade design. This absolutely does not ensure a better blade at all.

- Eulers equation is only relevant for a **single blade scenario.** Euler`s equation assumes that the water behaves continuously from one blade to the next, which is ridiculous. If a turbine had a pitch of 360 degrees (in other words it had one blade) then the water jet would be missing the turbine most of the time and would be useless. Thus Euler`s equation does not take the pitch of the turbine into consideration which is a decisive factor when designing a water turbine.

- Euler`s equations only takes into account directional losses and frictional losses. This is far from the truth. Losses due to flow phenomena such as turbulence also occur. Perhaps this frictional loss factor should be known only as a loss factor.

- Eulers equation only takes the incoming and outgoing directions of the water jet into consideration on a single 2-dimentional plane. The water jets entire path is not taken into consideration. Fortunately for the Pelton turbine, its water path is largely moving in a 2-D fashion and therefore Eulers equation is applicable.

I personally think the use of Euler`s equation is old fashioned and out dated. It cannot make any real conclusions about a real operating turbine. Its theory helps understand a great deal about optimal operating conditions and thus this is still very applicable when testing is done. An example of this is if we see that water is stopping and falling from the water turbines blades then we know the turbine is operating optimally. This is very important.

4. Ansys Workbench (CFX)

I will not be endeavouring into the mechanics of how The Finite element Method operates (see limitations section 1.6). Although I will need to understand some basics regarding how I intend using workbench and some of the choices it presents when simulating.

4.1. Simulations

The term "simulation" is used very broadly here. It refers to a five stage process.

Stage 1

The first stage refers to the creating or importing of the body to be analysed. During this stage I will be importing a geometry that was created on the program Solid Works Educational edition.

Stage 2

Stage two involves the actual meshing of the geometry. Here it is important to use a very fine mesh to create accurate results, although this does mean waiting longer. I will be using a automatic CFX-mesh which utilizes an octagonal element shape. This ensures calculations from one element to the next are smooth. All meshes will have over 250 000 elements.

Stage 3

Stage three is the real core of our simulations. It is here I can decide all of the preliminary criteria for the simulation. These can include everything from the type of flow, its behaviour to how it generally interacts with its surroundings. This stage of simulating is known as the setup on workbench CFX-Pre.

Stage 4

Stage four is the solving of stage three. Most of the work here is done by the computer here although one can choose a variety of settings as well. I usually choose the automated settings but adjust the number of loops to between 100 and 200. The number of loops refers to the number of increments the program calculates. If one chooses too few loops then the flow of interests may not reach its exit area. It is therefore better to have more loops than needed so that the calculations can reach some sort of stability so to speak. This stage can be adjusted in the CFX-solver manager window.

Stage 5

Stage five refers to the viewing of results. Here one can do this visually and through various graphs and illustrations. This stage is dealt with in CFD-Post and is where I will present most of the images for simulations in this thesis.

The real tricky area in the simulation process is the type of setup used.

4.2. Free Surface Flows (F.S.F) and Single Flow (S.F) setups.

Impulse turbines absorb energy from a Free Surface Flow (F.S.F). To know which simulation type is appropriate I need to fully understand what conditions our water turbine is subjected to in reality.

- Firstly I know that water is injected into a room filled with air. Thus I know that I will need to use a multi-flow simulation (F.S.F) of some sort. Here one fluid behaves as the activator or initiator; the water jet and one as inactive. The air around the water jet.

- The Free jet must have surface tension. This is caused by coulomb forces between the molecules which creates a type of cohesion between the water molecules. This also makes a free flow behave harmoniously as one. Here in Ansys I shall choose homogeneous flow which automatically induces surface tension.

- The flow experiences gravity. In Ansys Workbench one does this by choosing buoyancy and stipulating the gravitational direction as well as the density of the lightest substance.

- Surface tension between the two fluids will be set at 0.072 N/m^2 for water and air at 300 Kelvin.

Free Surface Flows (F.S.F) are extremely demanding to simulate and solve. Most conventional computers struggle to solve such simulations although improvements in both computer hardware as well as the simulation programs have made things easier over the years.

This all brings forth its limitations of what can be solved and what cannot. A real issue is the question of time.

Here underneath lies an example of the processes involved when simulating a F.S.F and a Single Flow (S.F) for a water jet, in a room filled with air at 300K. Gravity is in the negative y direction (predominantly down). The boxed room has dimensions of 3x3x3 meters.

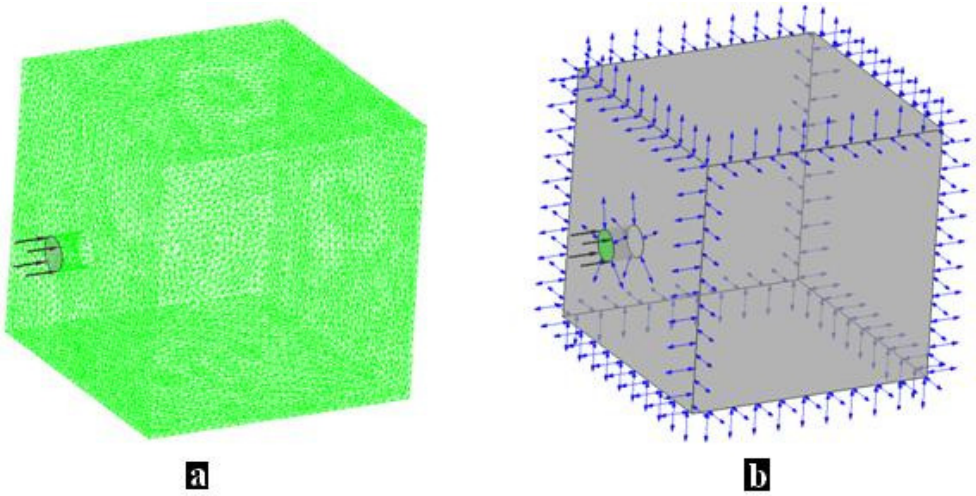

Figure 4.1. **a.)** The meshed box room with a protruding pipe on its left side. The mesh I used was a automatic CFX mesh which had about 350 000 elements. **b.)** Here we see the setup for our simulation. Inlet is shown in green whilst the rest of the surface area is subjected to atmospheric pressure (110230N/m^2).

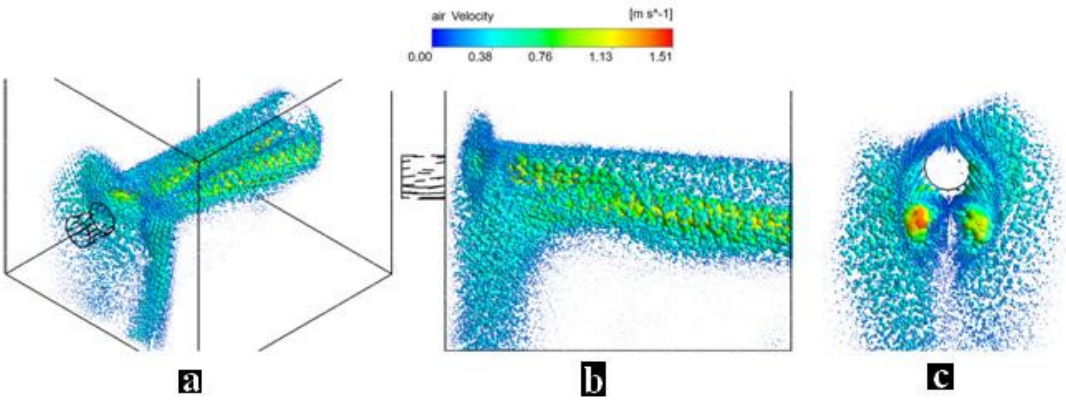

Figure 4.2. **a.)** An isometric view of the air around our water jet in a F.S.F. Air particles have been represented using spheres. **b.)** A right side view of the moving air around the water jet. **c.)** A front view of the moving air around the water jet. Notice a hole in the centre where water is moving.

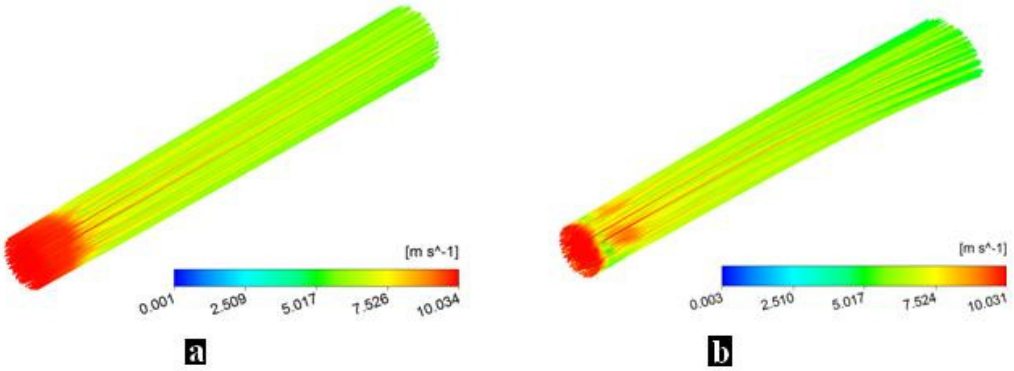

Figure 4.3. **a.)** This is a single flow using the same mesh as the F.S.F. Thus no air is present and thus the water is essentially cutting through a room filled with water. **b.)** A Free Surface Flow (F.S.F) of a water jet in a room filled with air at atmospheric pressure.

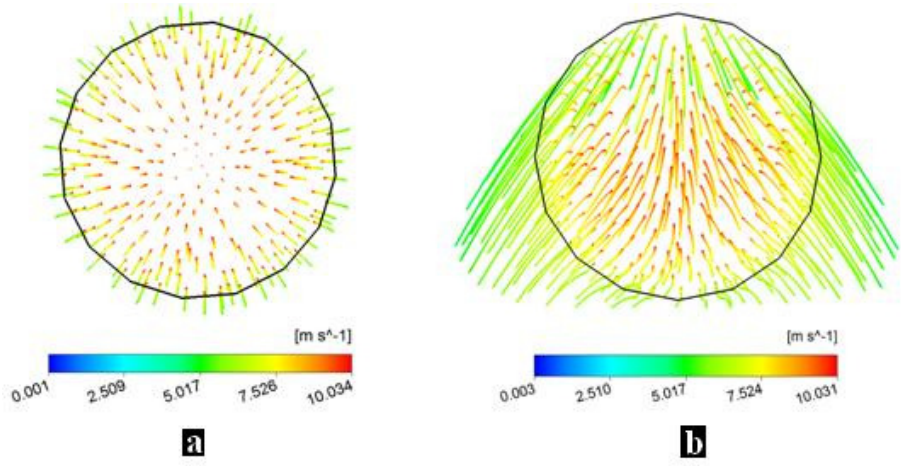

Figure 4.4. **a.)** Front view of a single flow (S.F) simulation. Water flows fastest in the centre and least on the circumference. **b.)** Front view of a Free Surface Flow (F.S.F). Gravity plays a role here by slowly morphing the water jet as time passes.

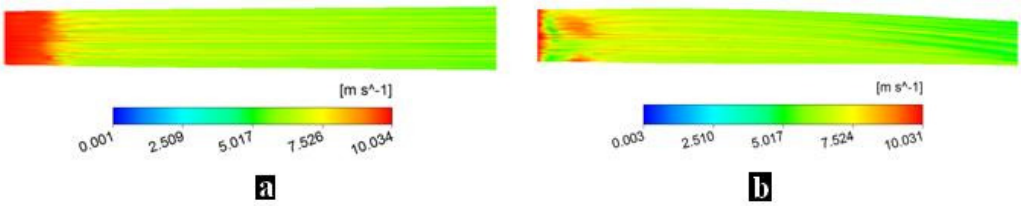

Figure 4.4. **a.)** A right side view of the S.F, notice it is perfectly straight. No gravity is included. **b.)** Gravity changes the water jets form, it starts to flatten and dip.

4.3. Simulation remarks

- There is very little difference between simulations of F.S.F and S.F flows over short distances and short time periods. The main noticeable difference is gravity. Gravity has no effect on a single fluid-flow because the flow has no buoyancy properties. Gravity affects free surface flows (water in air) in exactly the same way a stone would be affected, if thrown parallel to the surface of the earth.

- Free surface flows are more accurate but require much more time to solve than single flow simulations. This is because there are far more factors that have to be taken into consideration when simulating. This further increases the amount of data to be solved and therefore the amount of time to solve them as well.

- A typical mesh of 500 000 elements can take roughly 30 min to solve on the automatic settings and this is acceptable in my eyes. Therefore I will be using free-surface setups for all my simulation needs where possible. This will ensure a better design process and overall blade outcome. Concluding designs will be confirmed with accurate free surface simulations.

5. Physical boundary conditions

5.1. The housing of the Pelton turbine test rig

The Pelton turbines test rig at UMB has 16 blades that can be extracted and replaced. I could therefore install a different blade design in this test rig. This is possible if I adhere to some physical boundary conditions. If we look at figure 5.1 a below we see The Pelton Turbine Test Rig with 16 blades installed. In figure 5.1 b we can see a replica of the test rig drawn in SolidWorks.

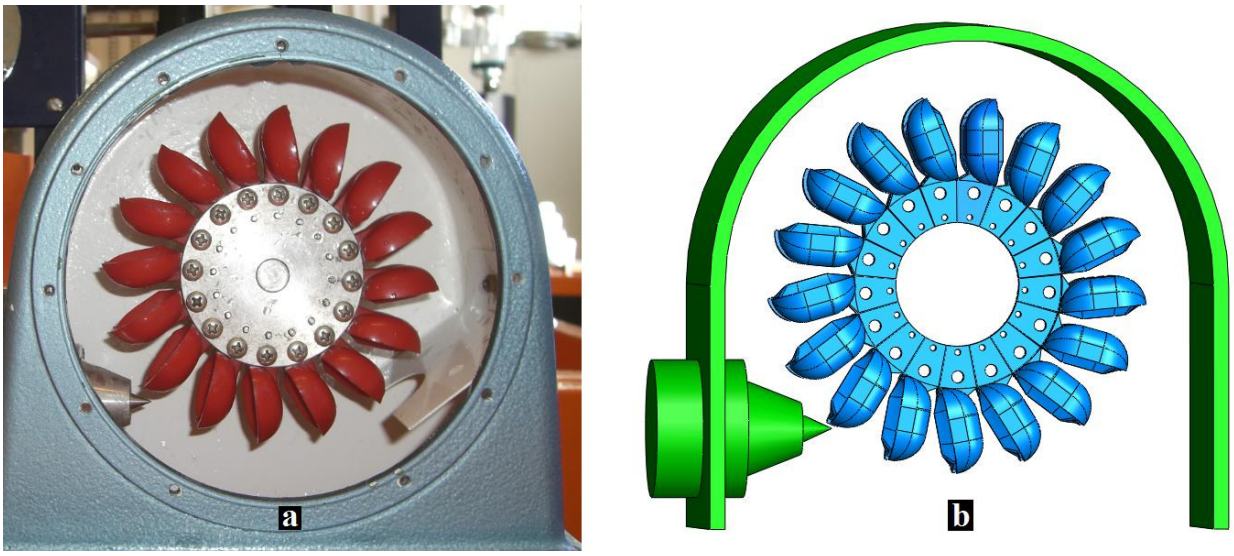

Figure 5.1. **a.)** The test rigs housing with The Pelton Turbine blades. **b.)** Visualization of The Test Rig without holding disks, screws, pins or the housings front and back walls. Green colour represents the outer physical boundaries inside the housing and the blue represents The Pelton turbine blades.

Measurements of The Test Rigs interior were done by hand with a Veneer Calliper. Any deviations in the readings were minimized by checking and re-checking. This is important because an error here can have severe consequences when a new design is later installed.

If we now look at figure 5.2, we see a front view of figure 5.1b with its important physical boundary conditions.

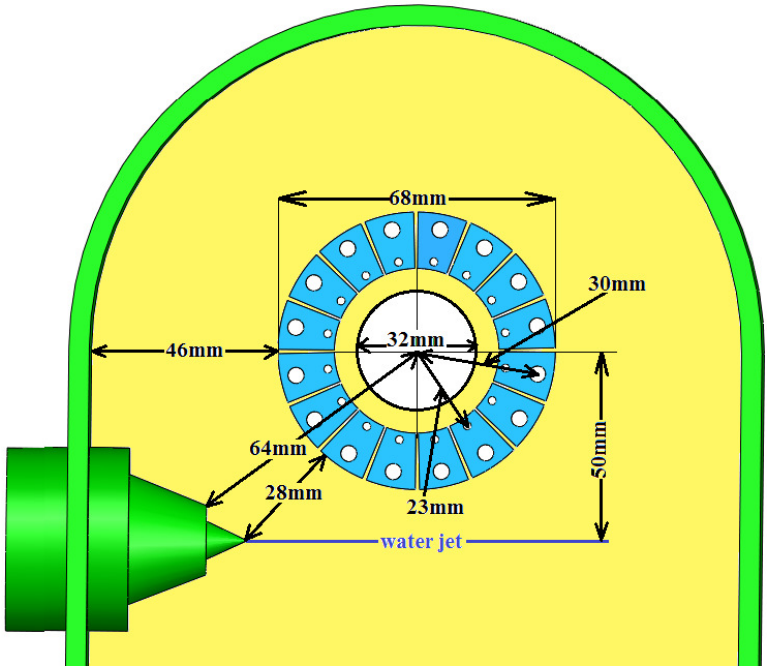

Figure 5.2. A front view of The Pelton Turbines rig setup, figure 5.2 b. Here we have outlined the important physical boundary conditions for a blade design that is to be installed. Yellow and blue represent available space. Green and white represents the permanent obstacles a blade design must be designed around.

Areas in yellow or blue represents available space. Green represents the side walls and The Water Nozzle. The white circles represent the turbines axial, screws and pins.

Notice how much The Water Nozzle is protruding in the housing space. This is a rather dramatic boundary condition on a potential blade design. If we now view figure 5.1 b from underneath we can see the available breadth dimensions shown below in figure 5.3.

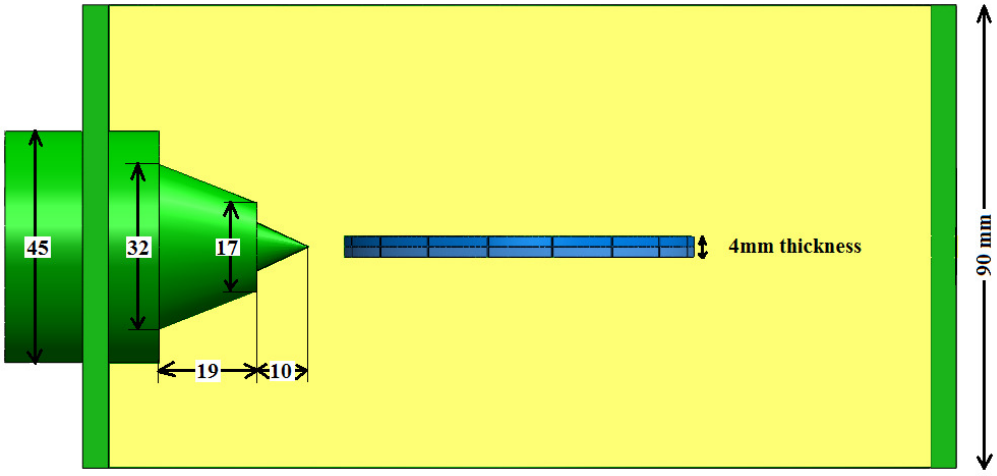

Figure 5.3. A bottom view of figure 5.1 b. The figure shows available space in yellow as well as physical boundaries in green. All units are in mm. The maximum breadth our blades can have is 90 mm. The water jet enters through the centre axis of its side walls, i.e. 45mm form each side and thus we could have a blade of 90 mm in breadth.

Again yellow represents available space whilst green represents the physical boundary conditions. The Water Nozzle and the blade sit with their centre axis 45 mm from each side.

5.2. The holder:

The holder is where the blade will be attached to the turbines axel. Here I are restricted to the following boundary conditions:

- 16 holes for the installation of 16 screws. This is the case because the metal disks that wedge the blade holders in place have 16 pre-made holes. Each hole has a diameter of 4 mm and is evenly spaced with a radius of 30 mm from the axis of rotation to the centre of the screw hole.

- 16 pins with a diameter of 2 mm with a radius of 23mm from the axis of rotation to the centre of the pin hole.

- The holder itself has a thickness of 4 mm.

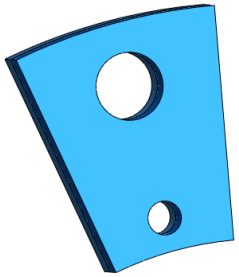

Figure 5.4. The Pelton turbines holder. I could adopt the exact same holder The Pelton Turbine uses but this is not a must. I am restricted to 16 holes and pins, the space around these holes must fit alongside one another.

5.3. Operating boundary conditions for the water jet

The general size of a designed blade is dependent on the water jets diameter. A very large water jet will also require some very large blades and vice versa.

After removing The Pelton Turbine Blades and manually measuring the water jets diameter with a Veneer Caliper. I concluded that the water jet ranged from approximately 5 mm in diameter to 6 mm depending on:

- The position from the exiting water jet. The water jet first decreases in size from the nozzle and converges to a minimal diameter and then increases in diameter as it moves further away.

- The velocity of the water jet. If the water jet is traveling over 14.85 m/s it will automatically begin to increase in its cross-sectional diameter (see cavitation, section 3.3). Although this needs far more time than is available. An example is industrial water cutters. These cutters routinely have a water jet of only 2 mm in diameter whilst converting up to 3000 bars of pressure. This creates a supersonic moving water jet, far faster than 14.87 m/s.

A blade can always tolerate a smaller water jet than it was designed for. The worst thing that can happen is that the water slows down (surface friction) far too much before it exits the blade. Not desirable but at least the water flow moved in the correct direction.

A water jet that is far larger than the blades design will effectively move over the blade in a very undesirable manner. Inadequate spreading can occur resulting in a lot of overflow and ultimately bad energy transfer from the water flow to the blades.

6. Blade design

6.1. Discussions and partial objectives

This concept involves the manipulation of an incoming water jet and propelling it out as effectively as possible. How effective a proposed blade design can become is dependent on several areas of study which must be overcome in order to create a useful blade design. What have we learnt thus far?

A. Desired operating behaviour.

Explanation

I want all of the water energy in the water jet to be deposited onto the turbine during operation. The energy in the water jet is in the form of kinetic energy and therefore in the form of movement. Thus I need to stop all movement of the departing water jet whilst the turbine is rotating. The only way this is possible is to create a water jet departing the blade in an opposite direction to the tangential velocity (u) of the blade at the point of departure, whilst moving in exact opposite directions. Thus we create the desired standstill of the water flow or a departing water jet with an **absolute velocity** of zero. If the turbine is rotating too quickly then an absolute velocity of zero occurs before the water can exit the blades creating undesirable water build up on the blades. Similarly if the turbine is rotating too slowly then water would not reach an absolute velocity of zero and exit the blade prematurely whereby energy would be wasted. The basic principal is true for all impulse blade turbines and is central to the success of a good blade design. See figure 3.17 and section 3.52.

Partial objective

How does this mean anything for our blade design? Well in order to satisfy this requirement, I will attempt to slow the incoming water to approximately half its velocity upon exiting. This should happen irrespective of the water jets incoming velocity. This will be done very roughly by looking at the direction of the exiting water jet. Unfortunately it is very difficult to see the overall flows velocity because of the continuity equation impact on F.S.F. The only time this can be used rather successfully is when I simulate a very thin water jet. Thick water jets show a range of different velocities in its cross-sectional area.

B. Catchment of the water jet.

Explanation

How effectively can a water jet be "accepted" without dramatically disrupting its flow-cohesiveness? I want to first capture the oncoming water jet (without breaking it up) as smoothly as possible and then once this is accomplished I want to exploit as much of its energy as possible.

Partial objective

I will accomplish this requirement by visually analysing that all water is captured on the blade. No abrupt surface will be encountered by the incoming water jet. Water will be directed on one blade at a time from various angles. I shall name this a **single blade setup** when performing simulations.

C. Water jet flow from one blade to the next.

Explanation

The oncoming water jet will move from one blade to the next as the water turbine rotates. This brings about a dilemma, whilst capturing water the blade design needs to provide easy access for the water jet to pass from one blade to the next. In this way water is always moving into the blades of the turbine, instead of being lost or misused. This section of the blade design is considered to be one of the most important. One can design the best blade in the world but if water cannot move effectively from one blade to the next it does not matter because most of the energy will be misused. This phase between the two blades also marks the beginning and end of the water jets travel on the blade design which makes it particularly interesting when designing.

Partial objective

This specification will also be accomplished visually. Water will be directed between two blades. Thus several blades will be necessary, and therefore this type of setup is known as a **multi-blade setup**.

D. Surface finish on the blade.

Explanation

The interface between the surface finish of the blade and the outer lining of the water jet on the blade; is where energy is transferred onto the blade. In order to do this, the water flow needs to move. Secondly it needs to move very close to the surface of the blade whilst cohesively changing in direction over the blade**.** An abrasive surface such as sand paper essentially creates a chaotic system of turbulence, vortices and misdirected flows at this interface zone. These chaotic flows transmit very little energy to the blade because they have a tendency to create apposing flows that cancel each other out.

Energy transfer occurs on a microscopic level. Water particles travelling closest to the blade wall experience the most flow resistance and therefore travel slowest. Other water particles travelling, that are not making contact with the surface of the blade wall, will essentially slide over one another and conserve more energy resulting in a faster velocity.

Partial objective

Ensure that the blades surface during simulations and testing is as smooth as possible. Simulations can adopt frictionless surfaces. I will use this because the reality is that a very smooth surface is what I will be trying to accomplish in practice. Thus I can simplify our simulations by just adopting a frictionless surface.

E. Length of flow from catchment to exit.

Explanation

Our blade requires enough length of travel over the blade to deposit its momentum. If this flow path is too short we can expect insufficient blade/ water flow contact. Flow energy would be conserved and energy that the blade could have captured would be wasted and escape the blade. If the water path is to long then surface friction in a real scenario will take its toll and water will barely leave the blade.

Partial objective

Design a blade that creates the shortest possible water path on the blade whilst abiding to the other design specifications. Ensure that the blade used is a sufficient size for the water jet. This will be done visually with Ansys Workbench (CFX).

F. Flow cohesiveness.

Explanation

I want the water flow to spread over the blade enough to deposit its energy. I also want water to stay together or behave cohesively. In this way we remove water effectively from the blade. Thus a balance is required between water spreading and flow cohesiveness.

If the designed blade is too compact, and the water jet is too large, then most of the flow will just slide over one another. Thus most of the energy will be conserved in the water flow and escape at the outlet of the blade. I want to find a balance whereby we spread the water flow enough so that it can deposit its momentum as well as manipulate its flow as much as possible so that its deposited momentum is utilized as effectively as possible.

Partial objective

During simulations avoid converging flows. Converging flows are the opposite of spreading, they tend to leave the surface as a result and conserve energy in the flow by becoming airborne. Make sure that the flow is moving together in more or less the same direction whilst retaining appropriate spreading over the blade.

G. Turn the flow 180 degrees without colliding with the next blade or water jet.

Explanation

This is the main weakness The Pelton Turbine has. It has to turn its water jet a maximum of 165 degrees to avoid collision with the back of its adjacent blade. If I can present a different blade design that can move a water jet 180 degrees instead, then I should theoretically speaking have a more effective single blade design than the Pelton turbine.

Partial objective

This requirement will be mostly fulfilled by deciding upon a blade design with the intention of moving the water flow 180 degrees. This will then be checked in a simulation. In other words, I will use, visualization of flow movement (in my imagination) to come up with a blade design. This blade design will then be checked on Ansys Workbench (CFX). Do note, visualization does not guarantee a perfect turn of 180 degrees but approximately 180 degrees.

6.2. Design procedure

1) Consider and design a blade model in Solid Works.

2) Prepare a new model that encloses the blade model for Ansys Workbench (CFX). This can be done in Solid Works although it is easier in workbench especially for Multi-blade simulations.

3) Perform simulations, then analyse results, conclude and make alterations to the design for improvements (point 1). If the model fulfils all the flow specifications as best possible then one can consider the blade design for construction.

7. Design category 1

This design category will be taken directly from the blade design used in course TMP301. I will add some symmetry changes to the original design so that it is more relevant to the housing boundary conditions. The basic flow principle is the same as those explained in figure 1.4 in section 1 entitled "Background".

7.1. Single blade scenario

By simulating a Free Surface Flow (F.S.F), I can test the flow movement over one such blade.

The basic setup for this simulation is a room filled with air at atmospheric pressure (example see figure 4.1). The room removes or depletes an object in it, as shown in figure 7.1b. This effectively retains the outline of our blade design. A hole or protrusion (on the adjacent side of figure 7.1b, not shown) can mark the diameter and position of the incoming water jet. Once this is accomplished I can mesh our object (figure 7.1 c) and create our multi-flow setup, solve and read results.

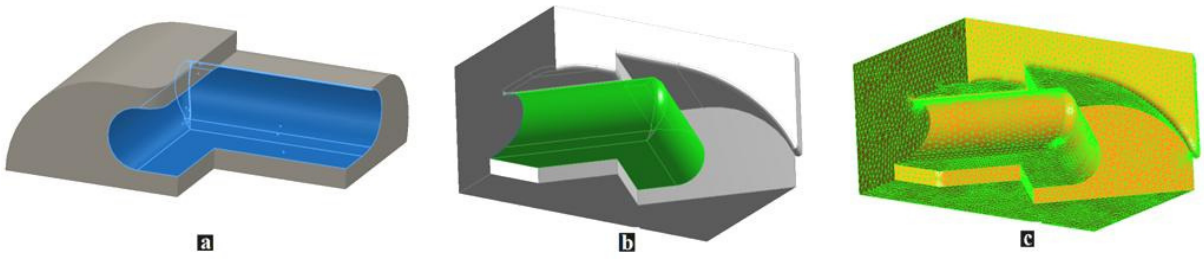

Figure 7.1. **a.)** The blade designed in Solid Works. Water/blade contact area is in blue. **b.)** A box that has enclosed the blade design. The blade in figure a, has been removed. Water/blade contact area is shown in green. **c.)** The meshed box over the blade with approximately 450 000 elements.

I shall start with a very thin water jet (3mm). Here I will try to create the behaviour of that which was visualised and shown in figure 1.4. The results for our blade design can now be read at various time intervals. The time intervals used here are about a thousandth of a second between each other.

Most incoming velocities' that were simulated resulted in the water jet stopping before it could escape the blade. This is a clear indication of what to expect if I were to bombard the blade with a very thin water jet.

The only way I could visualize the entire path of the water jet over the blade was to either increase the velocity or increase the diameter of the water jet. I preserved the diameter and increased the water jets velocity to 300m/s. This is a highly unlikely scenario. Underneath shows a purely Newtonian reaction from the water jet as shown in figure 7.2 below:

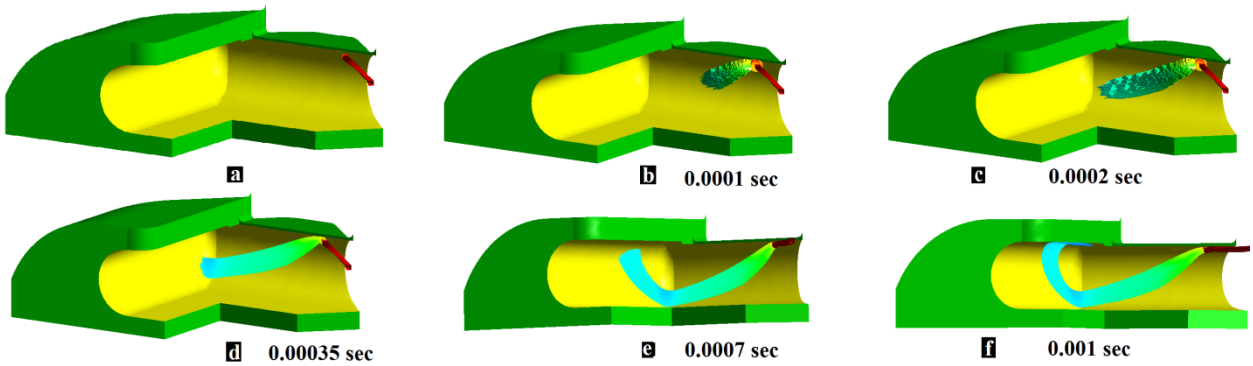

Figure 7.2. **a.)** Shows the blades face in yellow, the water jet will travel from the red hole. **b.)** At a tenth of a millisecond the water begins to move as predicted. Using 3-D arrow heads to mark the flow direction. **c.)** The water velocity has slowed down considerably, nearly halved in velocity. **d.)** Water has just passed the half way mark and I have changed to a streamline function instead of arrow-heads. **e.)** The water flow begins to move up the adjacent slope. **f.)** The water jet comes to a complete stop at the top of the adjacent blade.

Another way of visualizing how the water moved is to just view the last image of figure 7.2 f and then look at it from various angles.

Thus figure **7.2 a** can be viewed as figure 7.3 below:

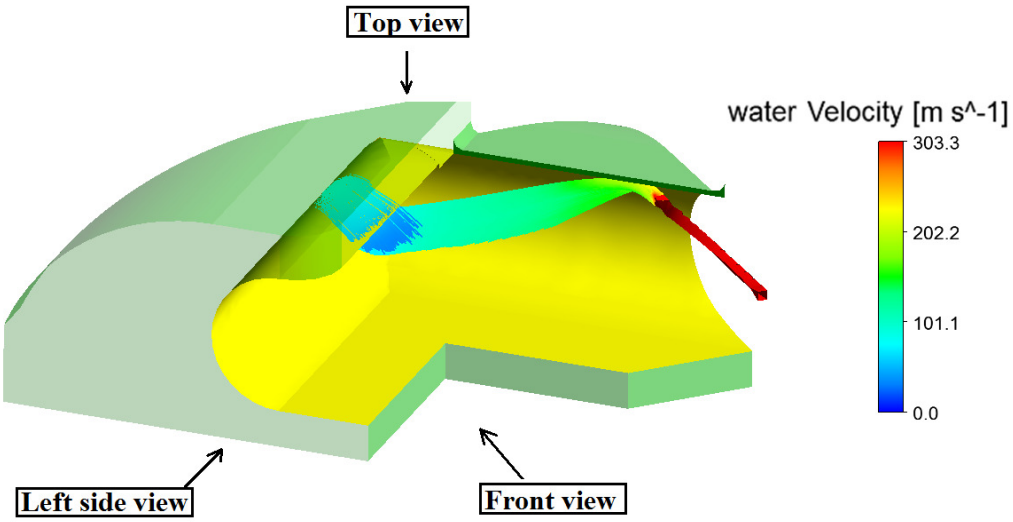

Figure 7.3. Shows an isometric view of the one blade setup. Three views are outlined. The incoming water jet has a maximum velocity of 303 m/s shown in red and diminishes in velocity until it exits, here it is barely moving. An outline of the velocities can be approximated with the colour/velocity index bar to the right of the figure.

The isometric figure above can be viewed from the three outlined views. I will remove the blade surface for a better view of the water flow.

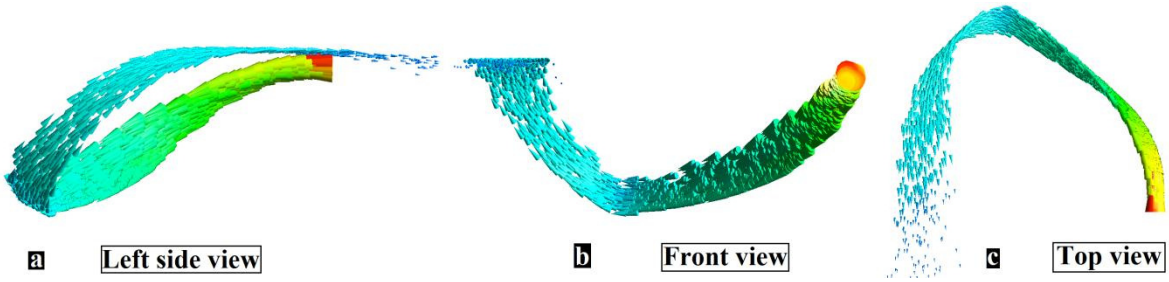

Figure 7.4. **a.)** The left side view shows the height at the beginning and end of the water jet. They are the same as expected. **b.)** The front view reveals the water jets height as well as the fact that water is entering and exiting at different positions. This avoids any collisions with itself. **c.)** The top view of the water jet can show some of the spreading behaviour upon water exit.

The simulation revealed that the blade design did indeed create the intended flow direction. I did not expect the water flow to just stop upon exiting. What happens if I increase the incoming water jets diameter? This duplicates a more realistic approach to the exceptionally thin water jet that was previously analysed? Below is the same simulation except with a water jet diameter of 6mm instead of 3 mm.

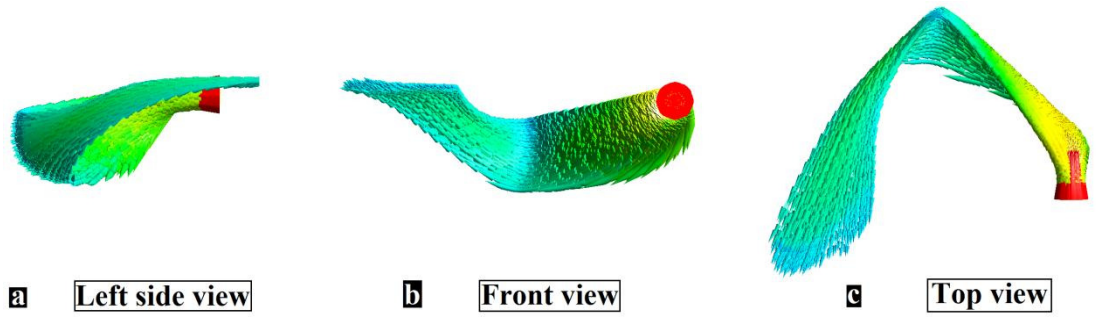

Figure 7.5. **a.)** We notice that the exit height is still the same. The base of the flow has a lot more spread behaviour. **b.)** Water exits at correct height, spread behaviour is evident. **c.)** The exiting water is vending to the left. This should be down the page as shown in figure 7.4 c. Regardless the water velocity has still declined too much. It is exiting at approximately a quarter of the incoming velocity.

Why did the water jet stop moving or decrease so much?

The answer to this lies in an inherent weakness when using Eulers equation. It is only useful for calculations on one plane. If we look at figure 7.4c again we see a water flow turning 180 degrees on the top plain. This is the only plain Eulers equation takes into consideration.

The fact of the matter is the water flow moves 180 degrees in another plane as well. This plain is the front plain. The movement in this plain is 180 degrees too but it is of no importance according to Eulers equation. The method used by Eulers Equation works on The Pelton Turbine because flow over its blade, for a thin water jet moves on one plane.

This is not the case in this blade design. The **effective** turn in the water jet is therefore 360 degrees. This turn occurs across two different planes. As it is shown in figure 3.7, a thin water jet travelling 360 degrees **effectively** will stop dead in its tracks as all its kinetic energy is depleted.

7.2. Multi-blade scenario

In a multi-fluid scenario we are faced with a predicament. The blade design must retain its general geometry in order to create the intended water flow. This is especially important where the water jet

first touches the blade, as it is shown in figure 7.2 b. Water must pass easily from one blade to the next with no obstructions.

If I now create a cross-sectional cut through the centre of the stationary water jet (diameter of 9 mm) and the rotating turbine we see the following:

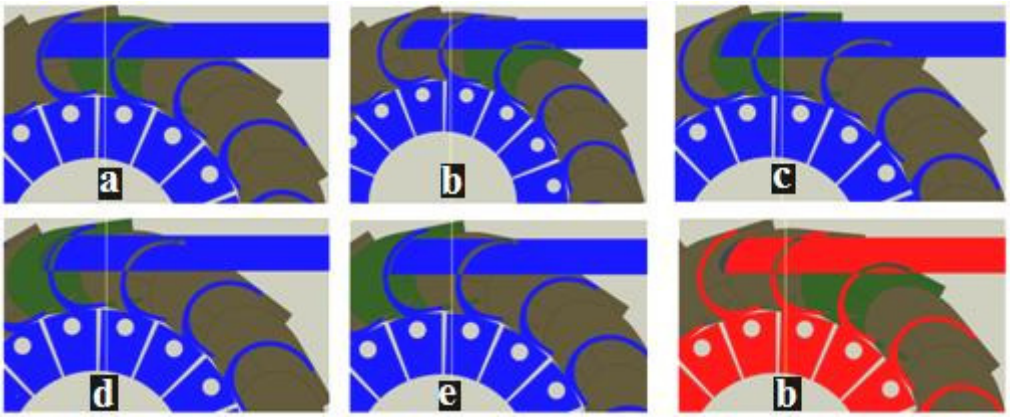

Figure 7.6. A cross-sectional cut (in blue) of the turbine with the suggested blades. The turbine is rotating in an anti-clockwise fashion whilst the water jet remains stationary. **a.)** The blade of interest starts here and lies directly below the water jet in blue. **b.)** The turbine rotates just enough to reveal that our blade of interest has an overlap with the water jet. This means the back of the blade is subjected to the water jet. This is definitely not desirable (shown in red). **c.)** Turbine rotates more and reveals acceptable blade water contact. **d.)** Acceptable water blade contact. **e.)** Acceptable water blade contact.

We can now capture several frames that record the start and end of a single blades encounter with the water jet. The turbine is rotating anti-clockwise and the blade in question sits directly under the water jet in frame **a**. As the turbine rotates I notice that there is an overlap of the blade with the water jet in frame **b**. In frames **c**, **d** and **e** there is no a problems. The behavior revealed in frame **b** is definitely unacceptable (shown in red).

I will not pay any more attention to finding solutions to this problem and its multi-blade design. The blade has failed the single blade setup and therefore there is no point in trying to find any solutions for the multi-blade setup.

Design conclusion for design category 1

- **Single blade setup:** A specification for the single blade setup was that water will exit at approximately half its incoming velocity. Simulations show that water flow comes to a near stop. Thus design category one **fails.**

- **Multi-blade setup:** A specification for the multi-blade setup was that water could easily pass from one blade to the next whilst retaining single blade objectives. Solid Works images reveal that this is not possible. The design category cannot create easy flow from one blade to the next and retain single blade flow objectives. Thus design category one **fails.**

8. Design category 2

8.1. Description of design category 2

A new design has been visualized mentally.

The concept was inspired by Norwegian Snow shovels. Snow shovels scratch the snow from the base of the road and lift it up sideways and off the road. I will be attempting something similar except I will lift the water (water is the moving fluid and not the snow shovel now) up, sideways and back in the direction (although different position) it came from. This time I have taken into consideration all possible turns in the water flow such that the **effective** turn in the water jet is a little over 180 degrees. This should only slow the water jet to approximately half its incoming velocity as desired for optimal operational conditions.

The basic concept to our new blade design is explained in more detail below in figure 8.1. The water enters the base of the blade shown in yellow. It is first split in two and then scooped up and deflected slightly. It is then flipped by two spoon-like geometries, shown in blue. Finally the area in green will correct the slight deflection created by the "scooper" in yellow and eject it at the correct height.

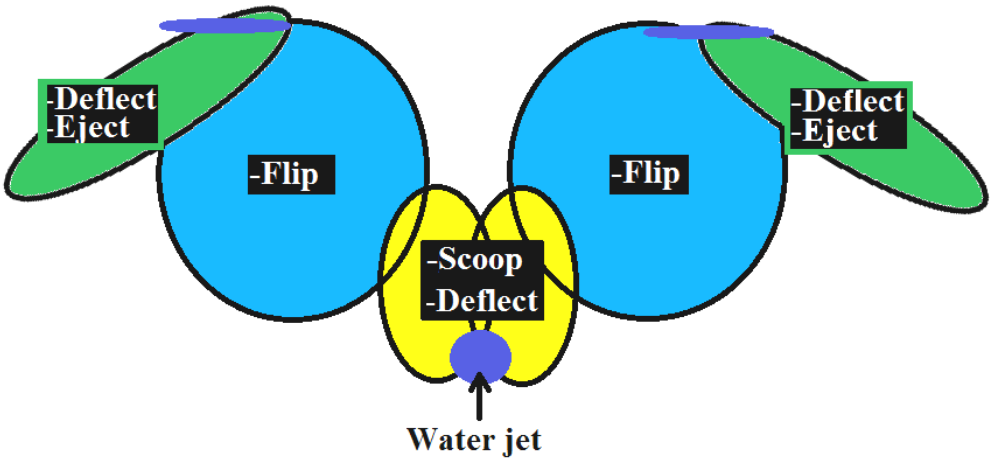

Figure 8.1. A front view of a potential blade with only its objectives of what each part of the blade should do to the water flow. The idea is to introduce symmetry to split the water jet in two. At the bottom of the figure we see the incoming water jet in dark blue. **Yellow region**. The water jet will be split in two and deflected only slightly to its respective sides. At the same time it will be scooped slightly upwards. **Blue region.** This region will only flip the water. It can have a semi-spherical or spoon like geometry. **Green Region.** This region will correct the slight deflection of that which was created in the yellow region as well as ensure the water jet leaves the blade correctly. The exiting water is shown as two dark blue ellipses that move directly out of the page.

This ejection of water at the top of the blade will take advantage of the blades circumference and avoid a collision with its adjacent blade. In addition ejecting water here provides the additional bonus of creating more torque from the same water jet. This is the case because of a larger radius from the area of water ejection to the centre of turbines axis of rotation.

In short a single blade setup (as the one described in figure 8.1.) has a similar blade design to our category 1 design. The difference is that now we are directing the water jet from the base of the blade instead of from the top. Thus for a single blade setup we would be using something like figure 8.2.

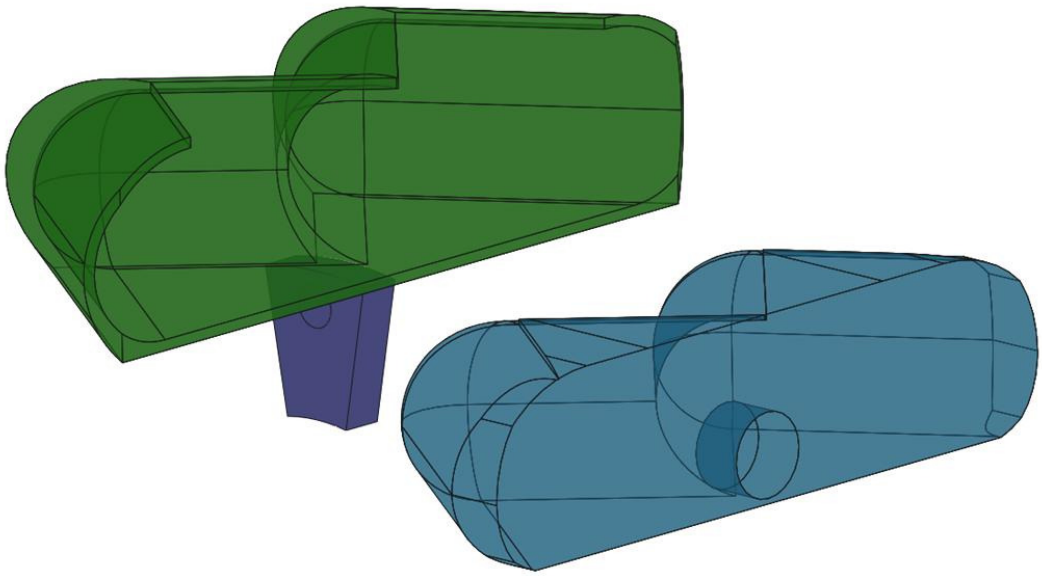

Figure 8.2. A symmetrical version of a Category 1 blade, in green. The so called box, for simulations in Ansys Workbench (CFX) is shown in light blue. Notice that the water jet hole is now at the base of the blade.

I can adopt a setup that is similar to a Pelton turbine setup for the water flow from one blade to the next (the centre of the blade). I can design the blade such that the base of the blade hides behind the one in front, a bit like scales on a fish. I can examine this later through various simulations of a multi-flow setup (chapter 9).

8.2. Building and naming sections.

Let us name and locate each section of this blade design. In this way I can identify changes made as I manipulate our design.

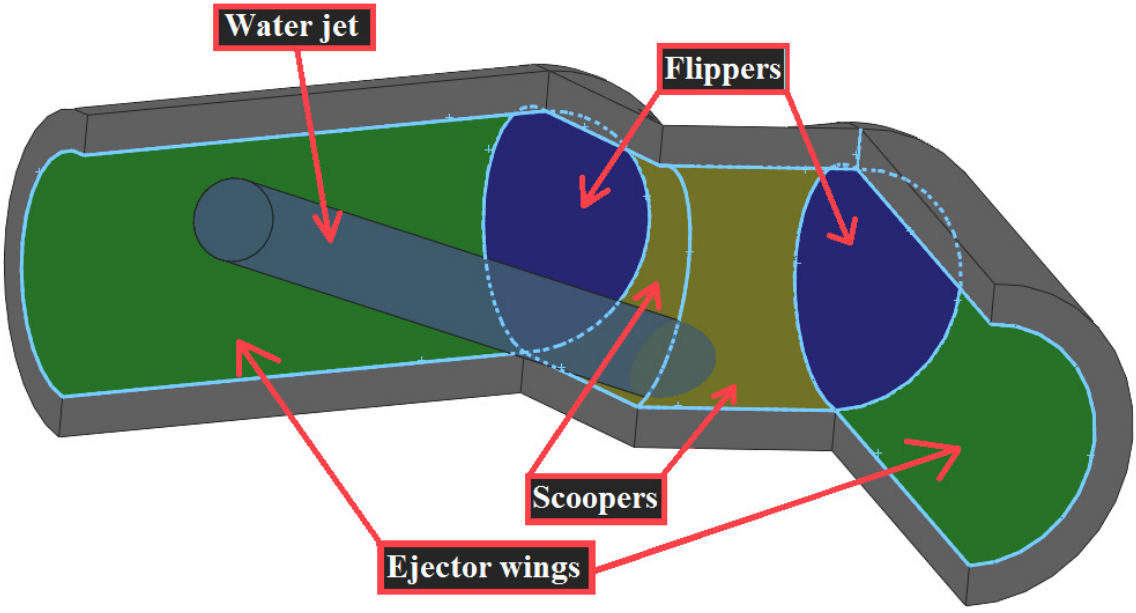

Figure 8.3. An isometric view of our intended blade design. The "**ejector wings**" will eject water and correct deflection, shown in green. The "**flippers**" will flip or invert the water flow, shown in dark blue. The "**scoopers**" will deflect or scoop up water, shown in yellow. The entire blade will be symmetrical such that the **water jet** moves through the middle as shown.

The "Ejector wings"

Ejector wings will rectify water deflection and eject water. The length (**L1**) can be changed as it is shown in figure 8.4 a.

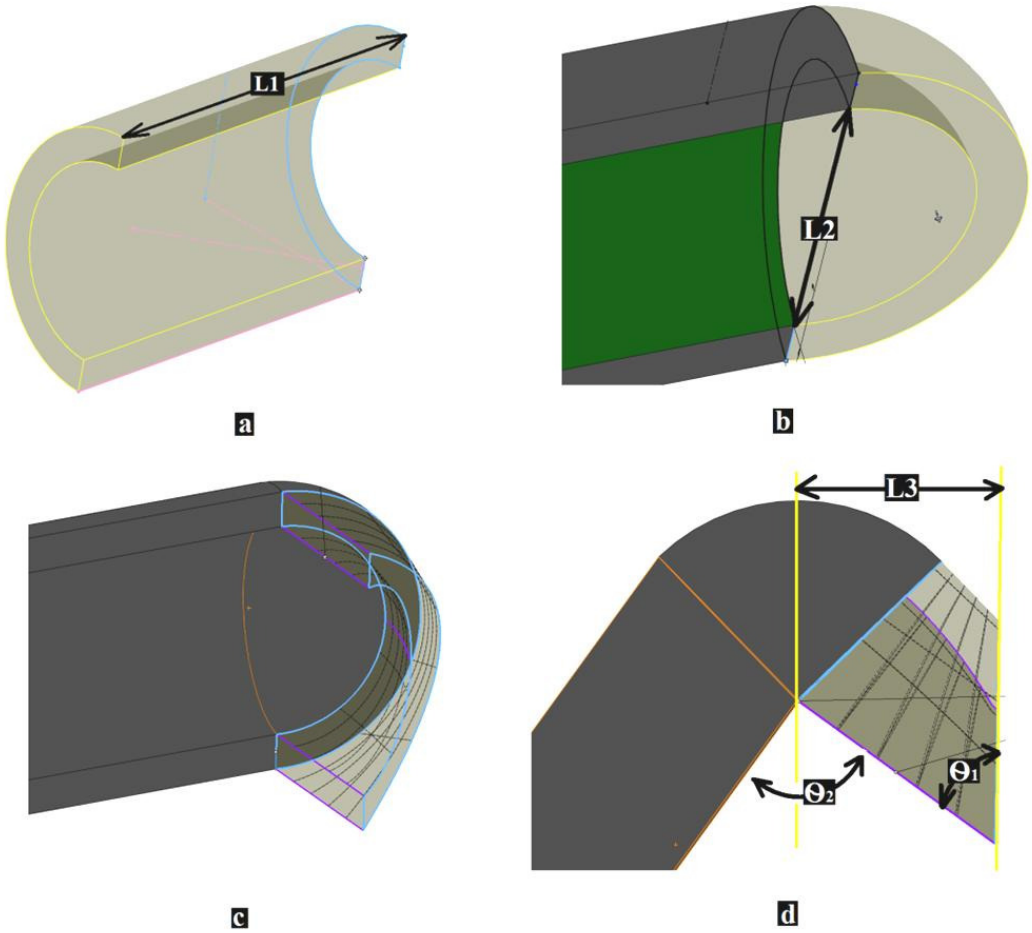

Figure 8.4. **a.)** Shows the extrusion of "The ejector wing". The length (L1) can be altered. **b.)** A rotation boss creates "The flippers". Here, the height (L2) can be chosen. **c.)** A lofted bend to create "The scoopers". **d.)** A top view of our blade. Here I can identify length (L3) between the centre plane of "the flipper" and the symmetrical plane, both are in yellow. The angle θ_1 and θ_2 are important variables when designing; these are usually around 90 and 45 deg respectively.

The "Flippers"

The flippers only have one function. That is to flip or invert the water flow. The geometry of its face (as shown in figure **8.4 b**) is essentially a quarter of a cylindrical sphere. This part can be thought as a type of spoon.

The "Scooper"

There are three main functions for the scoopers:

- Scoop up or lift the water flow slightly
- Deflect the water flow slightly
- Split the water jet into two.

Half of "The Scooper" is shown in figure **8.4 c** and **d** in transparent colour.

Positioning of blade with water jet

In order for this design to adhere to our boundary conditions we are going to have to lift the entire blade from its holder section. The distance of this, will be known as "the gap" and can be seen in figure 8.5 a. We also have our attack angle and the diameter of the water jet, shown in figure 8.5 b.

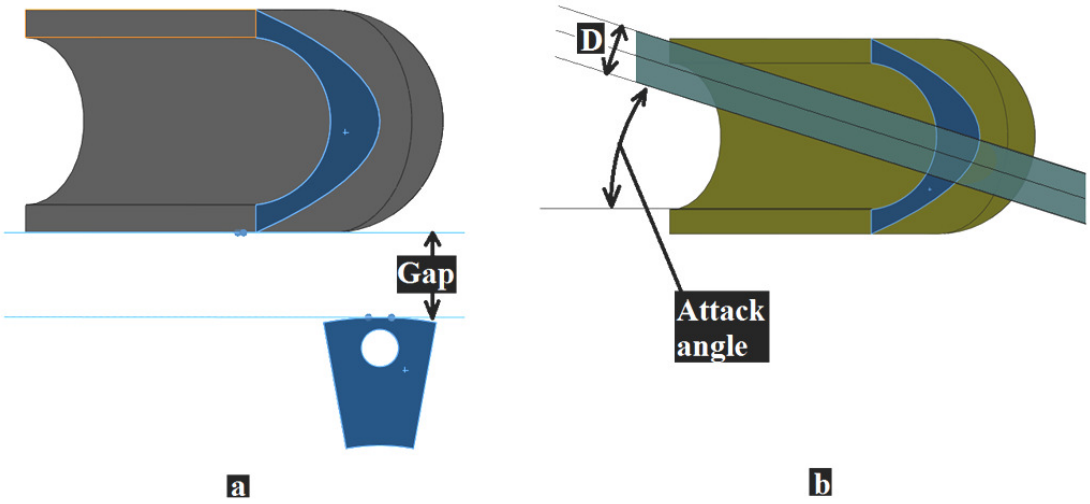

Figure 8.5. **a.)** Shows how the blade must be lifted, the distance the blade will be lifted is known as "the gap". **b.)** Shows where the attack angle is and the diameter of the water jet.

9. Single blade simulations of design category 2

Our single blade needs to deflect the water jet described in figure 8.1. The single blade setup needs to function correctly at different angles of attack. I shall first try a blade design that works with an angle of attack of zero, and later once this is accomplished I can increase it.

Every simulation will start with a small table that explains geometrical characteristics outlined in section 8. The table will also stipulate whether the simulation utilised a Free Surface Flow (F.S.F) or a Single Fluid (S.F) setup. The result for each simulation is then presented on the far right of each table.
Two main objectives are evaluated. The first being whether the flow behaviour is correct or not. The other checks whether 16 blades can fit together without colliding on one another as well as meeting the boundary conditions created by the turbines housing (chapter 5). The colour red describes a fail in the column and green a pass.

All simulations and there dimensions are recorded and logged in a table found in appendix I.
I shall not present and discuss every single simulation. Every change in design number represents a change made in the blades geometry (done on Solid Works). Simulations can sometimes use the same imported geometry although this is uncommon.

9.1. Simulation number 4

I shall start with blade design number 4. The designs characteristics are outlined in table 6.1 below.

Table 9.1. Phi angles ($Ø_1$) is being tested at 15 deg, whilst a phi angle ($Ø_2$) is being held at 80deg.

Sim num	Design num	L1 (mm)	L2 (mm)	L3 (mm)	Ø1 (deg)	Ø2 (deg)	Attack angle	Jet D (mm)	Sim type	Gap (mm)	Flow Results	Blade collision
4	**4**	20	15	16	15	80	0	8	F.S.F	7	Fail	Clash

As we can see in table 9.1 above, there is a dramatic choice of phi angles $Ø_1$ and $Ø_2$. The following happens:

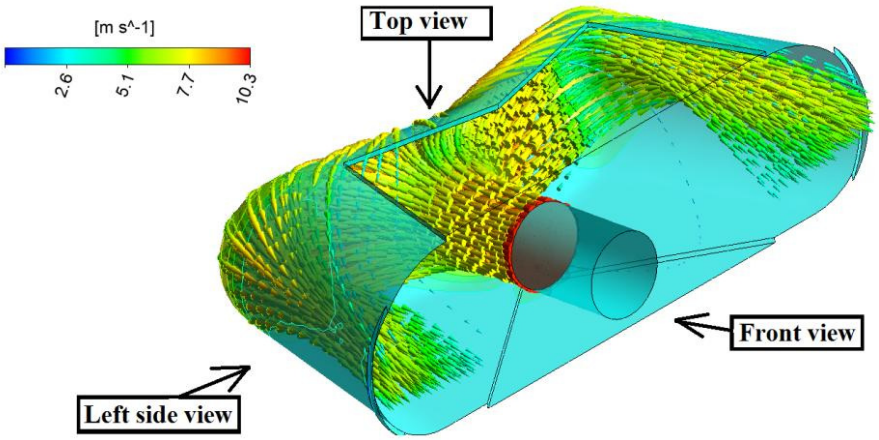

Figure 9.1. The flow is not gathering at the top of the blade on exit. The flow looses contact with the blade too early; it also gathers according to the continuity equation and retains or increases in velocity. The water flow is spreading too much. Three viewing angles are shown and a velocity index at the top left corner is shown.

Looking at figure 9.1 above we see a flow behaviour of nearly everything we don`t want. Let us now look at the viewing angles of figure 9.1.

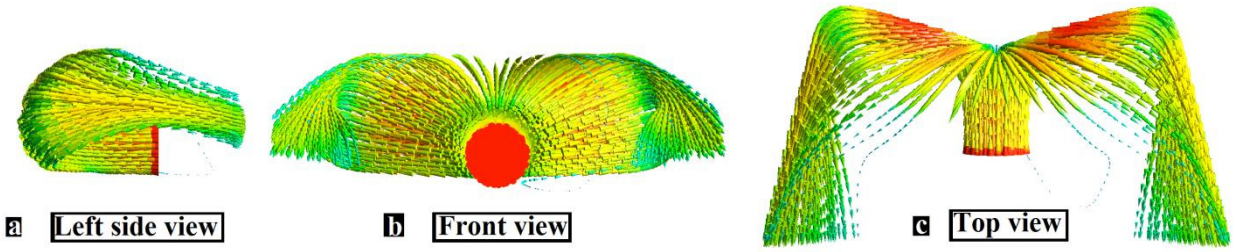

Figure 9.2. The blade has been removed. Thus only the water movement is visible. **a.)** The exiting water is pointing slightly downwards. **b.)** The front view shows too much spreading and far too little cohesion. **c.)** The top view. Water moves fast close to the blade on a frictionless simulation like this. Fast moving water is shown in red.

Since I chose a frictionless surface in our simulation we find that water can move faster on the surface of the blade than elsewhere. This is mainly due to air friction and surface tensions. Let us now increase phi angle two ($Ø_2$) by ten degrees and see what happens.

9.2. Simulation number 5

In this simulation I have increased phi angle two ($Ø_1$) by 10 degrees. Everything else has remained the same as design number 4.

Table 9.2. Simulation number 5`s characteristic table. Phi angle 1 ($Ø_1$) has been increased by 10 degrees in relation to simulation number 4.

Sim num	Design num	L1 (mm)	L2 (mm)	L3 (mm)	Ø1 (deg)	Ø2 (deg)	Attack angle	Jet D (mm)	Sim type	Gap (mm)	Flow Results	Blade collision
5	5	20	15	16	**25**	80	0	8	F.S.F	7	Fail	Clash

As we can see in figure 9.3 below, we cannot see any dramatic changes to the last simulation. I will have to look at the images various viewing angles of figure 9.3 first.

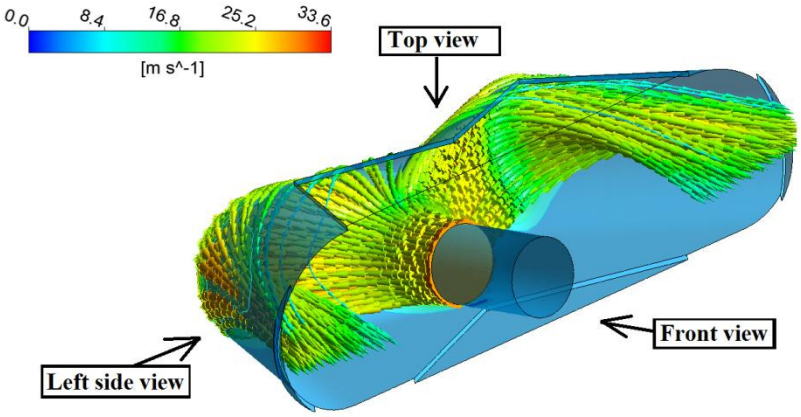

Figure 9.3. The isometric view of simulation number 5. Three views are pointed out as well as a water velocity index. Max velocity is in red whilst least is in blue.

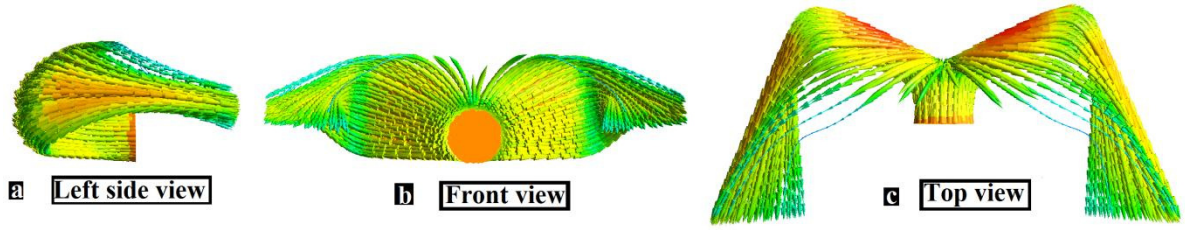

Figure 9.4. **a.)** The exiting water jet is still pointing in the wrong direction and is in the wrong position. **b.)** Nothing has changed really from simulation 4 here. There is still far too much spreading. **c.)** The top view of figure 9.3. Exiting water jet shows no improvements here either.

One can see a very slight improvement in the outgoing waters direction (figure 9.2 a and figure 9.4 a). Let us now increase the phi angle 1 ($Ø_1$) by another 10 degrees and see if there is further improvement.

9.3. Simulation number 6.

Table 9.3. Simulation number 6`s characteristic table. Phi angle 1 ($Ø_1$) has been increased to 35 degrees.

Sim num	Design num	L1 (mm)	L2 (mm)	L3 (mm)	Ø1 (deg)	Ø2 (deg)	Attack angle	Jet D (mm)	Sim type	Gap (mm)	Flow Results	Blade collision
6	6	20	15	16	35	80	0	8	F.S.F	7	Fail	Clash

We can now look at some of the results of simulation number 6. We see in figure 9.5 below an isometric view of simulation number 6.

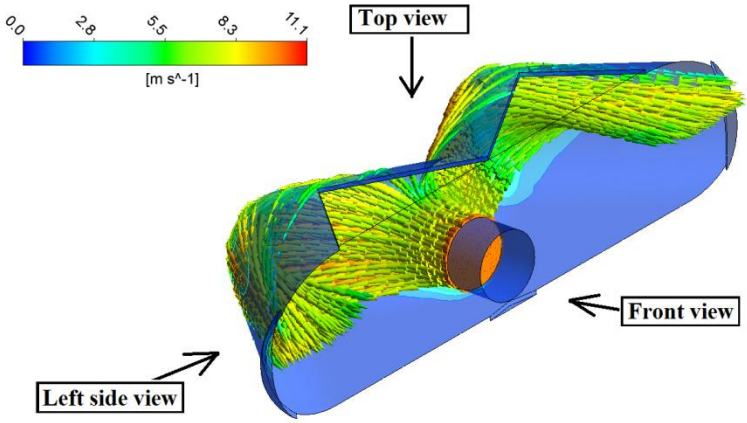

Figure 9.5. Simulation 6. An isometric view with velocity index.

Again I cannot see much change at all and must look at the various views of figure 9.5 in figure 9.6 below.

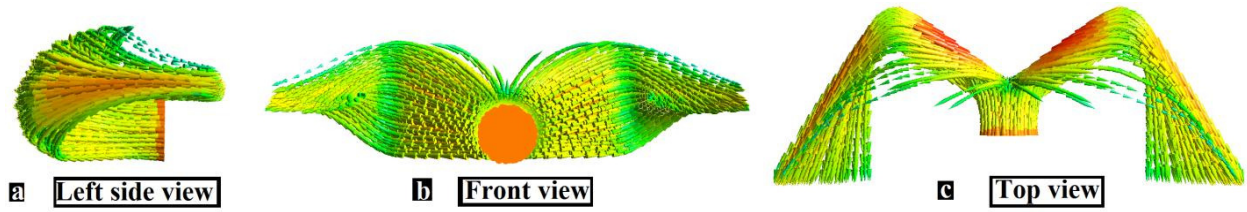

Figure 9.6. **a.)** The left side view. Exiting water flow seems to have lifted slightly to a more horizontal position. **b.)** As expected, the front view still shows too much spreading. **c.)** The top view shows no real improvements from the previous simulation either.

Figure 9.6 shows no real change except for the left side view. Let us now compare simulation 4,5 and 6`s left side views in figure 9.7 below:

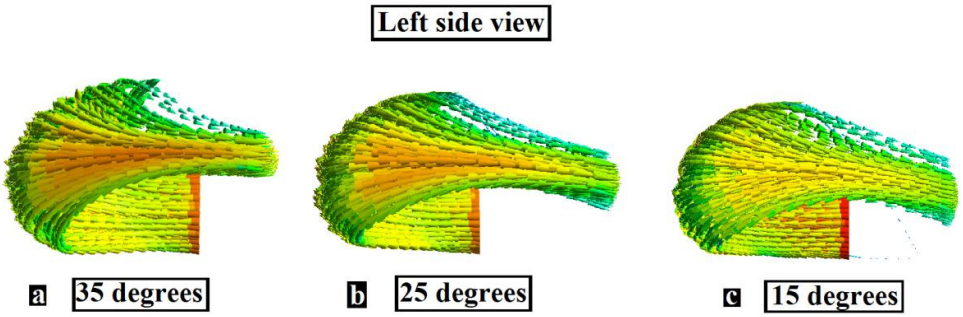

Figure 9.7. **a.)** Left side view of simulation number 6. **b.)** Simulation 5, left side view. **c.)** Left side view of simulation number 4.

Looking at figure 9.7 above we see that decreasing the phi angle ($Ø_1$) only makes our exiting water trajectory worse. I will therefore return to a phi angle one of 45 degrees.

I will now try to control the amount of spreading. I can reduce spreading by either increasing the blades height (L3) or decreasing the water jets diameter. The water jets diameter is 8mm and the expected diameter is 6mm. Thus we have a 25% safety margin. Let us rather increase the blades height (L3). In addition I can increase the length (L2) of our scooper part by 5mm. In this way "The Scooper" will have more space to do its job. The length of our "ejector wings" can be increased to 40 mm in case the water jet needs the space.

9.4. Simulation number 7

A general increase in the blades size has been implemented in this simulation.

Table 9.4. Simulation number 7`s characteristic table.

Sim num	Design num	L1 (mm)	L2 (mm)	L3 (mm)	Ø1 (deg)	Ø2 (deg)	Attack angle	Jet D (mm)	Sim type	Gap (mm)	Flow Results	Blade collision
7	7	40	20	28	45	90	0	8	F.S.F	-	semi-pass	Clash

Looking at figure 9.8 we see an immediate reduction in spreading from our previous simulations.

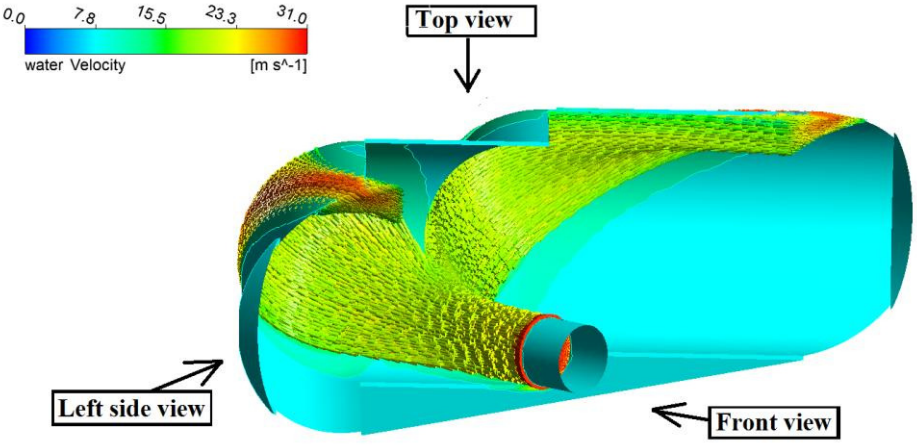

Figure 9.8. Simulation number 7`s isometric view with (3-D arrow heads). Velocity index is in the top left corner of screen. Water path shows improvement.

Let us now look at figure 9.8`s various viewing windows to get a better view of the water flow over this blade.

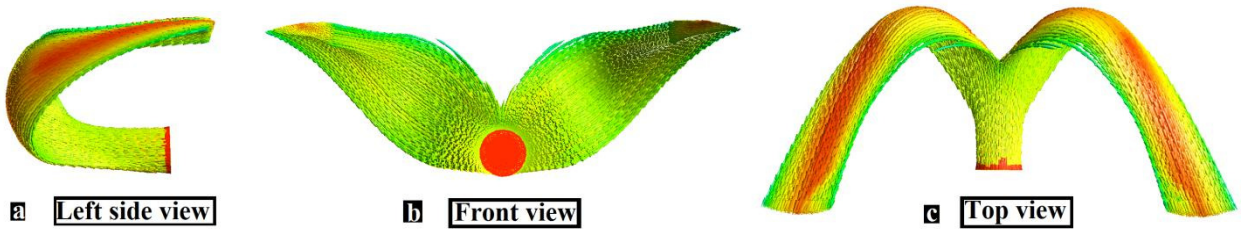

Figure 9.9. **a.)** The left side view shows a water jet that is ejecting water at the required height. **b.)** The front view reveals the fact that the exiting water is not approaching directly towards us. In addition the water is spreading correctly and then converging together again. **c.)** The top view shows a very clear out swing from our exiting water flow.

I have discovered a blade with an improved flow profile. Water is exiting at the correct height although its direction from this height is wrong (shown in figure 9.9 c). Let us now look at a pressure profile to see where water is having the most impact on the blade.

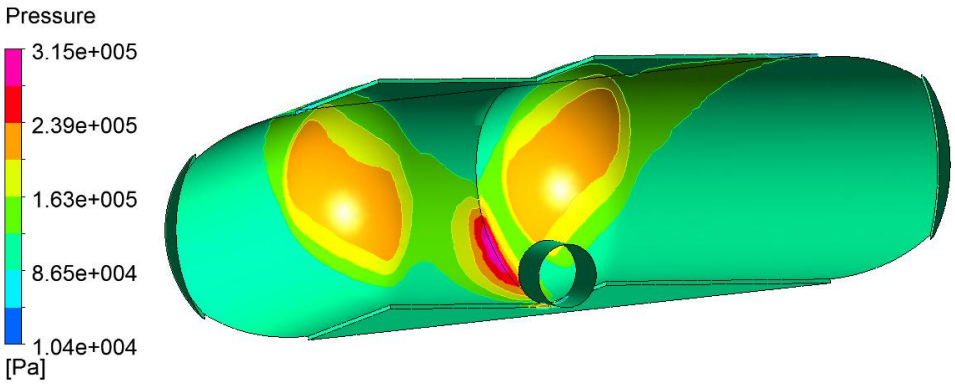

Figure 9.10. A pressure profile on the blade used in simulation 7. As expected, most of the pressure will be distributed onto "The flippers".

I notice from figure 9.10 above that the water flow deposits most of its momentum on "The flippers" on either side of the blade. This is the desired effect because this distributes the pressure on a large surface area.

Notice that the maximum pressure occurs at exactly the area where the water jet is split into two parts. I can reduce this pressure distribution here if I reduce our phi angle ($Ø_1$) of attack number one. I do not think this is urgent because if we look at the pressure profile on the left side of figure 9.10 we see that this maximum pressure does not exceed 3 times atmospheric pressure.

This blade is over 110 mm in breadth; our boundary conditions require less than 90mm. I will therefore have to shorten the length (L1) according to our boundary conditions (chapter 5).

In addition to this I will include a lofted bend for "The Scoopers" instead of a plain extrusion from "The Flippers". By doing this I can create a varying profile whereby "The Scoopers" attacking edge (in blue of figure 9.11) can be adjusted.

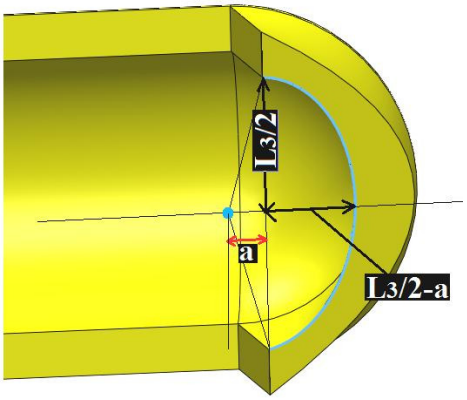

Figure 9.11. Half of the blade, which is divided by the blades symmetry plane. A lofted bend has been used on "The Scooper". Here we see how the attacking edge (blue line) can vary by a factor **a**. Notice that it is only the horizontal length that is varied. The height (L3) of the blade is conserved.

9.5. Simulation number 11

In simulations 8, 9 and 10 I found that shortening The Ejector Wings lengths (L1) made the water flow worse. In simulation number 11 below I found a balance (adheres to boundary conditions) for The Ejector Wings that were not too long or too short.

Table 9.5. Characteristic table for simulation number 11. A reduction in The Scoopers length to 12 mm as well as a reduction of the attack edge length **(a)** has occurred.

Sim num	Design num	L1 (mm)	L2 (mm)	L3 (mm)	Ø1 (deg)	Ø2 (deg)	Attack angle	Jet D (mm)	Sim type	Gap (mm)	Flow Results	Blade collision	a (mm)
11	10	30	12	28	45	80	0 deg	8	F.S.F	-	semi-pass	Clash	5

Simulation number 11 only used half of the blade design. Since the blade is perfectly symmetrical this is acceptable and necessary to reduce solving time for Ansys Workbench (CFX).

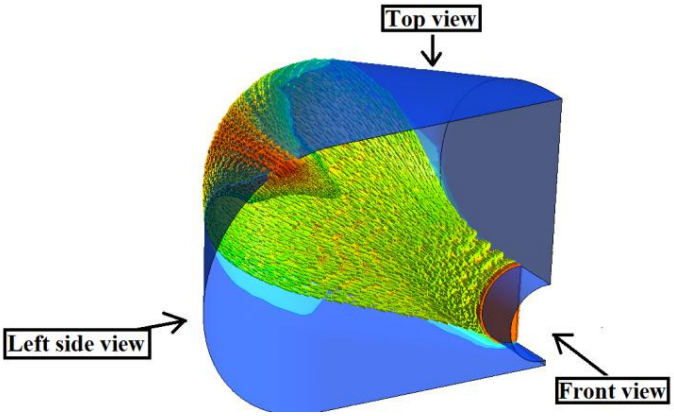

Figure 9.12. An isometric view of simulation number 11. Three viewing angles are present.

The figure above looks very similar to simulation number 7. We shall now look at figure 9.12`s viewing angles to get a better look at the flow over this blade.

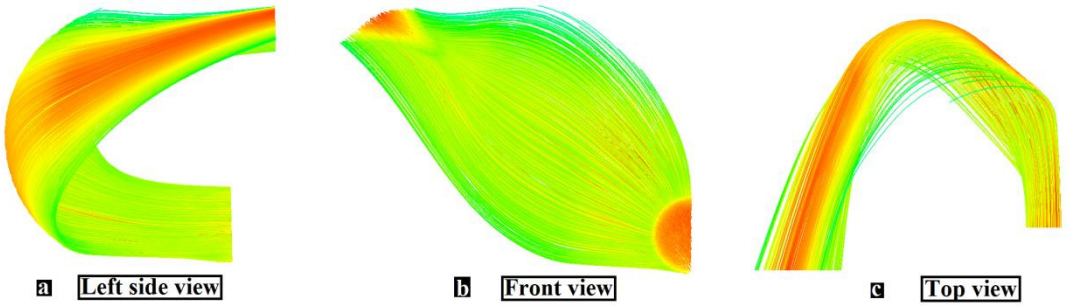

Figure 9.13. Three viewing angles of simulation number eleven. **a.)** The left side view seems more or less the same as simulation number 7. **b.)** The front view shows a good spreading of water although unwanted water gathering occurs at the water exit area. **c.)** The top view. Here we see the water is still moving slightly outwards instead of down the page.

Here we see an improvement of the direction of the flow but we are getting more converging of the flows at the same time. Flow direction improvements improves efficiency but flow accumulation gives way to flow losses. Which of the two are more important, I am not sure. Two problematic factors happen when two water streams accumulate, the first is a turbulence loss and the other is reduced contact with the surface of the blade.

9.6. Simulation number 14

In this simulation I have increase the height (L3) by 6 mm as shown in table 9.6 below.

Table 9.6. Characteristic table of simulation number 14. I have increased the height of the blade by 6mm in relation to simulation number 11.

Sim num	Design num	L1 (mm)	L2 (mm)	L3 (mm)	Ø1 (deg)	Ø2 (deg)	Attack angle	Jet D (mm)	Sim type	Gap (mm)	Flow Results	Blade collision	a (mm)
14	12	45	12	34	45	90	0 deg	8	F.S.F	-	Pass	Clash	5

After solving the Free Surface Flow I found the following results:

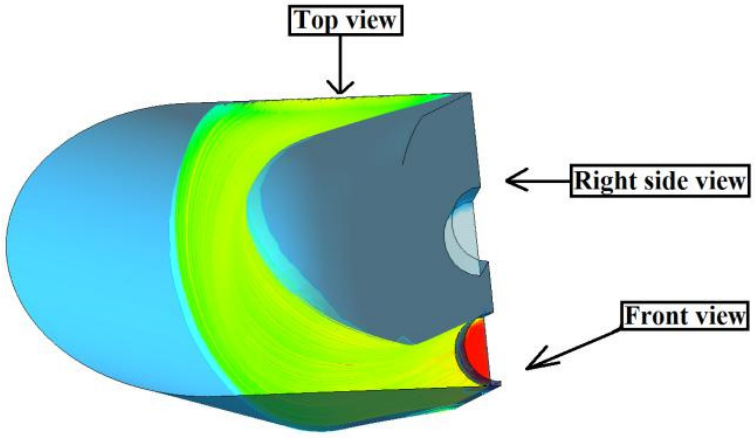

Figure 9.14. Isometric view of simulation number 14. Three views are shown.

Figure 9.14 above represents an isometric view of simulation number 14. The general flow pattern is behaving much better than in previous simulations. Let us now look at the various views to get a better look:

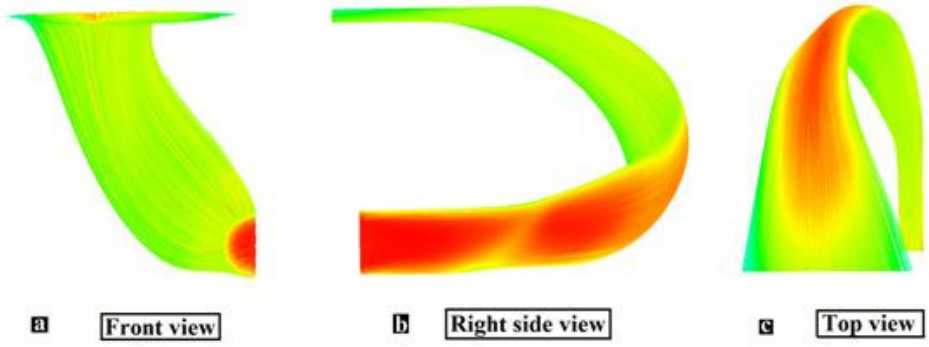

Figure 9.15. Three viewing angles of the water flow. **a.)** The front view shows the desired flow pattern laid out in our objectives. **b.)** The right side view shows the water leaving at the top of the face of the blade as desired. **c.)** The top view reveals that water is more or less leaving in the same direction it came from except from the desired position on top of the face of the blade.

We see in figure **9.15 a** above that water is reaching the top of the blade upon exiting. Spreading over the blade looks reasonable and not out of control as in previous simulations. It seems rather difficult to conclude from the colours that the water jet has effectively reduced its velocity to half its inlet velocity. Thus I will not show velocity indexes in figures and focus on the flow direction which should automatically deposit half its energy on the blade.

The velocity colour on the surface of the flow of figure 9.15 that is in contact with the air does not help at all. Irrespectively we can see that the water flow is turning approximately 180 degrees and therefore with relatively good spreading half the water flows energy should be deposited onto the blade.

9.7. Simulation number 15

I have now found a design we can work with that possesses better potential for our intended flow profile. It is important to consider as many of the flow scenarios our blade will encounter whilst being in operation. Thus as it was agreed upon, as soon as I have found some sort of blade that behaves itself I can implement new attack angles from our water jet.

Let us now use the same single blade design and see how it would behave with a water jet that has an angle of attack of 22.5 degrees.

Table 9.7. Characteristic table of simulation number 15. The attack angle of the water jet has been increased from 0 degrees to 22.5 degrees.

Sim num	Design num	L1 (mm)	L2 (mm)	L3 (mm)	Ø1 (deg)	Ø2 (deg)	Attack angle	Jet D (mm)	Sim type	Gap (mm)	Flow Results	Blade collision	a (mm)
15	12	45	12	34	45	90	22,5 deg	8	F.S.F	-	Pass	Clash	5

If we now look at the results of simulation number 15 in figure 9.16 below we see that this blade design has also managed to deflect the water in the desired manner. Water is reaching the correct height and position on our blade despite increasing our water jets angle of attack to 22.5 degrees.

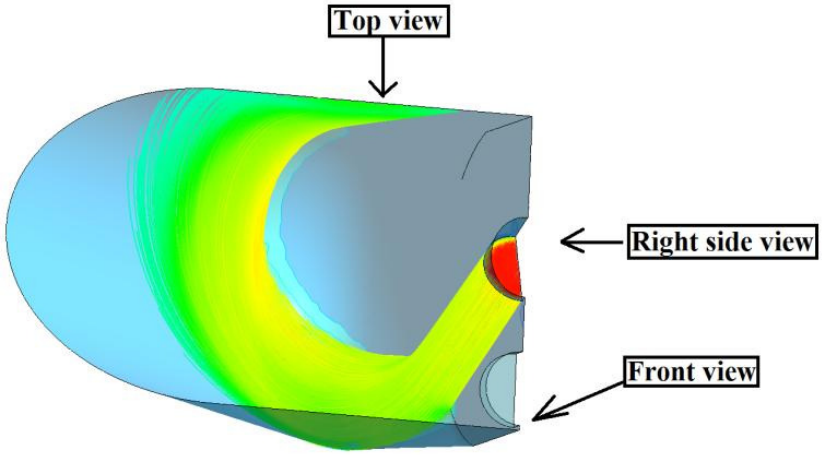

Figure 9.16. An isometric view of simulation number 15. Three viewing angles are shown.

Let us take a look at the various views. In figure 9.17 below:

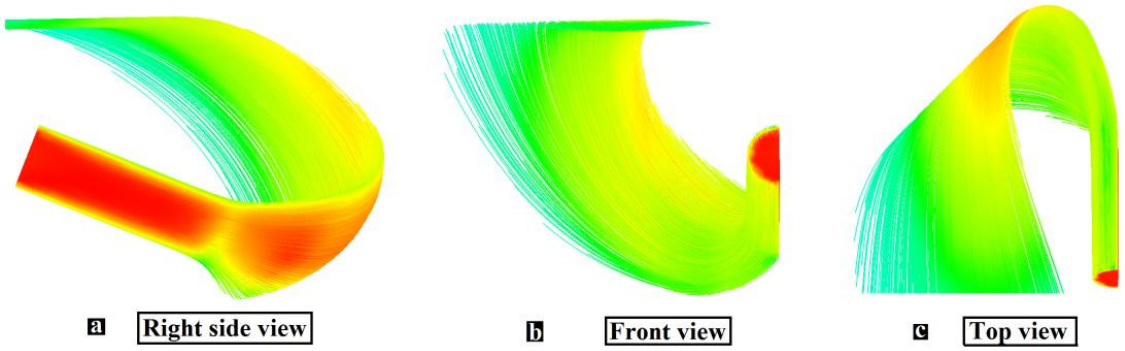

Figure 9.17. The water flow shown without the blade profile is in the correct position. **a.)** The right side view and its water flow. We see that water is reaching the desired height. **b.)** Here we see a good deal of spreading of the water flow. **c.)** Water is exiting in the correct direction although there is some variation in the speed of this flow which is dependent on the continuity equation.

We see in figure 9.17 the desired flow behaviour over our blade. Water is exiting at the correct height and in the correct direction. Spreading seems reasonable and the water velocity reading is rather difficult to read. Water velocities range depending on the flows cross-sectional area.

We are not expecting our blade design to encounter higher attack angles than 22.5 degrees because we will be using 16 blades. Thus a 16 blade turbine will have a pitch of 22.5 degrees and therefore each blade will have water passing over it for approximately 22.5 degrees of a rotation.

10. Multi-blade design of design category 2

10.1. Multi-blade challenges

So far I have only looked at single blade simulations. A very important requirement is that the water flow moves easily from one blade to the next. Let us have a look at our fundamental blade design again in its assembled form below in figure 10.1:

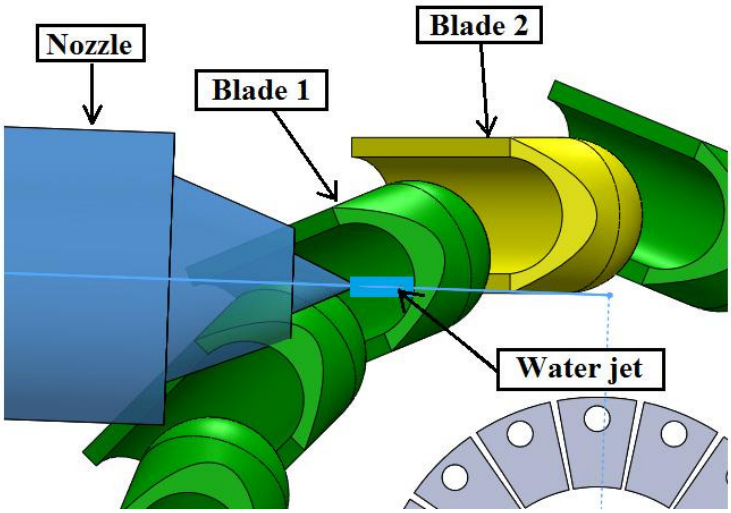

Figure 10.1. We see two major clashes. The first is the nozzle clashing with our blades and the other is our water jet has zero flow possibilities from one blade to the next. Blade one (in green) is completely blocking blade 2 (in yellow).

Looking at figure 10.1 above we see our water jet is unable to pass over from blade one (in green) to blade two (in yellow). The top part of our blades need to be cut away to give way for this requirement. In addition we see that the nozzle is clashing with our blade. This occurs because I had to lift the blade (the gap) such that the water jet could be "scooped" up. Let us take a closer look at how this nozzle is clashing with our blade whilst the turbine rotates in figure 10.2.

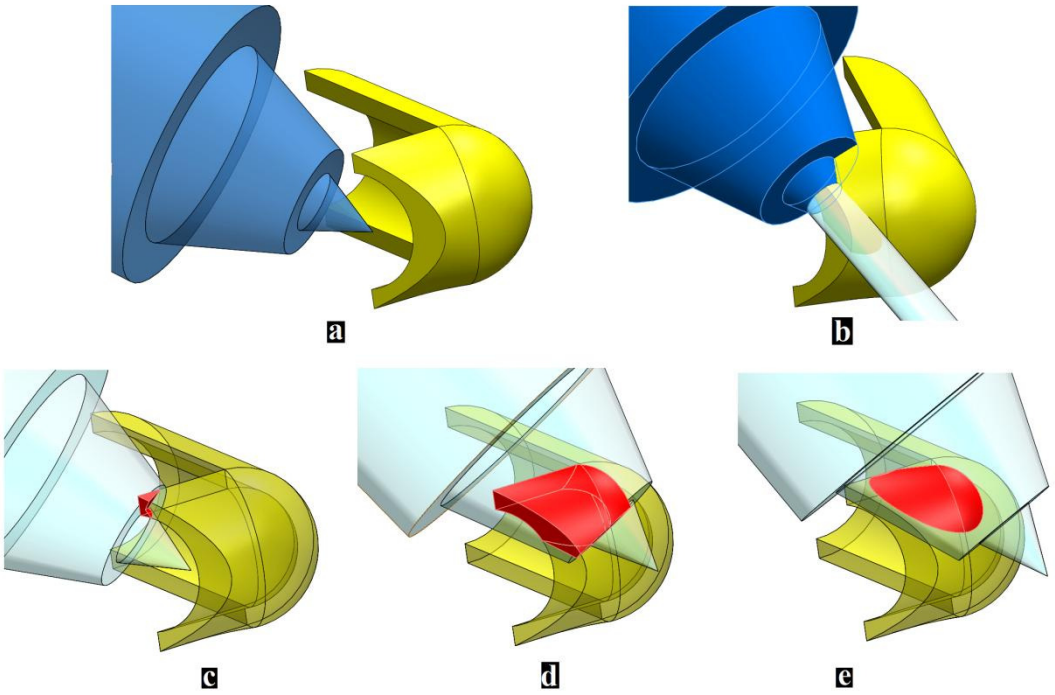

Figure 10.2. Interaction of one of the blades (in yellow) and the nozzle (in blue). **a.)** Here we see our water nozzle in blue and half our blade in yellow. The blade has been split through its axis of symmetry. **b.)** Here we see a clear clash of the nozzle with the blade upon rotation. **c.)** Here we see the beginning of the clash shown in red. **d.)** The majority of the blade and nozzle clash shown in red. **e.)** The end of the clash area shown in red.

After a lot of rotated-cutting on Solid Works, I found a solution for our blade that did not clash with the nozzle. This is shown in figure 10.3 below:

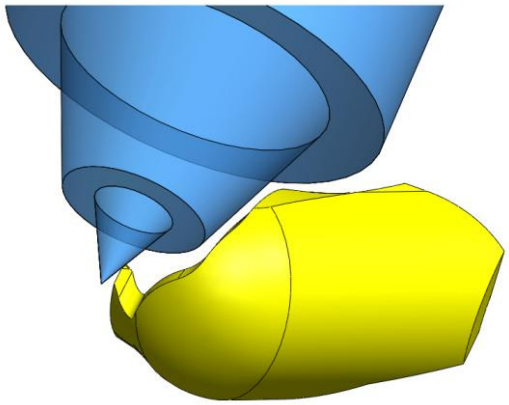

Figure 10.3. We see that the nozzle (in blue) is avoiding our newly cut blade (in yellow).

We see in figure 10.3 a blade design in yellow that avoids any clashes with the nozzle in blue. I did not want to cut too much blade away in order to preserve the blades flow design once the water does enter the blade. Thus the least amount of clearance this blade has with the nozzle is about one millimetre.

As it was laid out in our flow objectives water must flow easily from one blade to the next. This includes the avoidance of phenomena such as pressure waves. These can easily occur on a water jet if one hits it with a large blunt object. A pressure wave distorts the water jet and ultimately decreases turbine efficiency. Thus similar to The Pelton Turbine I will first “cut” the water jet by protruding an edge from the blade as it rotates. I will then slowly increase “the amount of blade” penetrating the water jet. This is shown in figure 7.4.

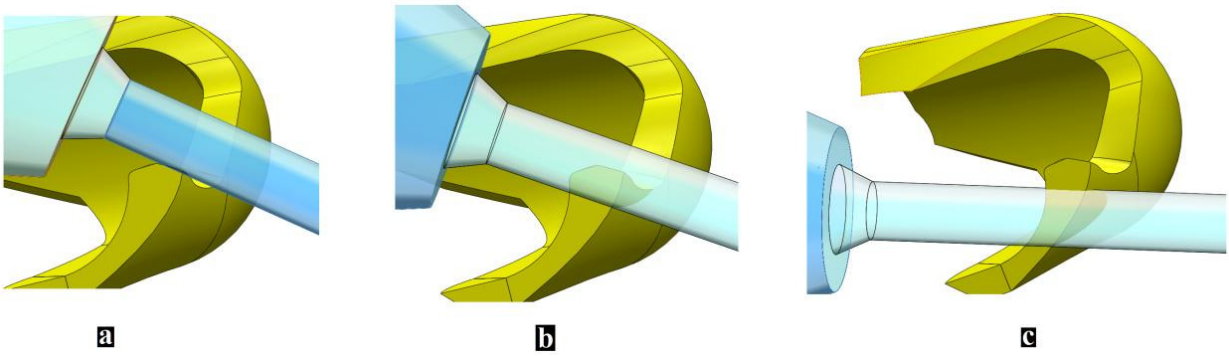

Figure 10.4. Half of the blade is split through its axis of symmetry with the water jet. As one of the blades rotates in the clock-wise direction the back of the blade will make contact with the water jet. **a.)** The beginning stage of the blade cutting through the water jet. Notice how only a slight edge is protruding. **b.)** At this stage the leading edge of the blade has been fully engulfed by the water jet and water is starting to move onto our blade in yellow. Water is also leaving its previous blade. **c.)** The blade has now rotated enough into the water jet that it receives the entire water jet over its blades.

Looking at figure 10.4 above we see how the water jet will be passing from one blade to the next. In figure **10.4 b** above we notice that this position over one of the blades marks the point in rotation where the water jet is making contact with two blades at the same time. The one blade is just beginning to receive water whilst the other is ending its encounter with the water jet. This is excellent to know for simulations because instead of taking many different simulations at various angles of attack we can just look at how the blades behave at this position or angle of attack. Let us now look closer at this angle of attack between two blades in figure 10.5 below:

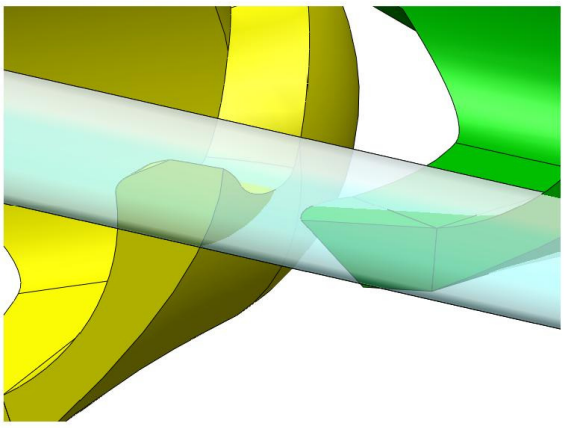

Figure 10.5. The water jet trajectory between two blades, Solid Works. Here we see the water jet passing over two blades. The blades have been split in two at its plain of symmetry in order to better see how the water jet behaves over them. The blade in yellow is beginning to receive water flow whilst the blade in green is ending its adventures with the water jet. Here we can also see how important it is to have the blade behind (in green) receives water on the top of its blade as planned and not under it.

If we look at figure 10.5 we see the water jets trajectory of flow between two blades. We can see how important it is that the blade behind (in green) is sitting below the blade in front (in yellow) such that water does not pass underneath it. This is an important consideration to be aware of when cutting material away in Solid Works.

We notice in the next simulations that if one increases the “gap” length; more material on the blade must be extracted in order for the water to pass over from one blade to the next.

The cutting process for each simulation is changed once the gap length has changed. I will not go into details as to how I cut away material for each simulation.

In the following simulations I have reduced the diameter of our water jet to a more realistic diameter of 6 mm. This gives us a lot more space to experiment with.

Let us now look at some simulations that aim the water jet between two blades. This marks the beginning and end of the water flow over the blade design.

10.2. Simulation number16

In simulation number 16 I have chosen an increased loft length (L2) and a gap of 10 mm as it is shown in its characteristic table below.

Table 10.1. Characteristic table of simulation number 16.

Sim num	Design num	L1 (mm)	L2 (mm)	L3 (mm)	Ø1 (deg)	Ø2 (deg)	Attack angle	Jet D (mm)	Sim type	Gap (mm)	Flow Results	Blade collision	a mm)
16	14	30	20	34	45	90	≈ 10 deg	6	F.S.F	10	overflow	Fail	3

The following results were discovered in figure 10.6 and 10.7 below:

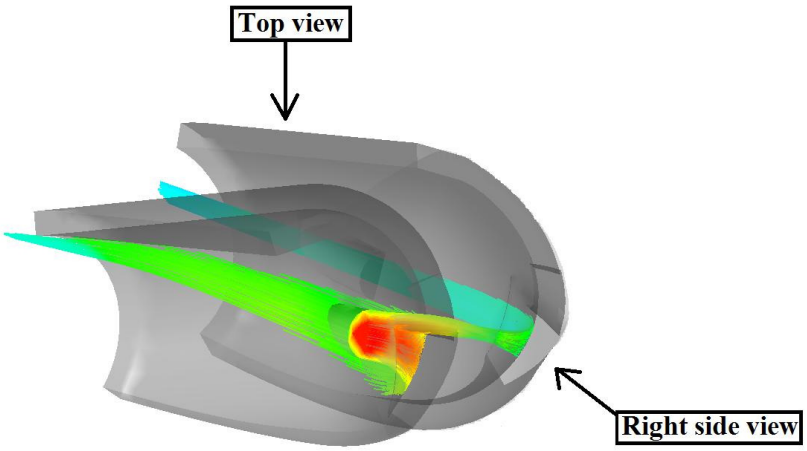

Figure 10.6. An isometric view of our water flow. It is immediately obvious that the water flow is not moving as it was intended.

Let us now look at the various views of figure 10.6 in figure 10.7 below.

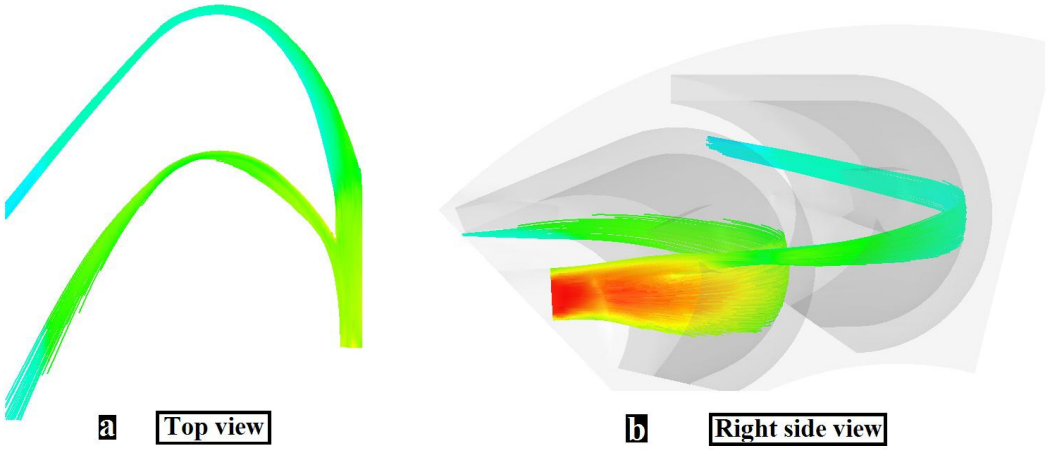

Figure 10.7. **a.)** The top view of the water flow in simulation number 16. Notice the water flow is in the wrong direction. **b.)** The right side view confirms that the water jet is not exiting at the correct height.

Looking at figure 10.7 we see a clear failure of both the exiting water position and directing on both blades. The flow seems to just swing outwards instead of upwards. The water flow is obviously getting too much time on the blade so let us reduce the lofted length (L2) to help correct this problem. In addition the water flow is not being scooped up at all which suggests that our "gap" height is too low.

These changes to our blades geometry were implemented in simulations 17 to 19 although it was obvious that our blades height (L3) was also still too large. Thus it was eventually reduced by 10 mm in simulation number 20 below.

10.3. Simulation number20

Simulation number 20 has decreased both lengths L2 and L3 as well as increasing the "Gap" length by 2 mm. Cutting over our blade has been increased because of changes made. The characteristic table of simulation number 20 is shown in table 10.2 below:

Table 10.2. The characteristic table of simulation number 20.

Sim num	Design num	L1 (mm)	L2 (mm)	L3 (mm)	Ø1 (deg)	Ø2 (deg)	Attack angle	Jet D (mm)	Sim type	Gap (mm)	Flow Results	Blade collision	a (mm)
20	16	25	**15**	**24**	45	90	≈ 10 deg	6	S.F	12	semi-pass	Nozzle	3

During the simulation process I used a Single fluid (S.F) type of simulation to speed up the process of finding the correct flow. Let us now look at an isometric view of the resulting flow over the new blade design, shown in figure 10.8.

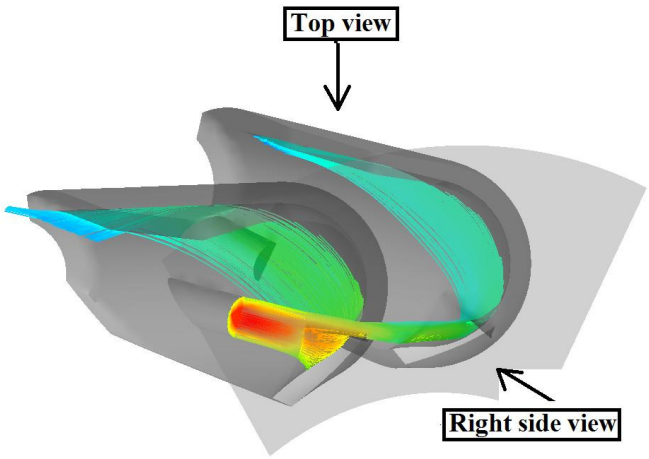

Figure 10.8. An isometric view of the water flow over blade design number 16. The top and right side views are indicated.

Let us now take a closer look at the two viewing angles of figure 10.8.

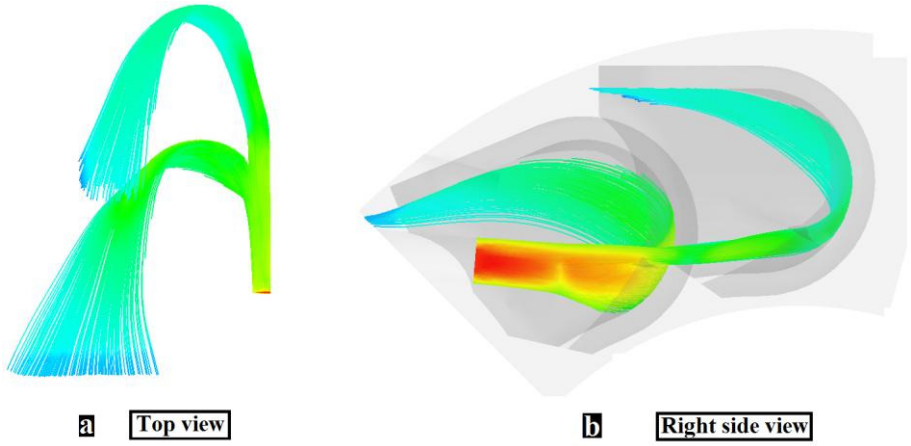

Figure 10.9. We notice that the water flow is not moving ideally over the first blade is encounters and spreads significantly upon exiting. The second blade on the other hand shows bettter results but has more out swing. **a.)** A top view of simulation number 20. We see a slight out swing with the first exiting water jet. **b.)** The height of our exiting water jet is acceptable.

Figure 10.9 has shown improvements in its flow behaviour both in direction and placement of the exiting water jet for both blades.

The behaviour of our water jet between the two blades is exceptionally dependant on the amount and way in which the material on the blades has been removed. The method and extent of the removed material will not be discussed. Although it is important to understand that although some simulation tables read the same data, they are usually not the same although they do possess the same information shown.

Let us now check how this blade design behaves with a water jet that has a slightly increased angle of attack and a little more material removed from its centre.

10.4. Simulation number 23 and 24

The characteristic table of simulation number 23 and 24 follows:

Table 10.3. Characteristic table of simulation number 23 and 24.

Sim num	Design num	L1 (mm)	L2 (mm)	L3 (mm)	Ø1 (deg)	Ø2 (deg)	Attack angle	Jet D (mm)	Sim type	Gap (mm)	Flow Results	Blade collision	a (mm)
23	**17**	25	15	24	45	90	**≈ 10 deg**	6	S.F	**13**	Pass	Nozzle	3
24	**17**	25	15	24	45	90	**≈ 14 deg**	6	S.F	**13**	Fail	Nozzle	3

Simulation number 23 and 24 has had more material cut from its centre as well as its gap length increased by 1mm. Let us look at a right side view of both simulations as shown in figure 10.10 below:

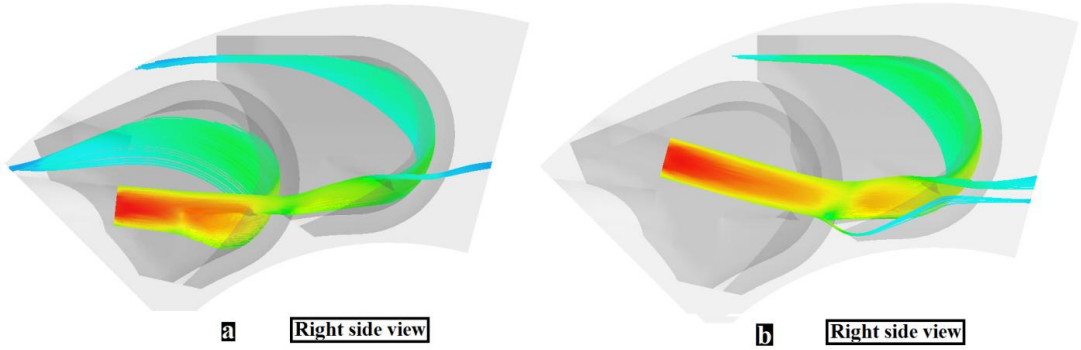

Figure 10.10. **a.)** A right side view of simulation number 23. Water flow appeared to move in an acceptable fashion. **b.)** A right side view of simulation number 24. As soon as we increase the angle of attack slightly, we see that some water is escaping under our blade. This is unacceptable water flow behaviour.

Figure **10.10 a,** shows an acceptable water flow over our blade design. As soon as I increase the water jets angle of attack over the same blade design we see that some water is escaping under the blade. Thus, simulation number 24 has failed its water flow criteria. I will have to yet again make some changes to our blade design such that "the back blade" hides better behind the blade in front of it. This proved to be more challenging than expected. Thus it was only until I came to simulation number 29 that I began to see better flow results.

10.5. Simulation number 29

Simulation number 29 has decreased its value of **a** (see figure 10.11) by 2mm. The blade has also made a series of small changes with the amount of material that has been cut from the blade.

Table 10.4. Characteristic table of simulation number 29.

Sim num	Design num	L1 (mm)	L2 (mm)	L3 (mm)	Ø1 (deg)	Ø2 (deg)	Attack angle	Jet D (mm)	Sim type	Gap (mm)	Flow Results	Blade collision	a (mm)
29	19	25	15	24	45	90	≈ 15 deg	6	F.S.F	13	Pass	Nozzle	1

Below lies an isometric view of simulation number 29. Viewing angles are provided.

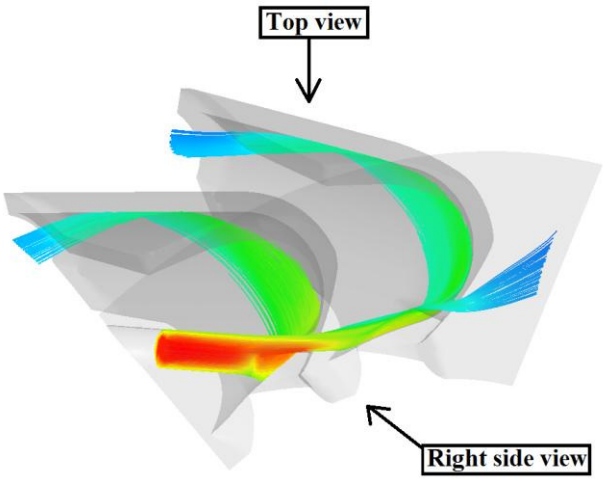

Figure 10.11. An isometric view of simulation number 29. Two viewing angles are indicated.

Let us now look at figure 10.11`s various viewing angles in figure 10.12 below.

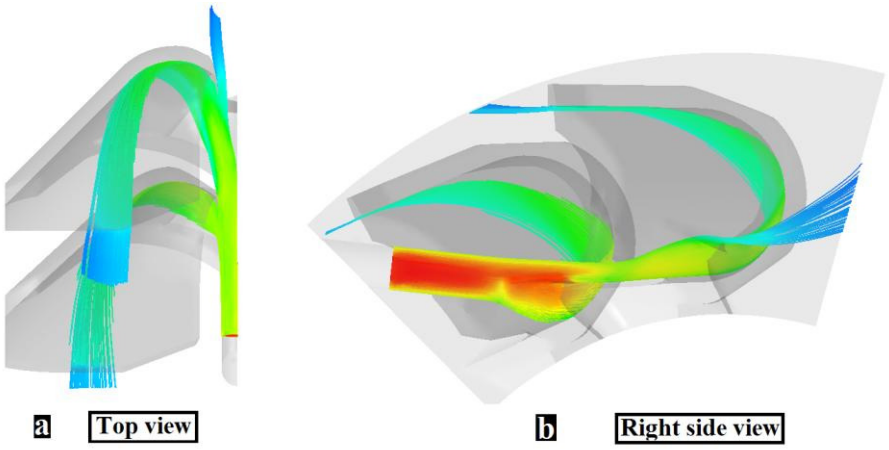

Figure 10.12. **a.)** The top view of simulation number 29. Flow behaviour over both blades is ideal in both direction and placement. We notice that the colour of the water jet suddenly changes from green to blue on exit. Only the surface of the water jet is visible and this colour change is expected when water flows in air. **b.)** The right side view of simulation number 29. Water flow is exiting at the desired height.

Both figure 10.11 and 10.12 reveal excellent flow behaviour. It is very difficult to accurately see if the water flow is moving at approximately half its incoming velocity with help from the velocity colour index (thus not provided). This is because as soon as the water jet leaves the blade it slows down where it is exposed to atmospheric conditions (only on the surface of the airborne water jet). Thus we see an immediate colour change (figure **10.12 a**) revealing that the water has stopped all together is misleading because it is not the true velocity of the exiting water jet.

10.6. Simulation number 30.

The following simulation is a very large simulation with approximately 1.45 million elements in its mesh. Water enters the blade setup at 120m/s here. A detailed report of actions made in Ansys Workbench (CFX) is found in appendix II for this simulation.

Table 10.5. Characteristic table of simulation number 30.

Sim num	Design num	L1 (mm)	L2 (mm)	L3 (mm)	Ø1 (deg)	Ø2 (deg)	Attack angle	Jet D (mm)	Sim type	Gap (mm)	Flow Results	Blade collision	a (mm)
30	24	25	15	24	45	90	≈ 10 deg	6	F.S.F	13	Pass	Fail	1

The simulation is of a F.S.F type and its purpose is to confirm that which occurred in simulation 29. This is a bigger, more accurate simulation. A very slight change in attack angle has occurred too.

A series of time frames will be taken in order to capture the waters movement step by step.

The first time frame is revealed in figure 10.13 below. This frame was taken after only 0.001 seconds.

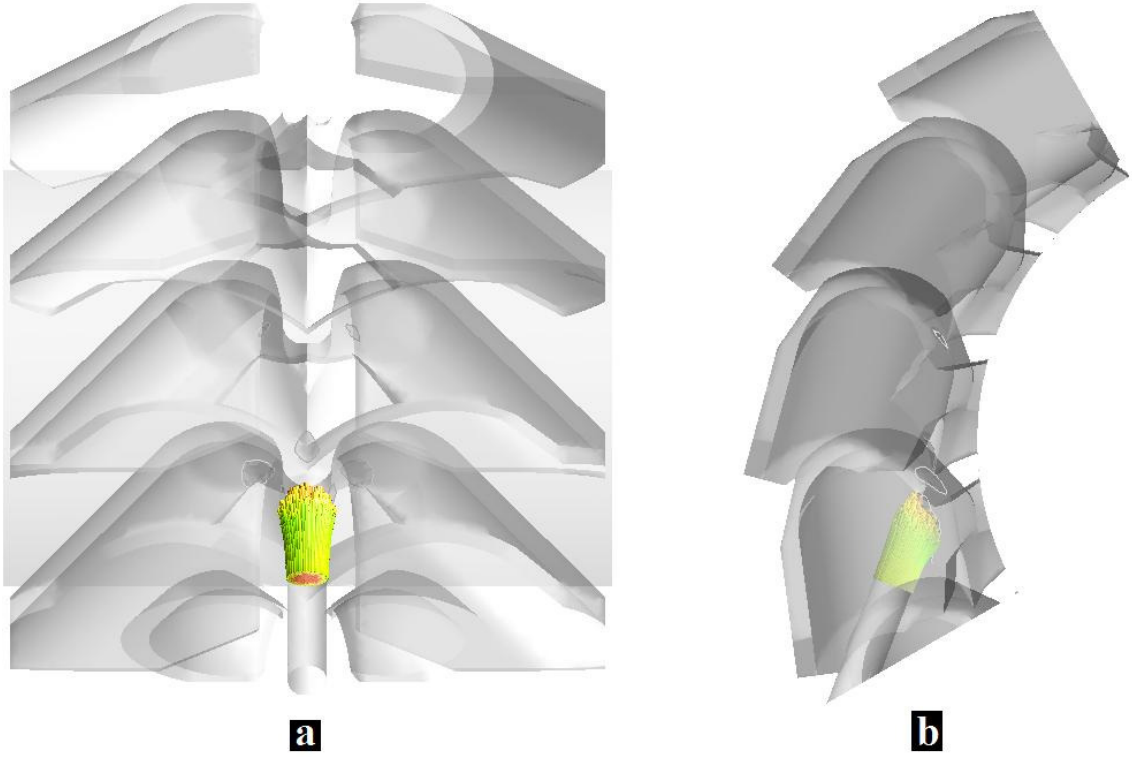

Figure 10.13. Here we see two views of simulation number 30 at a time of 0.001 seconds. **a.)** The top view of simulation number 30. **b.)** The right side view of the simulation number 30.

The second frame is shown in figure 10.14. This frame was taken after 0.01 seconds.

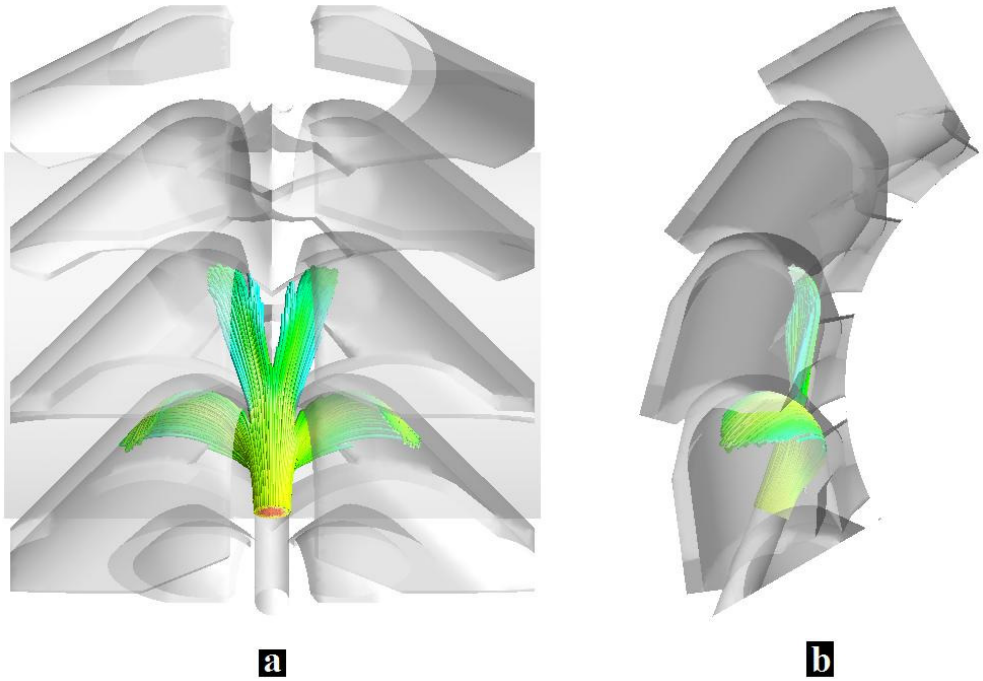

Figure 10.14. Two views of simulation number 30 at time 0.01 seconds. **a.)** The top view of simulation number 30. Water is effectively being split into two separate water jets. **b.)** The right side view of the simulation after 0.01 seconds.

The third frame is shown beneath in figure 10.15. This frame was taken after 0.015 seconds.

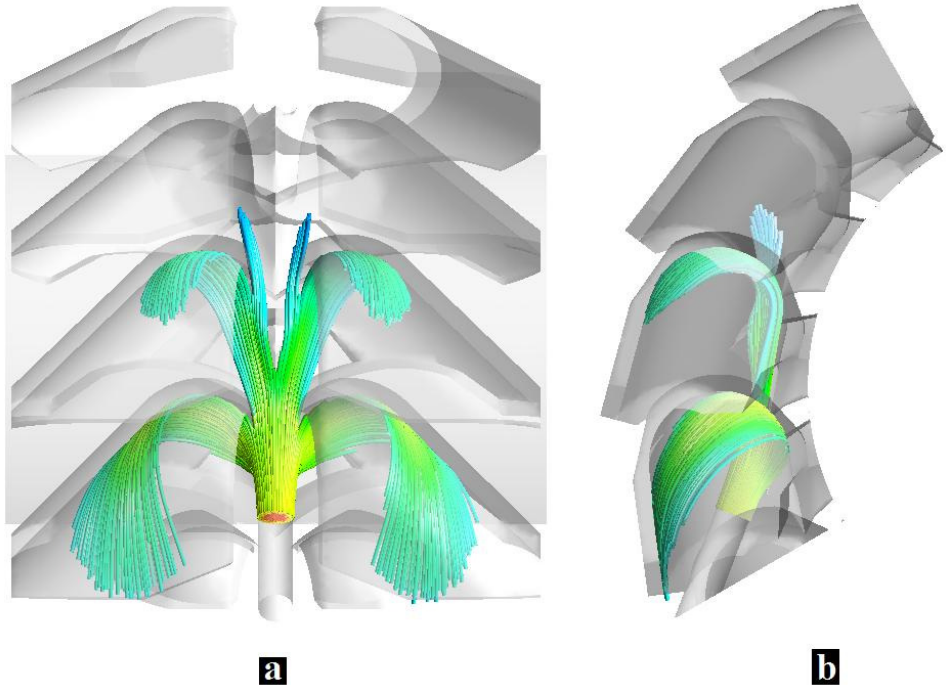

Figure 10.15. Two views of simulation number 30 at time 0.015 seconds. **a.)** The top view of simulation number 30. **b.)** The right side view of simulation number 30 after 0.015 seconds.

Finally the last frame is shown beneath in figure 10.16. This frame was taken after 0.02 seconds.

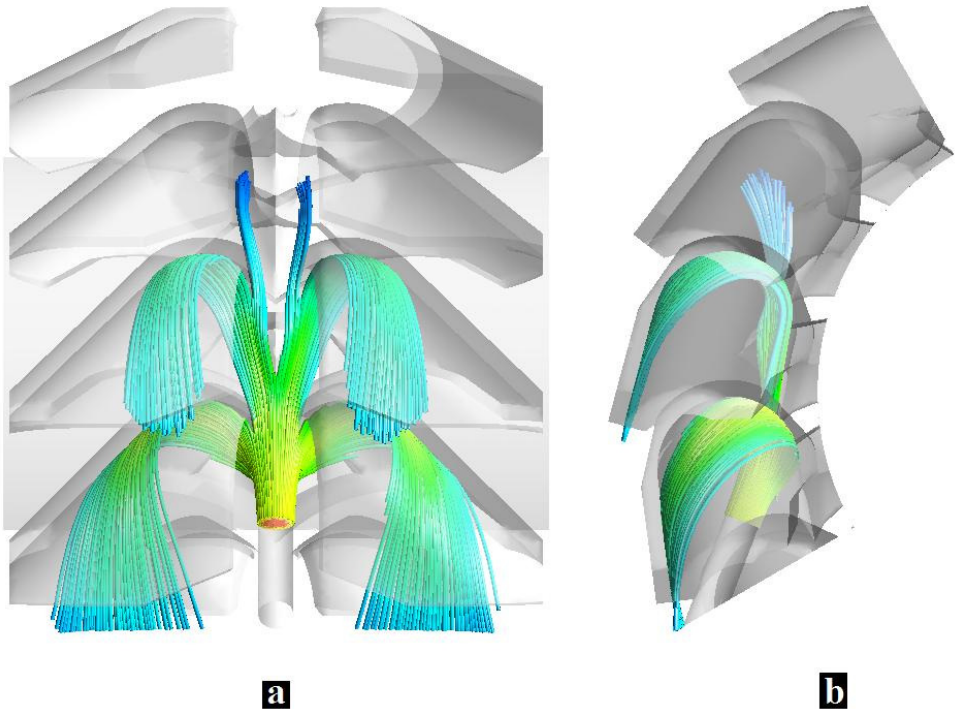

Figure 10.16. Two views of simulation number 30 at time 0.02 seconds. **a.)** The top view of simulation number 30. **b.)** The right side view of simulation number 30 after 0.02 seconds.

This flow behaviour is the best I have encountered thus far but there are still clashes with The Water Nozzle in the boundary conditions.

10.7. The chosen flow and subsequent blade design (simulation number 37).

All blade designs thus far have had clashes with the nozzle in our boundary conditions. Simulations 31 until 37 (shown in appendix I) was an attempt to see how much one could reduce the value of the blades height (L3), without serious disrupting our desired water flow pattern in simulation 30.
Reducing height (L3) and finding a solution here will make our blades smaller and more compact. It will also, more importantly save us from major collisions with the nozzle blade without cutting away too much off the blade. If it were not for the nozzle being in the way I would have gladly used simulation number 30 for testing.

Reducing the height (L3) created more spreading and out swing of the water jet. A compromise was made with a blade height of 18 mm instead of 24 mm in simulation number 30. This ensured that the underside of the blade design was not influenced when material was being cut away from the blade in order to make way for the water nozzle.

In simulation number 36 (characteristic table in appendix I) I used the exact same blade design as simulation number 37, except I had an attack angle of 10 degrees for the water jet. The flow over the blades behaved itself very well except for a very slight out swing of the flow. This is evident in simulation number 37 as well.

Table 10.6. Characteristic table of simulation number 37.

Sim num	Design num	L1 (mm)	L2 (mm)	L3 (mm)	Ø1 (deg)	Ø2 (deg)	Attack angle	Jet D (mm)	Sim type	Gap (mm)	Flow Results	Blade collision	a (mm)
37	24	25	15	18	45	90	≈ 20 deg	6	F.S.F	13	Pass	Pass	1

In simulation number 37, the water jet was just edging over the first blade. I checked the flow for any under flow, whereby there was none. Let us now look at the top view of this simulation.

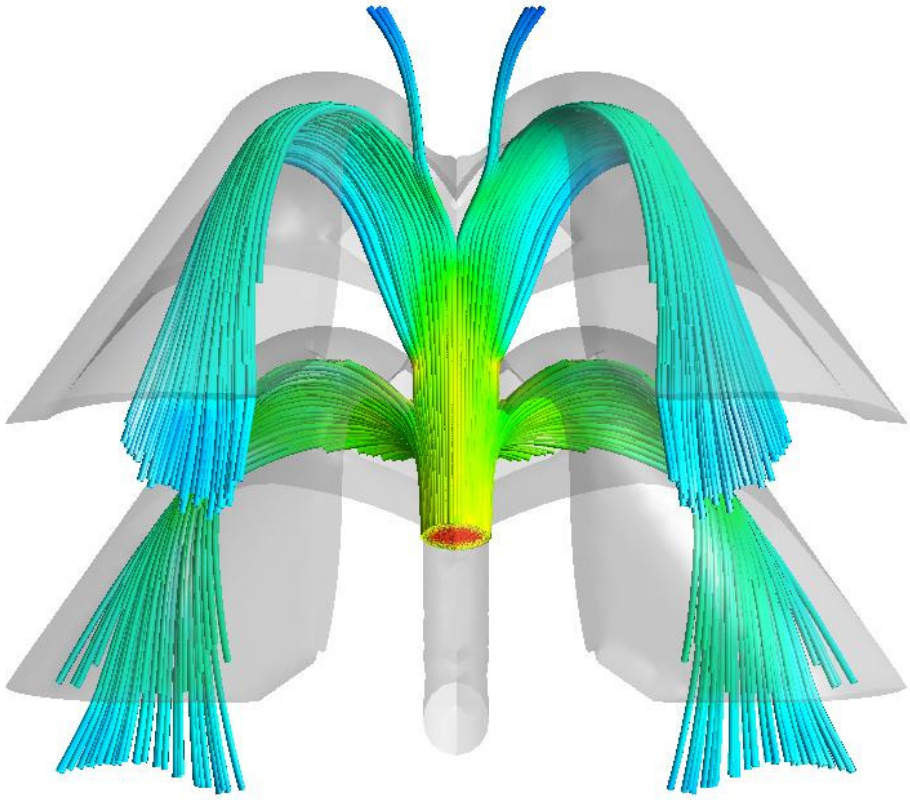

Figure 10.17. The top view of the last simulation. Notice a slight out swing of the water flow on the back blade.

Looking at figure 10.17 we see that the water flow is behaving very similarly to simulation number 30. The exception here is that there is a very slight out swing of the water jet behind the first blade. This also occurred in simulation number 36.

In addition, during higher angles of attack (Ø) the water jet (such as here) spreads slightly more and uses the outer reaches of the blade. This is different but quite acceptable. The water flow here represents a slight downgrade from simulation number 30 but it adheres to our boundary conditions and flow specifications (chapter 6). I will therefore use this blade design for further applications in this thesis.

11. Presentation of chosen 3-D blade solution

11.1 Single blade

Here we will present one of the 16 blades to be used in the turbine. All 3-D images will have their edges and constructional boundaries highlighted with a black line to help differentiate between various parts of the blade.

Isometric view

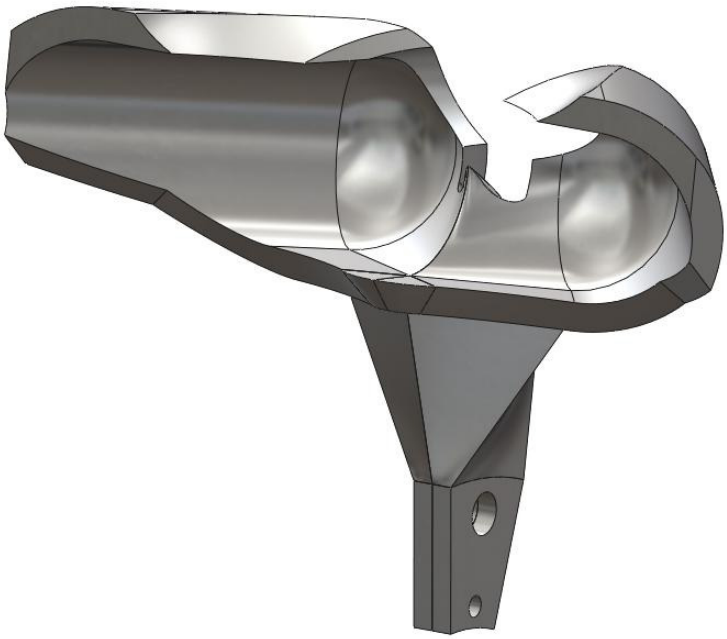

Figure 11.1. An isometric view of The Jack Turbine Blade. Black lines have been included onto all edges and part boundaries.

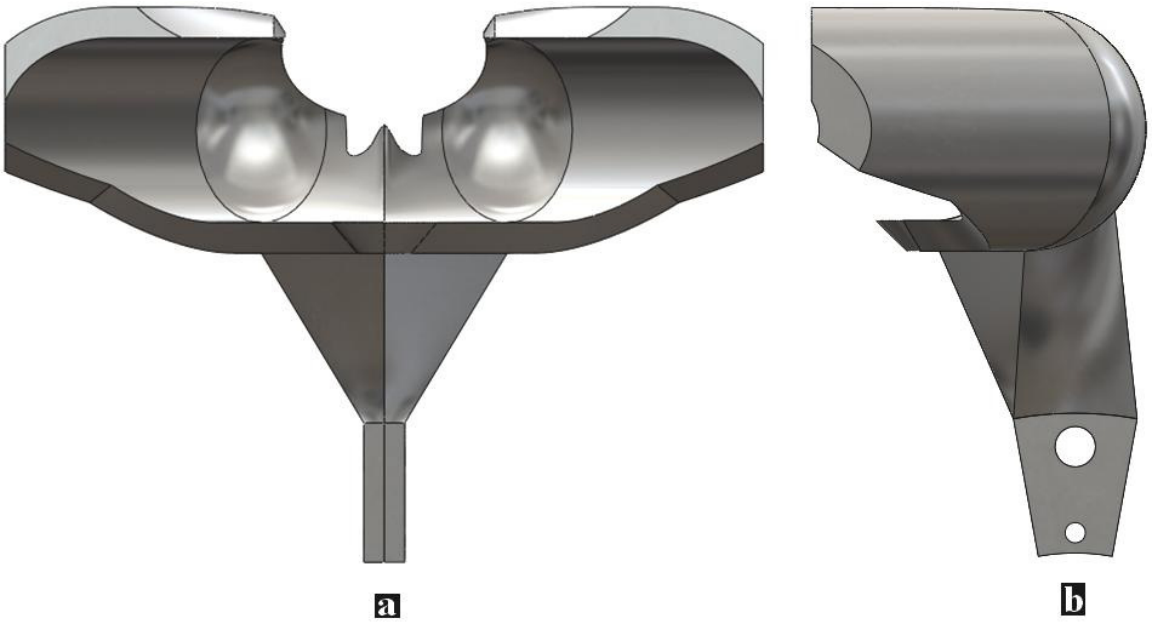

Figure 11.2. **a.)** A front view of figure 11.1. **b.)** The right side view of figure 11.1.

The majority of the top section has a thickness of 3mm. The section connecting “the holder” to the top body is a lofted extrusion. Sharp edges are expected to be sandpapered after construction.

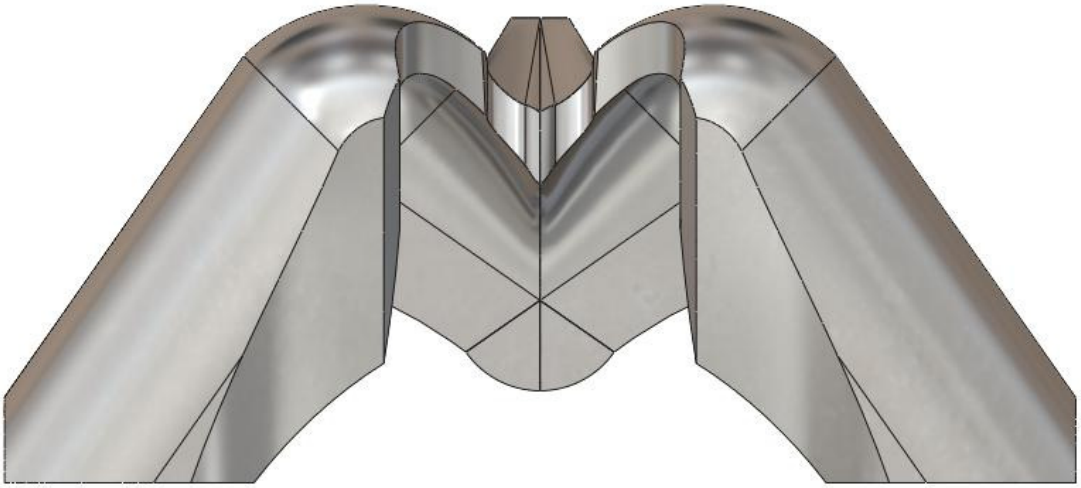

Figure 11.3. A top view of figure 11.1.

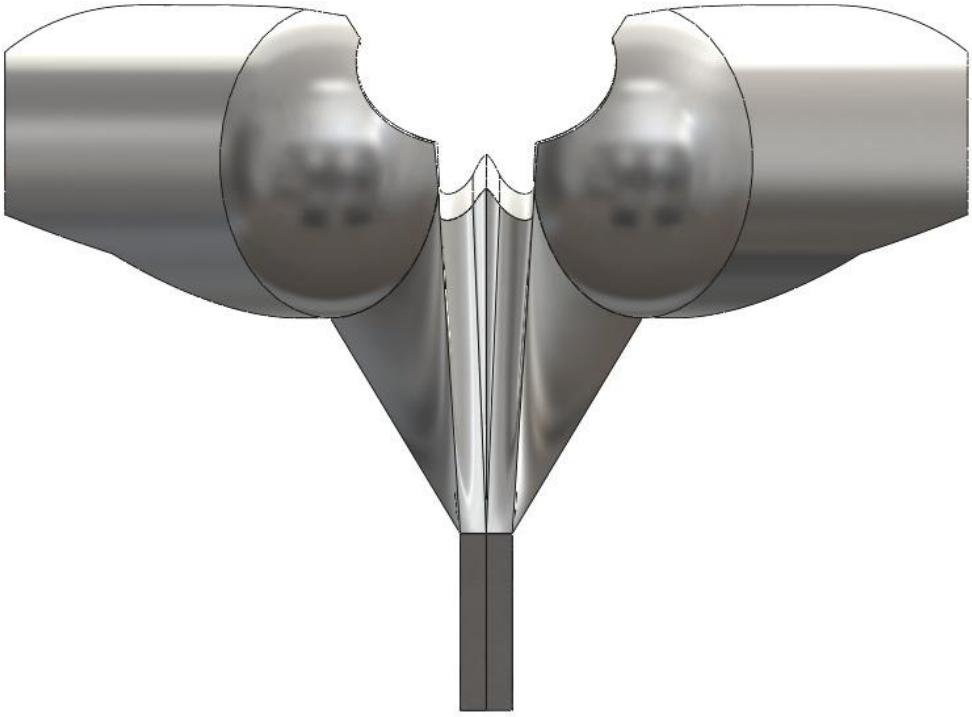

Figure 11.4. The back side view of figure 11.1.

A 2-D sketch is available in Appendix II. In this 2-D sketch I will outline the blades dominating measurements. I will not show details of all the measurements for this blade because it will be 3-D printed and not hand constructed.

11.2. Multiple blade assembly

Here we will visualize 16 blades as it is stipulated in our boundary conditions for testing. Beneath lies an isometric view of our multiple blade assembly.

Figure 11.5. A 16 blade assembly of The Jack Turbine Blade in isometric configuration.

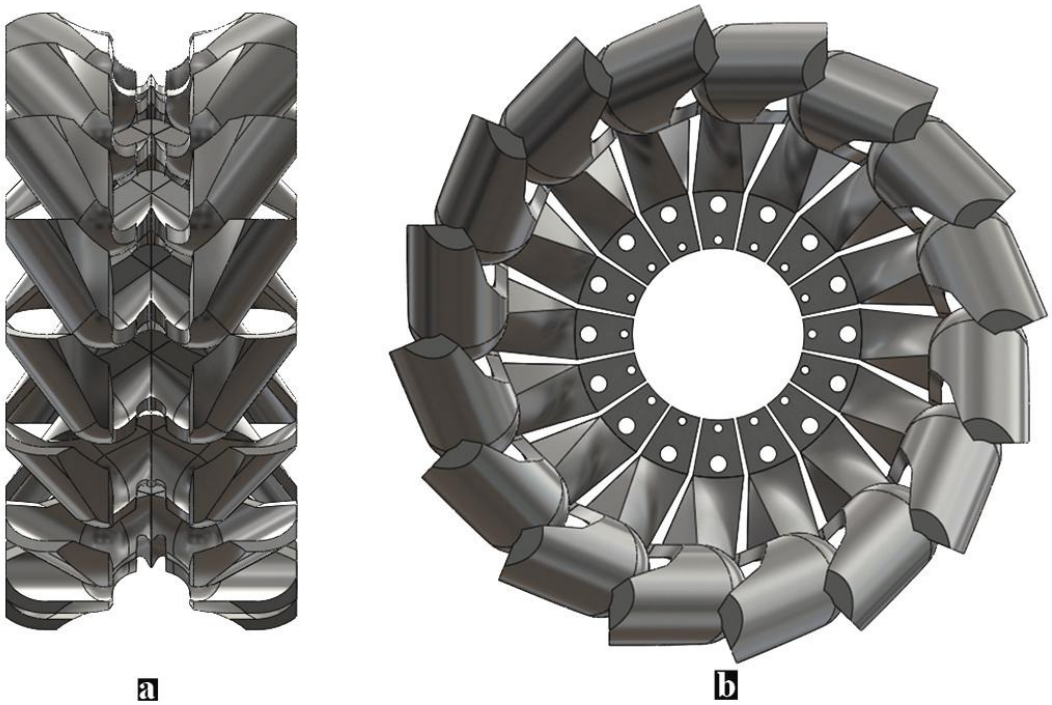

Figure 11.6. **a.)** A front view of figure 11.5. **b.)** A right side view of the assembled Jack turbine.

12. Operating loads for The Jack Turbine Blades

Unfortunately the construction of The Jack Turbines blade design cannot use conventional workshop methods. The blade design is too small and requires an exceptionally fine finish to minimize surface friction (k). Casting could be an option but 3-D printing seems to be the simplest method thus far. The advantage of having blades constructed separately is that I can do some hand sand papering and other finishing touches to each blade. In addition one can easily print far more blades than the required 16 blades. In this way I will have spares for both testing and manufacturing accidents.

The Norwegian University of Life Sciences (UMB) has a powder 3-D printer (explained in chapter 13). This is the only functioning 3-D printer available on campus. I can use it for our test blades if I in addition use an infiltrate or glue that can impregnate the powder construction. The disadvantage is that there is no information regarding the resulting materials properties. I must therefore conduct some rough tests and calculations on the resulting material before I can construct the blades.

12.1. The "worst case scenario".

Our so called "worst case scenario" will not occur when the water turbine is stationary and impacted by the water jet. This is because the water force on the blades will be the same irrespective of whether the blades are under stationary, pre-optimal or optimal operating conditions (see theory in chapter 3 and figure 3.17).

Optimal- and pre-optimal operating conditions occur when the turbine is rotating and absorbs no more than half the water jets energy. We must understand that The Pelton turbine and The Jack turbine blades are designed to extract no more than half of the water jets energy (tangentially to the direction of rotation) irrespective of the velocity of the water jet (see figure 3.9).

Only during post-optimal operating conditions will the blades extract less than half of the water jets energy.

Optimal operating conditions will include extra force variables such as centrifugal forces and fatigue. Other force variables such as vibration and harmonic frequency are also very real dangers although I will not be checking these due to time restrictions as stated in the limitations section of 1.6.
Single blade testing will not involve any rotation and should reveal whether or not our flow simulations were correct or not.

It is during multi-blade testing that the blade design will encounter its greatest challenge. Fatigue can occur rather quickly in micro-power turbines such as the one I will be using. With regards to harmonic frequency's I will just hope this does not occur and if it does, hopefully I have managed to gather enough data before failure.

In order to find out when the greatest forces occur on The Jack turbine we need to first find out more information regarding the maximum water force and the maximum centrifugal forces.

12.2. Estimate the maximum angular velocity

Previous studies on the Pelton Turbine rig setup done by myself and others show a maximum rotational velocity (ω) of approximately 2400 rev/min with a flow (Q) of approx 0,0004m^3/s.

I can expect The Jack turbine to have a slower angular velocity due to its larger radius. Thus I can be quite sure that during optimal operating conditions The Pelton turbine will rotate faster than the Jack turbine. The Jack turbine will produce more Torque because its point of water exit on its blade has a radius of 68mm where as The Pelton Turbine will exit its water at approximately -+ 5 mm from the radius of entry (50 mm) due to spreading.I can use the same flow (Q = 0.0004 m^3/s) on the Jack Turbine as that experienced when The Pelton turbine reached its maximum angular velocity (ω =2400 rev/min).

I first need to make a few assumptions:

The first being that the blade design cannot absorb more than half the water jets energy and the other being that the water jet has a diameter of 5mm. By selecting a smaller diameter (measured 6mm) for the water jet I can exaggerate our "worst case scenario" as follows:

I know that water will exit The Jack Turbine at a radius of approximately 68 mm. Thus substituting the continuity equation into equation 3.14 below with its relevant values we find:

$$u = \frac{1}{2}v_{in} = \omega r$$

$$\Rightarrow \quad \omega = \frac{\frac{1}{2}\left(\frac{Q}{A}\right)}{r} \cong 150\ \frac{rad}{s}\ or\ 1432\ \frac{rev}{min}$$

It is very likely that The Jack Turbine will reach a higher angular velocity at some entirely different flow (Q) and therefore produce a different water jet diameter (d) too. I will therefore increase this estimated angular velocity (ω) by approximately 25 percent to 2000 rev/min.

12.3. Maximum force due to water flow

From equation 3.12 in section 3 we have:

$$F = \rho Q(v_{in} - v_{out})$$

Since our blade design will extract a maximum of half the water jets energy. Equation 3.12 becomes:

$$F = \rho Q(v_{in})/2$$

Substituting a flow (Q) of 0.0004 m^3/s, velocity (v_{in}) of 20 m/s and a water density (ρ) of 997 kg/m^3, we find a force of approximately:

$$F \cong 4N$$

12.4. Centrifugal forces at 2000rev/min

I do not have the mass required to calculate the centrifugal force on our blades because I have not yet built any blades for weighing yet. I can estimate the mass by choosing a material on Solid Works. To get some idea of the weights involved, ABC plastic produces only 11 grams for one blade and a heavy non-metal such as a ceramic weighs roughly double this. The material that comes out of the 3-D printer is exceptionally light and fragile (lighter than most plastics). Glue will be added to these blades. Thus an estimated mass of approximately 20g per blade should be

appropriate. I can also find the centre of mass for the material and thus estimate the radius (r= 0,04m) at which this occurs when the blade is installed on the turbine. Again this is an estimate because the lower part of the turbine blade will be clamped between two metal disks and thus not be affected by the centrifugal motion. Thus slightly less weight is affected by centrifugal motion during testing but I will ignore this in our calculations for exaggeration purposes.

The centrifugal acceleration is therefore as follows:

$$a_c = \frac{u^2}{r} \qquad \text{(eq}^{\text{n}}\text{ 12.1)}$$

$$a_c = \frac{(\omega r)^2}{r} = \omega^2 r = \left(\frac{2000 \times 2\pi\ rad}{60\ s}\right)^2 (0{,}04m) = 1754 m/s^2$$

The expected force on our blade due to centrifugal accelerations is the product of the acceleration and the blades estimated mass. Such that:

$$F = ma = 0{,}02kg \times 1754 \frac{m}{s^2} \cong 35N$$

Here we can see that the force on our blades due to centripetal forces is far larger than those caused by the water jet (4 N).

12.5. Structural stresses on blade during "worst case scenario".

I can now estimate the tension on the base (least cross-sectional area) of the blade due to the centrifugal forces. A tensile stress due to centrifugal forces is estimated as follows:

$$\sigma_{ten} = \frac{F}{A} = \frac{35N}{(0{,}012m)(0{,}004m)} \cong 0{,}729\ MN/m^2$$

This value should be increased due to the bending affects of the water jets force. Thus let us now consider the impossible case of maximum centripetal force (35N) whilst including the maximum water jet force (4N) onto the blades. Due to the complexity of the blade I will avoid any hand calculations due to their inaccuracy and gather results using Ansys Workbench.

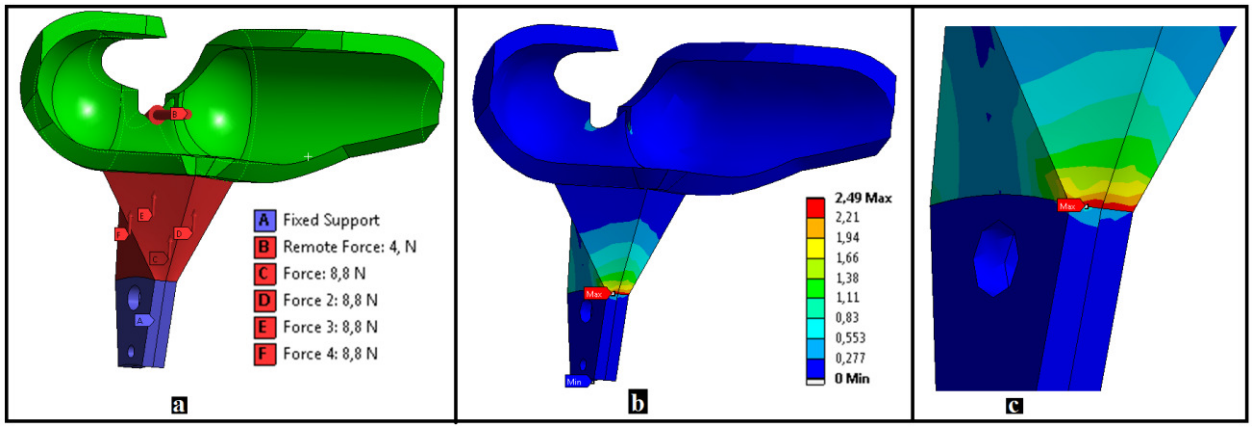

Figure 12.1. **a.)** The blue section is held tight, marked as fixed support. I applied the centrifugal force on the base of the blade. Four forces of 8.8 N evenly distributed. A single force of 4 N was applied to the entire body of the top section of the blade (shown in green) to duplicate the water force on it. **b.)** A von Misses maximum stress of 2.49 MN/m^2 occurs at the base of the blade in red. A small red box points vaguely to this area. Let us now try zoom into this area indicated a red. **c.)** A close up of the maximum stress area shows that it is mostly concentrated on the edge, shown in red. I could thus smooth this area out with glue upon construction.

Thus our "worst case scenario" will create a stress of 2.49 MN/m^2. This is a relatively low stress which leaves us open to wide range of acceptable materials including various plastic types. In our case we will estimate the material properties of an epoxy resin that infiltrates the material produced after 3-D printing. The 3-D printer (ZPrinter 450) produces layers of gips held together by a weak binder. This composite material is roughly investigated in section 12.5 below.

12.6. Rod testing for <u>minimum</u> material stresses.

Let us create sample rods of this composite for testing.

Each test category produced 8 test rods, 4 of the rods were printed up the rods shaft and 4 were printed across it. I expected the material to have different strength in different directions, similar to wood. After the rods were 3-D printed I soaked them in the epoxy mixture (Aeropoxy 101 and 205) for about 10-15 min. Whilst the rods were in the mixture, air bubbles were produced; this is because air in the rods was being replaced by the epoxy mixture. I therefore waited until the rods stopped producing air bubbles before I extracted them from the mixture for drying. I left the rods to dry for 2 days as shown in figure 12.2 below.

<u>Figure 22.2.</u> The test rods. Each rod had a square cross-section of 3x3 mm and was 45mm long. Drying took 2 days at room temperature.

Tensile strength

It was during tensile testing that I found the <u>lowest</u> stresses on the test rods. Figure 12.3 below shows the type of experimenting that was done for tensile testing.

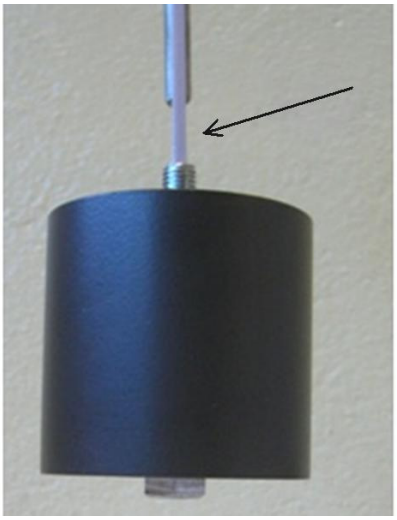

<u>Figure 12.3.</u> The test rod here was glued to the side of a metal pin at the top (shear force) and the base was glued to the weight. The tensile testing area is indicated with a black arrow. The mass here was only 2.5 kg.

It was difficult to attach a gradual amount of weight to the test rod. In the end I attached the test rod to a bag and in the bag I placed the weights whilst holding the test rod stationary.

The 8 rods could carry loads varying from around 7.5 kg to 11 kg depending on whether it was printed up the rod or across it. The shorter the rod the more force it could hold as well. I shall use 7,5kg to account for the least possible force encountered during rod testing.

This reveals a tensile stress of approximately:

$$\sigma_{ten} = \frac{F}{A} = \frac{7{,}5kg \times 9{,}81m/s^2}{(0{,}003m)(0{,}003m)} \cong 8{,}18\ MN/m^2$$

Calculations for bending, torsion and shear were also tested and can be seen in appendix IV.

Safety factor:

Our Ansys Workbench simulation produced a maximum stress of 2.49 MN/m^2 and tests on the material showed a minimum stress of 8, 58 MN/m^2. I can therefore find the safety factor involved for our worst case scenario.

$$SF = \frac{\sigma_{ten\ rods}}{\sigma_{worst\ case}} = \frac{8{,}18\ \mathrm{MN/m^2}}{2{,}49\mathrm{MN/m^2}} \cong 3{,}29$$

I have constantly exaggerated forces in our "worst case scenario" in order to compensate for unforeseen loads and or situations under testing. A dynamic safety factor should be over 3 in our case and so the safety factor found here is only just acceptable.

12.7. Conclusions for testing and construction

The truth is that I should perhaps use a different material such as ABC plastic but this would mean using a different 3-D printer outside UMB. I will therefore despite the risks of failure use the same method used on our test rods for the construction of The Jack Turbine Blades.

During multi-blade testing I will try to avoid maximum rotational velocities. This means I should avoid zero axial load conditions.

Some sandpapering at the base of the blades will be necessary to remove excess epoxy layers for installation. The sandpapering will destroy the surface finish and therefore some super glue over the surface will be used to cover these abrasions. I expect the super glue layer over the base of the blades will help prevent crack propagation and ultimate fatigue. Super glue has an exceptionally low viscosity which makes it perfect for absorption into materials. Its downfall is the fact that it dries in seconds. This makes working with it challenging.

I think it is important to remember that the data presented is not very trustworthy but can be thought of as an indicator and not a decisive factor.

13. Construction of The Jack Turbine Blades.

13.1. 3-D printing

The 3-D printing process was done by a Gips Powder Printer known as "ZPrinter 450" at UMB. The printer machine can print most 3-D construction drawings including Solid Works. It prints in a series of layers. Each layer is approximately 0.1 mm thick. The 3-D printer places a combination of powder and binder in each layer. The object is thus constructed via a series of layers consisting of binder and powder. After a few hours the construction is finished and the 3-D construction lies amongst loose powder. The blades dry for approximately 2 hours before been extracted from the powder. The machine vibrates such that excess powder falls away resulting in figure 13.1 below.

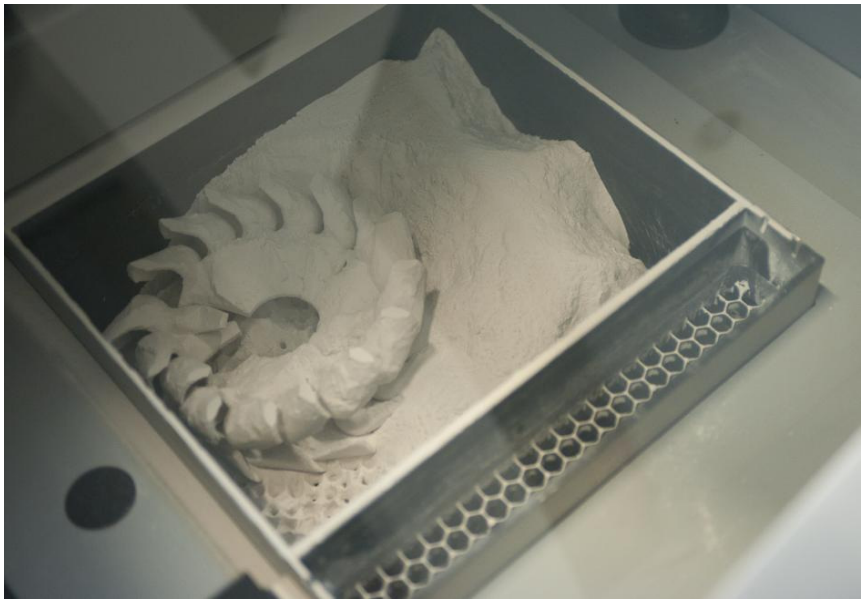

Figure 13.1. The remaining blades after 3-D construction. The blades are loose and thus needed to be extracted carefully from the powder.

The blades are then moved to a separate compartment where excess powder is carefully removed as shown in figure 13.2 below.

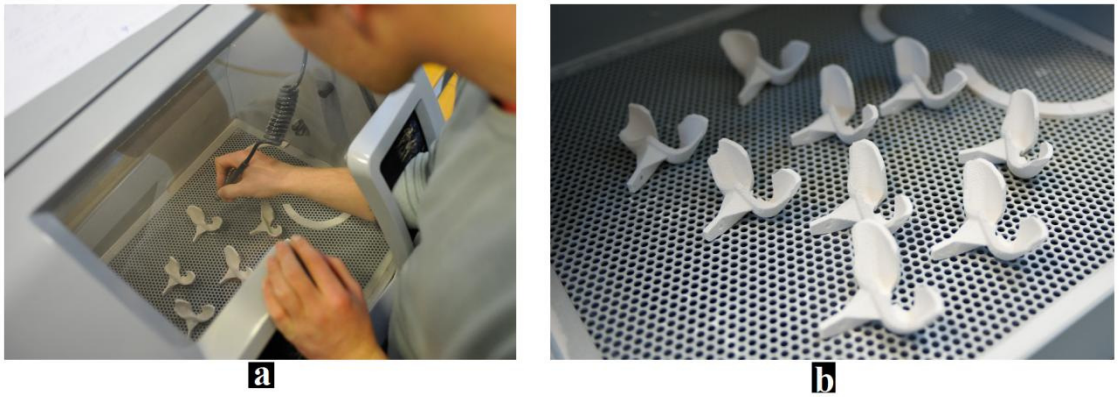

Figure 13.2. After drying the blades are carefully moved to another compartment. **a.)** Here excess powder is carefully removed by blowing air onto the blades. **b.)** The finished blades after 3-D printing.

13.2. Quality control

The first few days of printing did not produce well printed blades. These blades had to be discarded because they were exceptionally fragile. Only about 20 % were successfully removed from the printer machine. I found that this was due to a faulty print head as well as old binder. After these were ordered and replaced, the 3-D printer machine produced much better quality blades. The blades used, can be seen in figure 13.3 below.

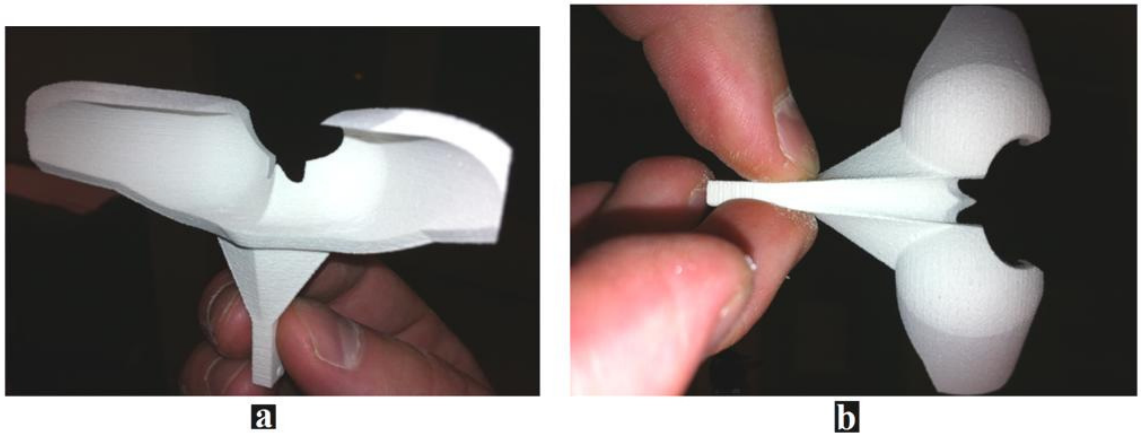

Figure 13.3. **a.)** A front view of the finished blade. The Blade is hard and has sharp edges. **b.)** The back of the blade after 3-D printing.

These blades were very sharp at its edges and had good detail. In addition every single one of these blades did not break or get damaged when being removed from the machine. During this print session a batch of 32 blades were printed and placed in a tissue box (figure 13.4 below).

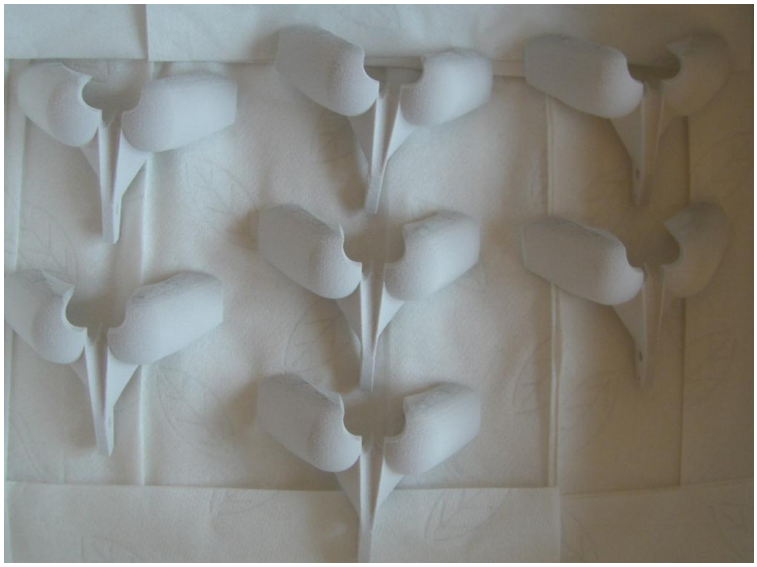

Figure 13.4. Finished blades were stored in a tissue box. Totalling 32 blades.

13.3. Infiltration of glue

In order to give the blades its strength I used the same epoxy that was roughly tested in chapter 12.5. Once the two epoxy resins have been mixed together (ratio 2:1) it begins to harden. The reaction is exothermic and therefore becomes warm. This also makes it less viscous for only 35 minutes.

During these 35 minutes all the blades are drowned in a bath filled with an epoxy mixture. Below in figure **13.5 a** is the bath used.

Figure 13.5. **a.)** The epoxy bath used to soak the blades in. **b.)** After 10 min, the blades stop producing bubbles and are removed for drying.

Whilst the blades were in the epoxy bath, air in the blades were displaced with epoxy mixture and bubbles escaped to the surface of the bath. It took about 10 minutes for each blade to stop producing bubbles at which point they were taken out to dry.

13.4. Drying and finishing touches

Drying took about 2 days at room temperature. The blades were placed on a stick free surface as shown in figure 13.6 **a** below.

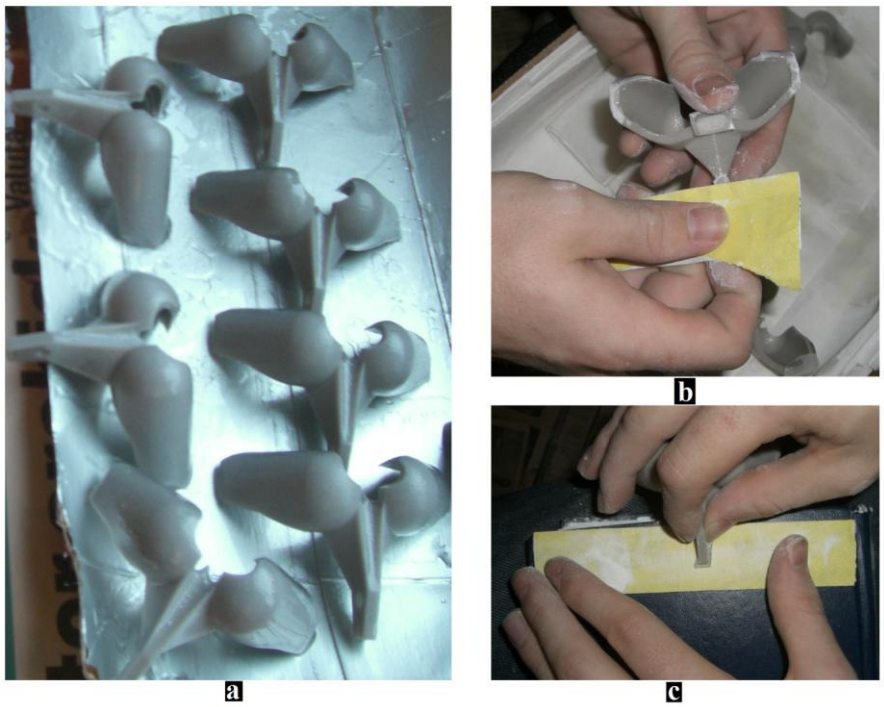

Figure 13.6. **a.)** Shows the drying blades on a stick free surface. Inside of a juice container. **b.)** Sandpapering was necessary to remove unwanted glue. **c.)** Some areas required a lot of work to remove excess glue.

After the drying process was completed, excess material was removed by sandpapering. The surfaces of the blades were rather coarse after the first time they were impregnated with glue. This was not acceptable and thus 2 more sessions of dipping the blades in glue was made. Each time, excess glue was removed after drying. This produced blades with an acceptable surface finish.

13.5. Installation

As mentioned earlier the blades are expected to be wedged between two metal disks. The disks have two holes for each of the 16 blades. Thus each blade (known as the holder in section 5.3) has two holes as well. The lower hole at the base of the blade will contain a thin pin through it of 2 mm in diameter. The other hole will have a screw penetrating through it of diameter 4mm.
During the installation of the blades, it was obvious that most of them needed more material removed at the base in order to fit in the turbine housing. After rigorous fine adjusting (used fine sandpaper) and fiddling I had about 24 of the 32 blades that could fit into the turbines housing.

The sandpapering at the base of each blade made tiny scratches that could later lead to propagation cracks and failure. I therefore dipped the base of each blade in super glue which made a thin but very strong layer over the scratches. After more fine adjustments I had 19 blades that could fit in the turbine housing. I then checked that each blades centre aligned itself with the tip of the water nozzle, as it is shown in figure 13.7 below.

Figure 13.7. The centre of each blade was checked to line up with the water nozzles tip. None of the blades were perfect but most were very close. The nozzles axis from its tip has been drawn over the picture as a black line. Here the entire axel had to be nudged upwards for the blades to align better.

Two blades were discarded as they did not align well at all, as shown below in figure 13.7.

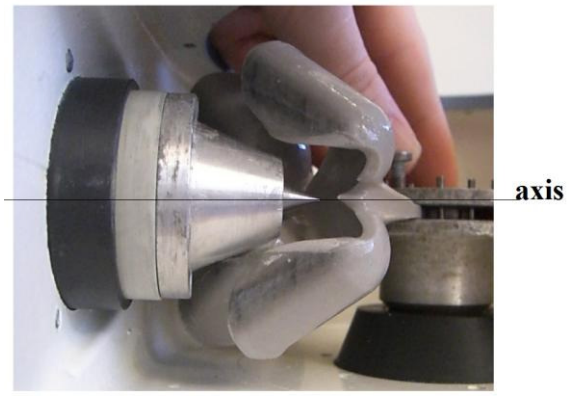

Figure 13.7. This blade had to be discarded because it deviated from the turbines nozzle axis by about 1mm.

Thus 16 Jack Turbines blades were successfully installed in The Peltons Turbines housing. None of the blades were 100 % perfectly aligned. Some were pointing over the nozzles tip and others under. This proved that the alignment-issue was because of the blades and not the turbines axel position.

14. Pre-testing background

In this section we will become more familiar with the equipment I will be using. In addition I will try establish what it is I want to achieve from testing.

14.1. Goals and expectations for testing

Main goal

The main goal for the testing of The Jack Turbine Blade is to simply retrieve as much data as physically possible. The much tested and less worrying Pelton turbine will be tested for comparison purposes. Milestones for testing would be to confirm flow behavior that was made in section 6 and to retrieve some efficiency readings.

Expectations

I will try to avoid any expectations and just do the lab rather mechanically. This will ensure unambiguous data readings.

With regards to The Jack Turbine blades, I do expect these blades to eventually break off at some point if sufficient operating time is provided. I therefore hope that this does not happen in the beginning of testing and rather after a few days or never. I will try avoiding any maximum angular velocity (no load) in the beginning of the testing of these blades.

14.2. Equipment and its function

14.2.1. The hydraulic bench

The hydraulic bench essentially contains everything that occurs whilst the laboratory is in progress. Beneath in figure 14.1 lies the hydraulic bench used in testing.

Figure 14.1. The hydraulic bench records and contains everything that happens during testing.

The tank records the amount of water passing through the turbine by means of a water gauge shown as the vertical white object on the left of figure 14.2 a.

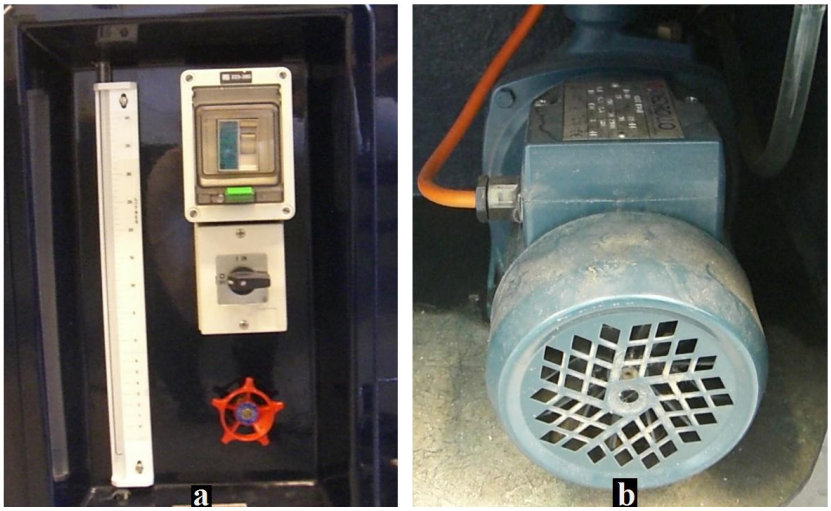

Figure 14.2. **a.)** The controls on the hydraulic bench. On the left in white, we have the water gauge and centred to the right, we have the on/off switch. The red lever on the bottom right is the main water valve; this is always fully open during testing. **b.)** The pump used. The pump reaches a maximum of 23 m water head (h) and 90 L/min flow (Q).

The time a specific amount of water passes through the turbine can be recorded via a conventional stop watch. In this way I can determine the flow passing through the turbine by dividing a certain volume of water by the recorded time it took to complete this volume.

The tanks single pump (figure 14.2 b) can produce 23 meters of water pressure at zero flow and a maximum flow of 90 L/min.

14.2.2. The Water Turbines Rig

The Water Turbines Rig is placed on top of the hydraulic bench. It has rubber padding under it and weighs about 14kg. Gravity and the turbines rubber padding is used to stabilize the turbine during operation. Piping from the Water Turbine Rig is connected to The Hydraulic Benches` Pump.

The Water Turbines Rig has three changeable criteria.

a) It can alter the water flow (Q) and water head (h) via the adjustable Water Nozzles Handle (figure 14.3 a).

b) It can vary the belt force by manipulating a belt/pulley system (figure 14.3 c, 14.6 a and b). This consequently creates variable torque and angular velocities on the turbine.

c) The water turbine rig can utilize different types of turbine blades.

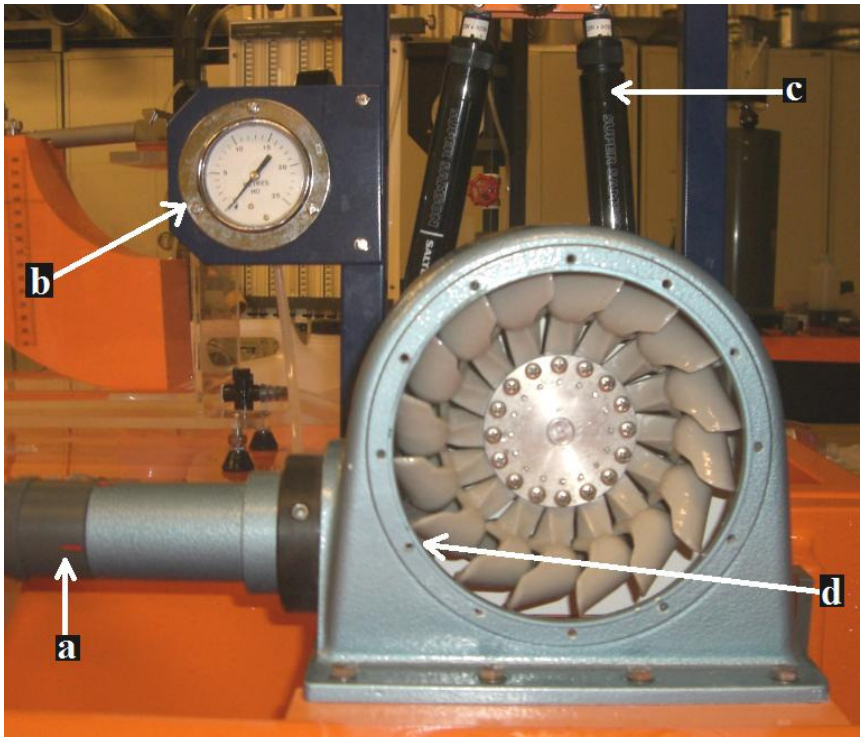

Figure 14.3. The Water Turbines Rig with The Jack turbine blades installed. **a.)** The adjustable water nozzle handle. **b.)** The pressure gauge records water head (h) in meters. **c.)** Springs at the back of the test rig record the force differences when the turbine is in operation. **d.)** The housing with The Jack turbine blades installed. The nozzle is hidden within the blades and is not visible.

14.2.3. The Tachometer

The tachometer (figure 14.4a) records the angular velocity of the operating turbine in revolutions per minute. A white sticker is placed on the pulley at the back of the turbines housing. The tachometer releases a red laser beam that also receives reflected beams back whilst the turbine is rotating. In this way if one holds the tachometers stationary over the white sticker's radius one receives a reading. This is shown in figure **14.4 b** below:

Figure 14.4. a.) The tachometer. **b.)** A white sticker is attached to the turbines axel (shown via black arrow). The tachometer is aimed and held stationary at a point where the sticker passes. One needs to hold the tachometer steady at this point for longer than five seconds in order to receive accurate readings.

14.2.4. The belt and pulley.

There is one pulley that is attached to the turbines axel. Around this pulley lies the belt that is attached to the force springs at each end. The pulleys diameter (L4) is 60 mm where it makes contact with the belt. This is shown in figure 14.5 below.

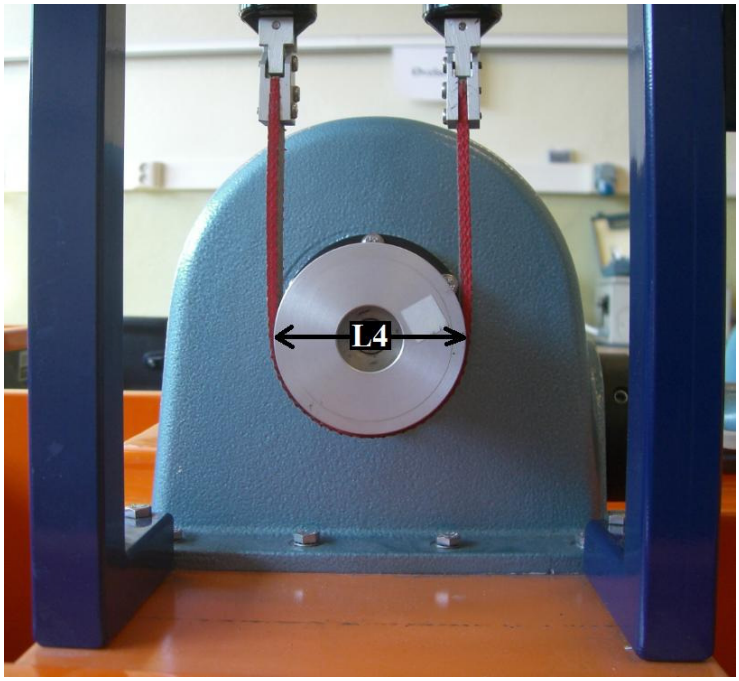

Figure 14.5. The back of the turbine with the belt in red, as well as the pulley. The pulleys diameter (L4) is 60mm.

The belt/pulley system uses friction to convey the axels torque. Slip produces unwanted friction on the pulley and thus efficiency losses.

14.2.5. Springs and adjustable force arm.

The belts ends are attached to two springs that are calibrated to record the forces at each end. These springs are shown in figure 14.6 c below.

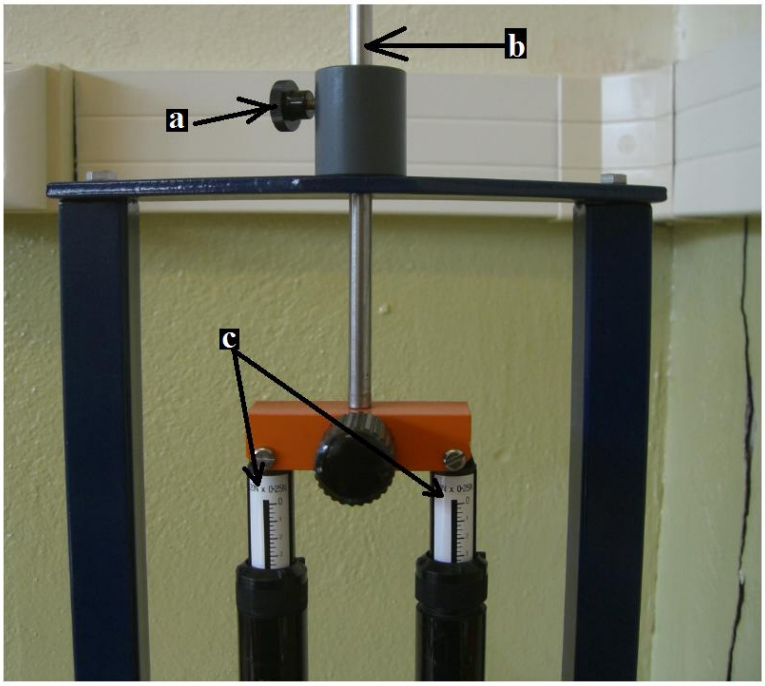

Figure 14.6. **a.)** A screw for tightening the steel rod in place. **b.)** The steel rod. It can be adjusted vertically and therefore vary the amount of resistance on the axel. **c.)** The two springs are attached to the ends of the belts. Each spring is calibrated to record the amount of *force in Newton's.*

The entire spring and belt system can be lifted via the steel rod in figure 14.6 b. This effectively varies the amount of resistance. I shall call this **The Belt Force**. Positioning this steel arm in place is done by tightening a screw shown in figure 14.6 a above.

14.2.6. Waters inlet to outlet

Water first enters the turbines housing from the pump via the piping shown in Figure 14.7 c below.

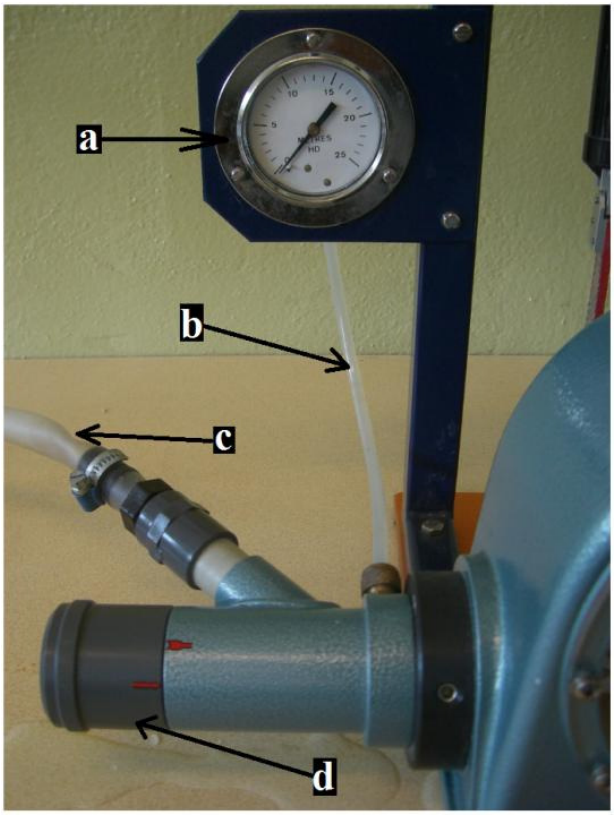

Figure 14.7. **a.)** The pressure gauge. Water pressure is measured in meters water height. **b.)** The piping from the water flow before the water nozzle to the pressure gauge. It is important that only water is present in the piping, thus no air bubbles. **c.)** Main piping from the pump to the water turbine rig. It is important that the piping is not tangled and does not vary in cross-sectional area. As shown here there was a little impression in the piping that had to be pressed out. **d.)** The nozzle handle can rotate and vary the water flow.

The amount of flow can be adjusted via The Nozzle Handle in figure 14.7 d above. A thin pipe (figure 14.7 b) connects the pressure gauge (figure 14.7 a) with the water flow before it exits the water nozzle.

Let us now have a closer look at the nozzle handle and its subsequent water jet nozzle in figure 14.8.

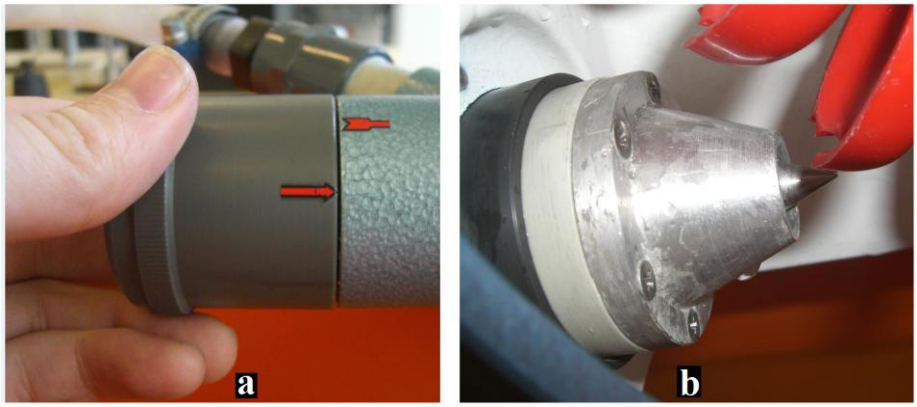

Figure 14.8. **a.)** The adjustable nozzle handle pulls and pushes the steel point of The Water Jet Nozzle, shown in b. **b.)** The Water Jet Nozzle. The steel point protrudes out and water flows out from its sides.

In figure 14.8 a, we see The Nozzle Handle. Any rotation of this handle will pull or push the steel point (in figure 14.8 b) out or in. This subsequently controls the amount of flow of the water jet. It is here I will manipulate the amount of flow over our turbine.

14.3. Preliminary checks and comments

The first day of testing proved to be a failure and thus data was discarded. I noticed that when I rotated the water turbines handle to the same position I did not receive the same flow (Q) and water head (h) as expected. Upon opening the nozzle assembly I found that the steel rod (which is a part of the steel tip) was essentially a long shaft that was screwed onto the nozzle handle. The rod was not properly fastened to the nozzle handle and thus this issue was fixed. This improved readings substantially. The nozzle produced relatively consistent flow (Q) and water head (h) readings when turned to the same position.

Variation in water head was usually because of some air bubbles that would enter the piping (as shown in figure 14.7 b) to the pressure gauge.

I also made sure that the piping from the pump to the turbine was not being obstructed in any way. Any fold in the piping automatically slows water down and subsequently varies the hydraulic Power to the turbine.

All these checks were done before and during the testing procedure.

15. Testing procedures

Here we will discuss the order and actions of everything that happened during laboratorial testing.

There are two areas of testing; single and multiple blade setups.

15.1. Testing procedure for The Single Blade Setup

a) Here I installed a single blade in the turbine housing.

b) I then held the pulley at the back of the housing to stop any rotation of the axel.

c) I turned the pump on and adjusted the nozzle handle such that water would flow over the blade.

d) I then made observations of the waters flows behavior over the blade.

e) I then repeated steps **a** to **d** with the other type of turbine blade.

f) I attached a string to the back of the axels circumference which hanged off the side of the bench by some weights (figure 15.1 c).

g) I then created a water flow and aimed the water jet onto the single blade without holding the pulley.

h) I then varied the amount of weight on the end of the string to an equilibrium point whereby the blade would be on the verge of rotating through the water jets flow.

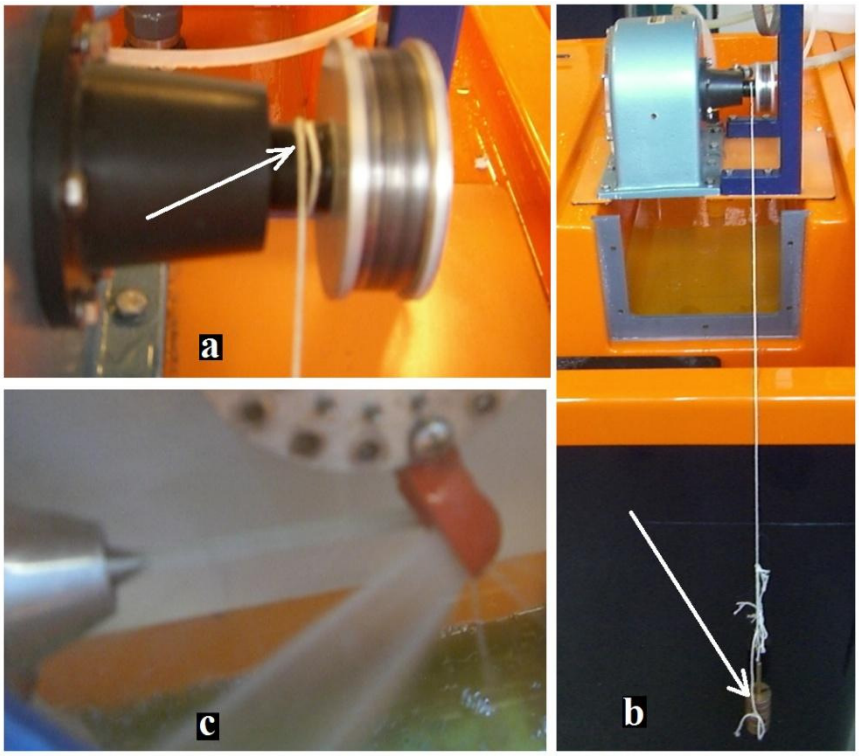

Figure 15.1. **a.)** A string is attached to the turbines axel. A white arrow points to attachment point. **b.)** The string is connected to masses and left to hang over the wall of the hydraulic workbench. Masses indicated by white arrow. **c.)** A Pelton Turbine blade left to fight the water jet.

15.2. Testing procedure for The Multiple Blade Setup

In this area of testing I would test the overall capability`s of the turbine with all of its 16 blades installed. In essence we are testing two things at the same time:

- How effectively water flows from one blade to the next
- How effectively the blades utilize the waters jets power.

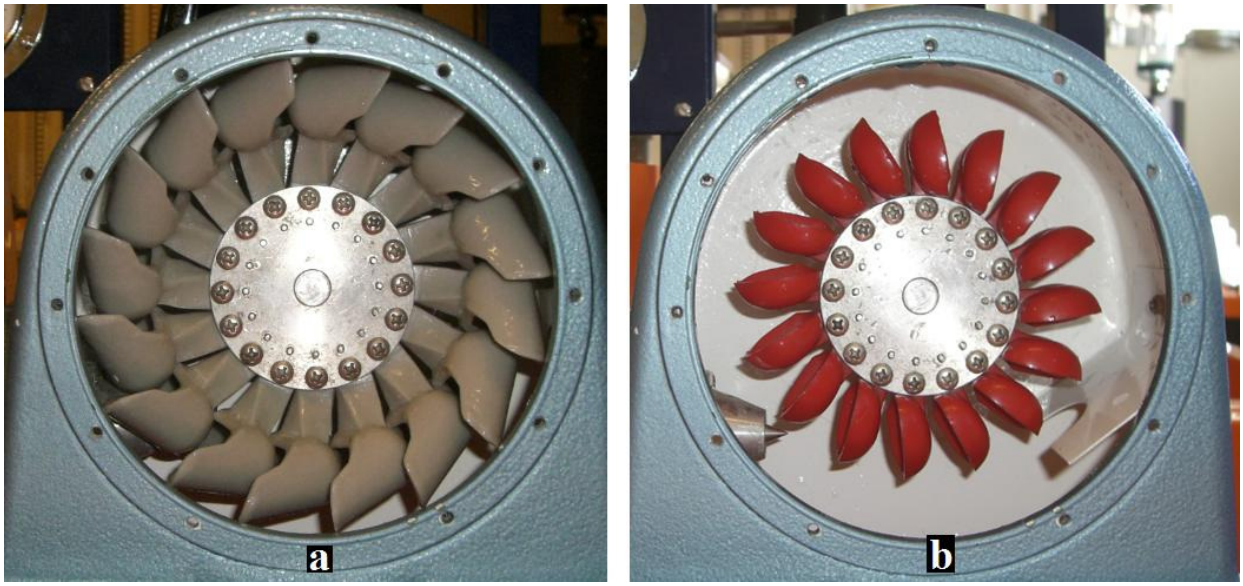

Figure 15.2. **a.)** The Jack turbine in its housing. Notice how the nozzle is hidden within the blades. **b.)** The Pelton Turbine in the same housing. Here the nozzle is more visible.

The list below was the order in which I performed all testing of blades.

a) **Pre-lab checks.** These include checking that there are no air bubbles in the piping, especially leading up to The Pressure Gauge. I then turned on the main water valve handle to make sure there were no obstructions in the water flow surrounding the pump. This ensured that it was only the water nozzle handle that could regulate the water flow.

b) **Installation.** I gently flipped the turbine housing (such that water stayed in it) on its side and inserted the desired turbine blades, bolts, washers etc. Once this was complete I checked that the centre of the blade was perfectly aligned with the centre of The Water Nozzles tip. I also checked to see that none of the blades were loose and the turbine rotated without any collisions what so ever.

c) **Pre-lab changes.** I applied the desired load on the axel by the belt/pulley and spring-system. I then made some last minute checks to make sure I had everything in place and turned on the pump

d) When the pump read that it was over 20m in pressure head (thus no air in the piping), I gently opened The Nozzle Handle to let the water out. I stopped turning the opening nozzle leaver at a desired pressure of interest.

e) I waited a few seconds until things stabilized. I then shut the tank (thus stores water) and started timing when the water level reached the zero mark on the water gauge.

f) Whilst I waited for the water level to reach the desired height in the tank (25 liters); I recorded angular rotation (n), forces on springs and the pressure on the pressure valve. When the water level reached the desired level (for example 25 liters) I stopped the timer. This was all recorded on paper.

g) I gently closed the nozzle valve and turned off the pump.

h) I transferred paper data onto an excel sheet on my laptop and looked at efficiency's and other important data to try predict what was most appropriate for the next run on the turbine.

i) Started at point c again.

j) I would run several cycles of point c) to i) with different loads whilst consistently holding the same pressure (h) and flow (Q). I started a new cycle (a new constant flow and water pressure) when I thought the data in the excel page showed a completion of the characteristic efficiency/load curve. I did the same if I noticed the turbine had reached its extreme point[5].

k) When The Turbines laboratory objectives were complete on the first day. I started on point a) on day two and installed the next turbine blades. During the Jack turbines testing I avoided maximum angular velocity because of reasons outlined in chapter 12.

Note: **I always turned off the nozzle valve before turning off the pump. Similarly upon starting I turned on the pump before I adjusted the nozzle valve**. If I turned the pump off before the nozzle valve then the water sitting in the pipe and pressure sensor would fall out before I could close the water valve and air would replace it. The air in the piping leading up to the pressure valve would give me entirely false readings. In addition the water leading up the pipe behind the air bubble, creates an explosive type of exit from the water nozzle. This is not good because I want a gradual approach of the water jet onto the blades. In this way the turbine will gradually start rotating instead of being bombarded at a given moment.

As expected, The Jack turbine Blades did eventually break of the turbines axel. After about 3 or 4 hours into the testing procedure I had gathered enough data to make comparisons to the Pelton Turbine. I then decided to try risk it and find “that specific flow” that brings forth the turbines maximum efficiency. I therefore had to play around with various belt loads and flows (adjusted the nozzle handle). After a few minutes I heard a vibrating sound and I thought at the time the turbine was really working well here perhaps. So I tried focusing on the sound until suddenly the blades just exploded off the axel. Afterwards I realized this must have been the blades harmonic frequency that I was hearing and feeling. The blades were absolutely not checked for this (see limitations section 1.6) and consequently failed here.

[5] Extreme point refers to either when the turbine has no load or it has far too much load and cannot rotate.

16. Results

16.1. Single blade results

Here, I only made tests of one of each of the blades in the housing at a time.

16.1.1. Failed single force readings

Let us look at figure 15.1 again.

This process proved unsuccessful because the blade stabilized over a large range of random forces that were not at all consistent? I would for example increase the amount of mass of the side until it stabilized at 2.5 kg. I would then continue increasing the mass to 5 kg until the blade finally pushed through the water jet. I would repeat the same conditions and receive completely different results ? The maximum weight varied depending on how the string was sticking more than how the turbine blade was behaving. What I think happened was the string I was using was sticking to the tanks edge by means of friction. In addition the blades were vibrating and bouncing slightly which did not help at all.
I could not see any significant difference in this behavior or results when I used the Jack turbine blade.

I needed a belt/pulley (belt can roll over the pulley) system over the edge of the hydraulic bench for this experiment to work properly. This was unfortunately not available at the time.

16.1.2. The Jack Turbines single blade flow analysis.

As far as I could see the water flow over the blade was generally moving as it was simulated in simulation number 37.
Water was leaving the blade over the top part of the blade and it had a slight deflection to its sides as predicted in simulation number 37. This is partially shown in figure 16.1 below although the deflection may seem exaggerated because of the angle at which this picture is viewed.

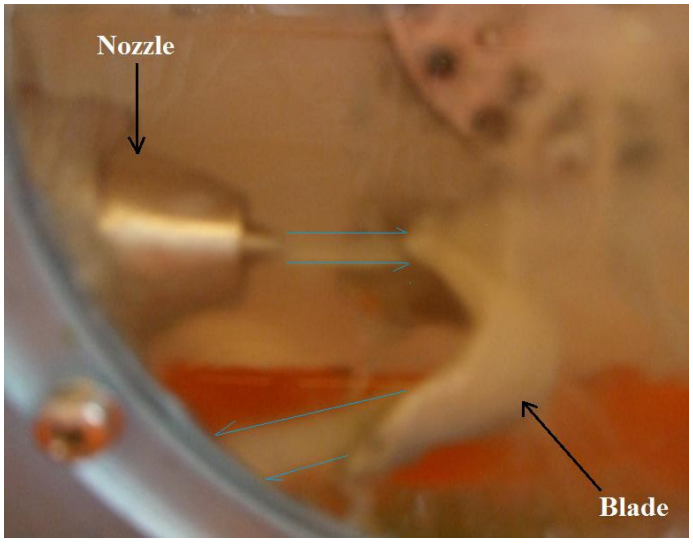

Figure 16.1. We see The Jack Turbine Blade and the nozzle. Both are indicated, the water flow has been bordered by thin blue lines to better see its direction. The water flow exiting The Jack Turbine is in actual fact more flat than it is shown here.

The actual water path is slightly difficult to see in figure 16.1 above because the viewing window is at the wrong place on our Water Turbine Rig. I had to lift the turbine (whilst holding the pulley stationary) and look underneath (got wet) in order to fully confirm flow behavior.

16.1.3. The Pelton Turbines single blade flow analysis.

The Pelton Turbines blade behaved as expected except for one exception. The blades showed that they were slightly angled as shown in figure 16.2 below. As to exactly why the manufacturers at Armfield did this I do not know. I suspect this is to compensate for a shorter radius. A shorter radius increases the turbines angular velocity and decreases its torque capabilities.

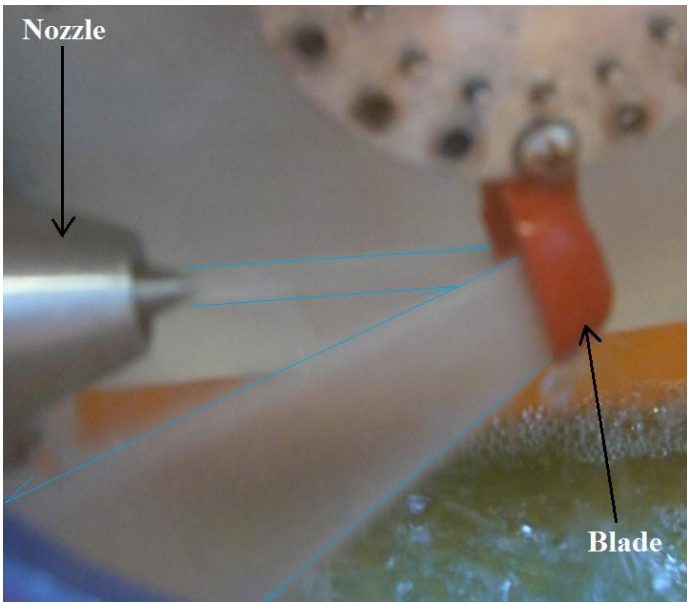

Figure 16.2. The nozzle and the blade are marked. The water jets boundaries are marked in with a thin blue line. Here the blade was positioned with its axis vertically or perpendicularly to the water jet. The water flow was deflected over the sides of the blade as expected, although it was also angled slightly downwards.

This Turbine Rig is not good at recording torque but excellent at recording angular velocity so it makes sense. This is not a good sign for our Jack turbines blades which are expected to rely more on torque to deliver mechanical power than The Pelton turbines blades design.

16.2. Equations used for results in multiple blade analysis

After the laboratorial tasks were completed I tabulated them (in appendix V) and used the results for further calculations in the tables outlined in section 16.3. The origins of the data used in these tables are described as follows:

- **Belt force (N)** was implemented on the springs and is therefore taken directly from the tabulated data in Appendix V.
- **Flow (Q)** was calculated by dividing the displaced volume by the time it took to complete this displacement. The units were converted to cubic meters per second.
- **Pressure (P)** was taken directly from the pressure gauge and its units are in meters.

- **Hydraulic Power (E_{hyd})** is calculated by using equation 3.8.

$$E_{hyd} = PQ = \rho ghQ$$

- **Force difference** is the difference between force 1 and force 2 read from our springs. These force readings are documented in appendix V. Units are in Newton's (N).
- **Torque** is calculated by multiplying the force difference by the radius of the pulley. This radius is 30 mm. Units are Newton's meter (N.m).
- **Angular Velocity (ω)** is taken directly from our tachometer readings and converted to radians per second.
- **Mechanical power (E_{mec})** is calculated by multiplying the torque by the angular velocity.
- **Efficiency (η)** is calculated by using equation 3.17.

$$\eta = \frac{energy\ out}{energy\ in} = \frac{E_{mec}}{E_{in}} = \frac{T\omega}{PQ}$$

16.3. Multiple blade results, scenario 1

- Here I chose a constant flow (Q) of approximately 0, 45 liters per second. This flow also produced a relatively constant water head (h) of 12 meters.
- I then adjusted the belt force on each and recorded readings as tabulated in Appendix V.
- After using the equations and explanations outlined in section 16.2 I found the following results for both The Pelton and Jack Turbine setups:

Table 16.1. Reveals test readings of The Jack Turbine Blades when subjected to varying Belt forces with constant flow (Q) of 0.45 L/s and a Pressure (P) of 12 m. We notice a maximum efficiency of 54 percent.

Test	Belt load (N)	Flow (m^3/s)	Pressure (m)	Hydraulic power (W)	Force Diff (N)	Torque (N.m)	Angular velocity (rad/s)	Mech power (W)	Efficiency (%)
1	9	0,00045	12,00	52,40	5,25	0,16	120,74	19,02	36,29
2	10	0,00045	12,05	52,61	6,75	0,20	116,66	23,62	44,90
3	11	0,00044	12,00	51,48	8,25	0,25	110,06	27,24	52,92
4	12	0,00044	12,05	51,69	9,75	0,29	96,03	28,09	54,34
5	13	0,00045	12,00	52,40	10,00	0,30	90,69	27,21	51,92
6	14	0,00044	12,00	51,48	10,40	0,31	83,04	25,91	50,33
7	15	0,00043	12,10	51,01	10,00	0,30	76,76	23,03	45,14
avg		0,00044	12,03	51,87					

Looking at table 16.1 above we see that the turbine has reached a maximum efficiency of 54 %. The hydraulic Power for the turbine averaged at about 52 Watts. Let us now have a look at how The Pelton Turbines blades reacted to the same conditions of flow (Q) and water head (h).

Table 16.2. Reveals test readings of The Pelton Turbines Blades when subjected to varying Belt forces with the same constant flow (Q) and Pressure (P). A maximum efficiency of 65 percent was recorded.

Test	Belt load (N)	Flow (m^3/s)	Pressure (m)	Hydraulic power (W)	Force diff (N)	Torque (N.m)	Angular velocity (rad/s)	Mech power (W)	Efficiency (%)
1	4	0,00045	12,10	52,83	3,00	0,09	203,26	18,29	34,63
2	6	0,00044	12,10	52,36	4,25	0,13	190,17	24,25	46,30
3	8	0,00044	12,00	52,02	5,50	0,17	171,74	28,34	54,47
4	9	0,00044	12,00	51,48	6,25	0,19	158,76	29,77	57,83
5	10	0,00044	12,00	51,48	6,50	0,20	163,99	31,98	62,12
6	11	0,00045	12,00	52,68	7,50	0,23	150,06	33,76	64,10
7	12	0,00044	12,00	51,84	9,20	0,28	121,27	33,47	64,56
8	13	0,00044	12,00	51,48	9,80	0,29	112,57	33,10	64,29
9	14	0,00044	12,00	51,12	10,50	0,32	99,17	31,24	61,11
10	15	0,00044	12,00	51,48	10,50	0,32	98,96	31,17	60,56
11	16	0,00043	12,00	50,59	11,10	0,33	82,31	27,41	54,18
12	17	0,00041	12,00	48,10	12,50	0,38	44,51	16,69	34,70
avg		0,00044	12,02	51,45					

The tabulated results of The Pelton Turbine are shown above. We notice that the maximum efficiency for this turbine reached an impressive 65 % with the same conditions as the Jack turbine. Let us now compare data. We can start with the turbines angular velocities (ω) with respect to the varying belt force (N) below in figure 16.3. Notice the values highlighted in yellow of the table above. This was due to friction from the pulley/belt system such that angular velocities increased with increased belt load. Thus cooling time was necessary between readings.

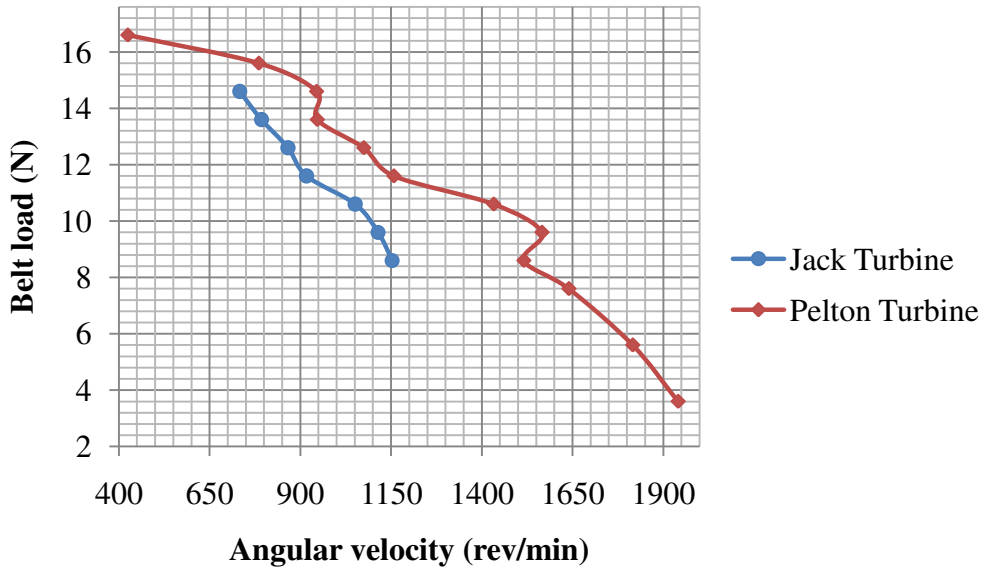

Figure 16.3. **Belt load (N) vs Angular velocity (rev/min).** Here we can see the Belt Force (N) on the y axis and the angular velocity (rev/min) on the x axis. All data points had approximately the same hydraulic force acted upon the blades. We notice that the lines are not very constant and can be attributed to variations in slip and other errors. It shows that the Pelton turbine is consistently producing a higher angular velocity than the Jack turbine.

In figure 16.3 we notice that The Pelton Turbine is consistently producing higher angular velocity (ω) values despite having the same belt force placed over the turbines axel.

The other variable that makes up the mechanical power is the turbines torque (T). Let us now see how the two turbines torque varies in comparison to a changing belt force.

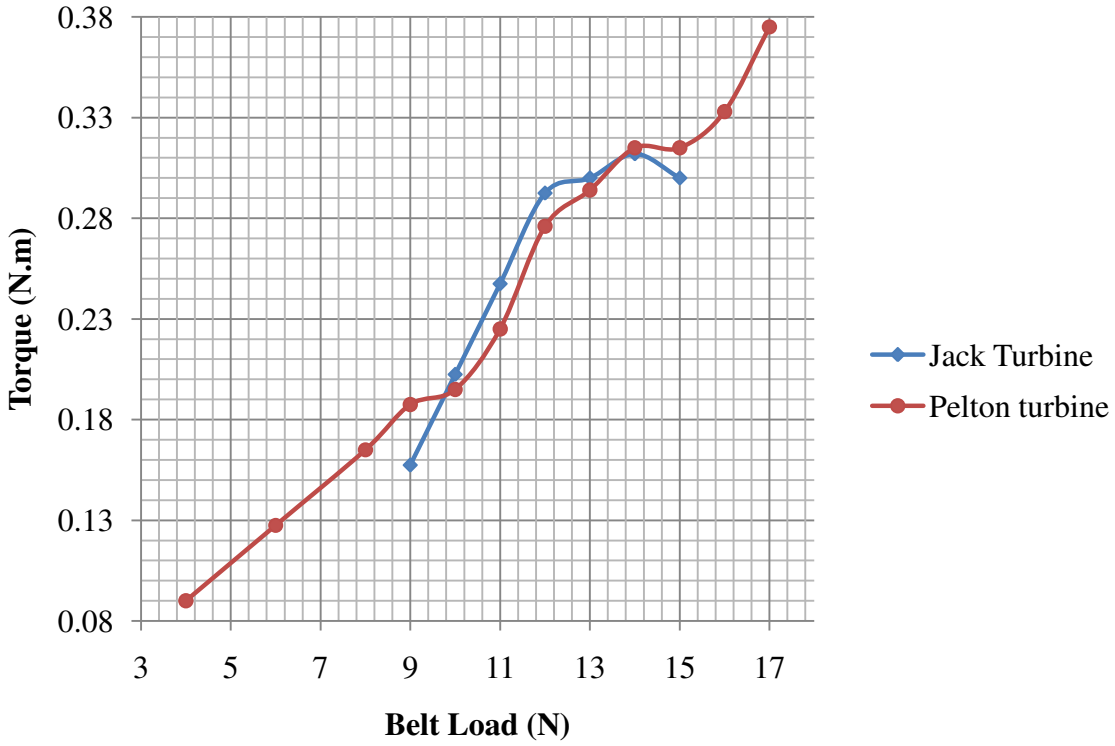

Figure 16.4. **Torque (N.m) vs Belt Load (N).** Here we can see how both turbines vary in torque as the belt force is varied. The blue line represents The Jack Turbine and the red line The Pelton Turbine. Both lines are not very consistent. The Jack turbine seems to be producing torque that lies somewhere between the same and slightly more torque than The Pelton Turbine.

Looking at figure 16.4 above we see two lines representing The Jack and Pelton Turbines. Both lines do not make up a smooth line. Although I can estimate that The Jack turbine is producing more or less the same torque values as The Pelton Turbine for the same belt load (N).

Let us now look at the two turbines efficiency`s vs. belt load in figure 16.5 on the next page:

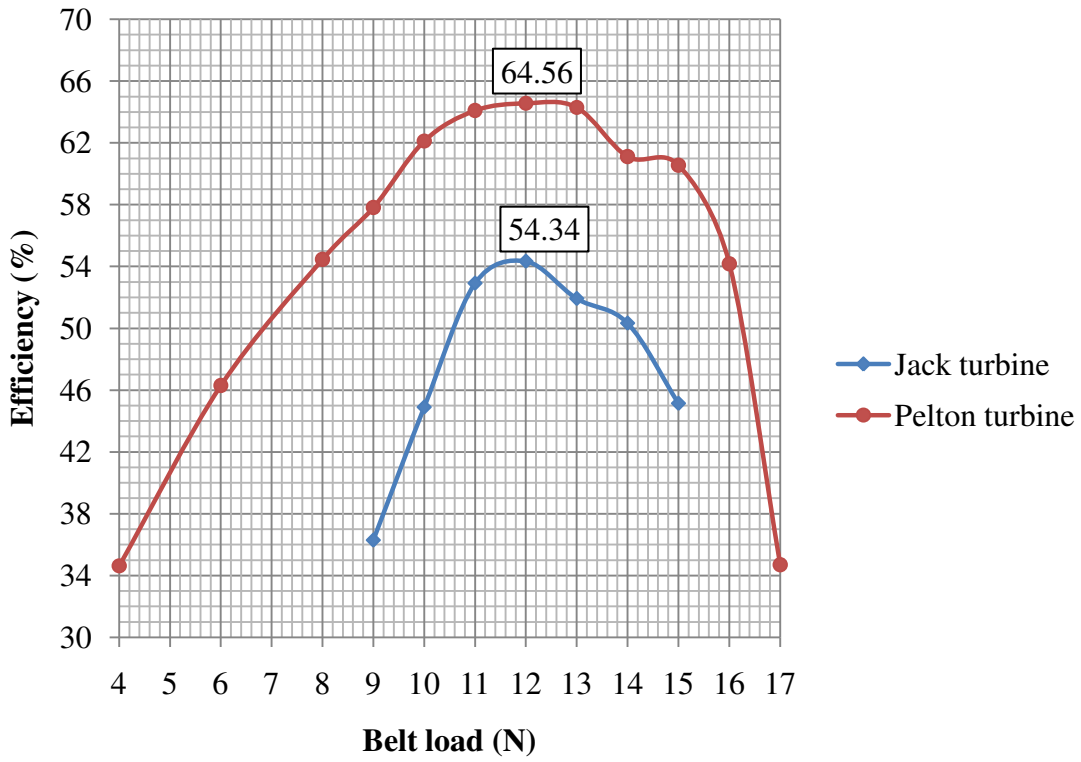

Figure 16.5. Efficiency (%) vs Belt Load (N). Here we have the efficiency on the y axis and the belt load on the x-axis. The red line represents The Pelton Turbine and the blue line The Jack Turbine. The Pelton Turbine reaches a maximum efficiency of 64.56 percent and The Jack Turbine 54.36 percent.

We see in figure 16.5 that there is about a 10 percent difference in maximum efficiency`s between the two turbines. This efficiency difference varies slightly for different belt loads but it averages at 14.1 percent for the 7 different belt loads.

16.4. Multiple blade results, scenario 2

In order to confirm that section 16.3 was not some freak coincidence let us now compare a different flow (Q) and water head (h) for the two turbines.

- Here I chose a constant flow (Q) of approximately 0, 5 liters per second. This flow also produced a relatively constant water head (h) of 9 meters.
- I then adjusted the belt force on each cycles and recorded readings as tabulated in Appendix V.
- After using the explanations outlined in section 16.2 I found the following results:

For The Jack Turbine I managed six readings at different belt loads. The results are shown in table 16.3 below.

Table 16.3. Test readings of The Jack Turbine Blades when subjected to varying Belt forces with constant flow (Q_{avg} = 0.00051m^3/s) and Pressure (P_{avg} = 9.01m). We notice a maximum efficiency of about 53 percent.

Test	Belt load (N)	Flow (m^3/s)	Pressure (m)	Hydraulic power (W)	Force diff (N)	Torque (N.m)	Angular velocity (rad/s)	Mech power (W)	Efficiency (%)
1	9	0,00051	9,00	44,91	6,35	0,19	113,62	21,64	48,20
2	10	0,00052	9,00	45,85	7,00	0,21	108,49	22,78	49,69
3	11	0,00050	9,00	44,01	7,75	0,23	99,38	23,11	52,50
4	12	0,00050	9,00	44,01	8,25	0,25	91,94	22,76	51,70
5	13	0,00052	9,05	46,10	9,05	0,27	84,30	22,89	49,65
6	14	0,00052	9,00	45,85	9,50	0,29	78,64	22,41	48,89
avg		0,00051	9,01	45,12					

Looking at table 16.3 we see that The Jack turbine gained a maximum efficiency of approximately 53 % for a hydraulic power that averaged 45 Watts. Let us now see how this compares to The Pelton Turbine below using the same conditions.

Table 16.4. In this table we have the results of The Pelton Turbines blades being subjected to a varying belt force whilst retaining a constant flow (Q) and pressure (m). A maximum efficiency of 62 percent was reached.

Test	Belt load (N)	Flow (m^3/s)	Pressure (m)	Hydraulic power (W)	Force diff (N)	Torque (N.m)	Angular velocity (rad/s)	Mech power (W)	Efficiency (%)
1	6	0,00049	9,00	43,15	3,75	0,11	167,97	18,90	43,79
2	8	0,00050	9,00	43,75	4,90	0,15	155,61	22,88	52,29
3	9	0,00050	9,10	44,23	5,25	0,16	150,48	23,70	53,59
4	10	0,00051	9,00	44,55	6,00	0,18	142,00	25,56	57,38
5	11	0,00051	9,00	44,91	6,75	0,20	136,55	27,65	61,57
6	12	0,00051	9,00	45,09	7,25	0,22	126,40	27,49	60,96
7	13	0,00051	9,00	44,46	7,65	0,23	117,18	26,89	60,49
8	14	0,00049	9,10	43,37	8,50	0,26	101,89	25,98	59,90
9	15	0,00052	9,00	45,61	10,00	0,30	82,41	24,72	54,21
10	16	0,00051	9,00	44,91	10,75	0,32	74,25	23,94	53,32
11	17	0,00052	9,00	46,04	11,50	0,35	55,50	19,15	41,59
avg		0,00051	9,02	44,55					

The table above shows a maximum efficiency of approximately 62 percent for The Pelton Turbine. This is a 9 % difference in maximum efficiency. The average difference in efficiency is calculated to be 8.8 %. Let us now look at how the two turbines angular velocities (ω) and torques (T) compares to the varying belt loads.

We can see in figure 16.6 below that again The Pelton Turbine has consistently produced a higher angular velocity than The Jack Turbine.

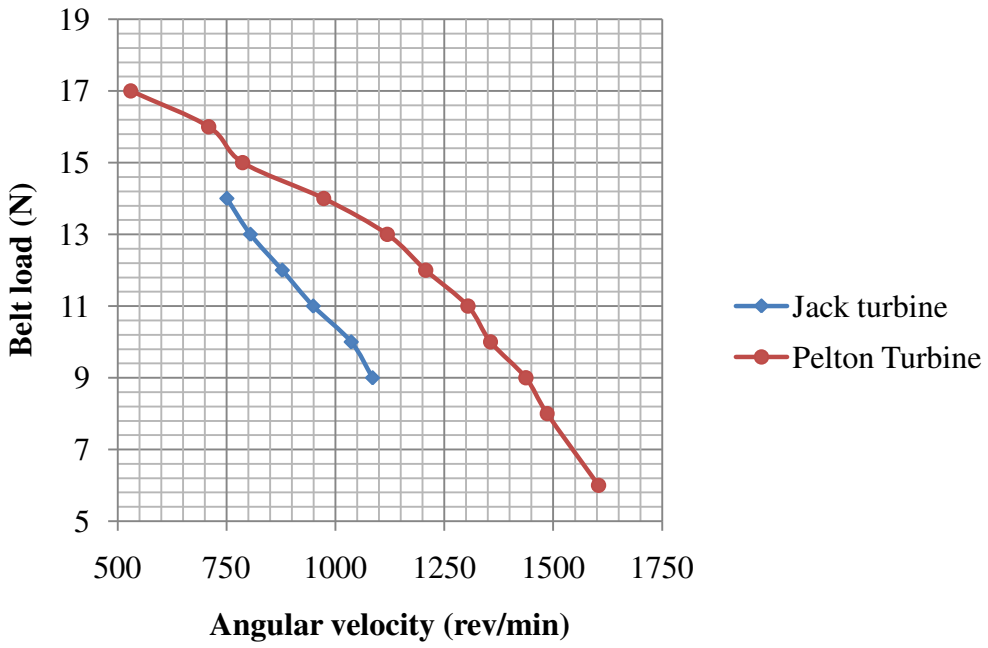

Figure 16.6. **Belt load (N) vs Angular velocity (rev/min).** The varying belt force (N) compared to the angular velocity (ω) in revolutions per minute. We notice that again such as it was shown in figure 16.3 The Pelton Turbine consistently produces higher angular velocities than The Jack turbine.

In figure 16.7 below, we have compared the torque (T) to the belt load (N). Unlike in figure 16.4 we have managed to gain some consistency. Cooling time was given in scenario 2. The Jack Turbine is definitely producing more torque than Pelton turbine under these conditions.

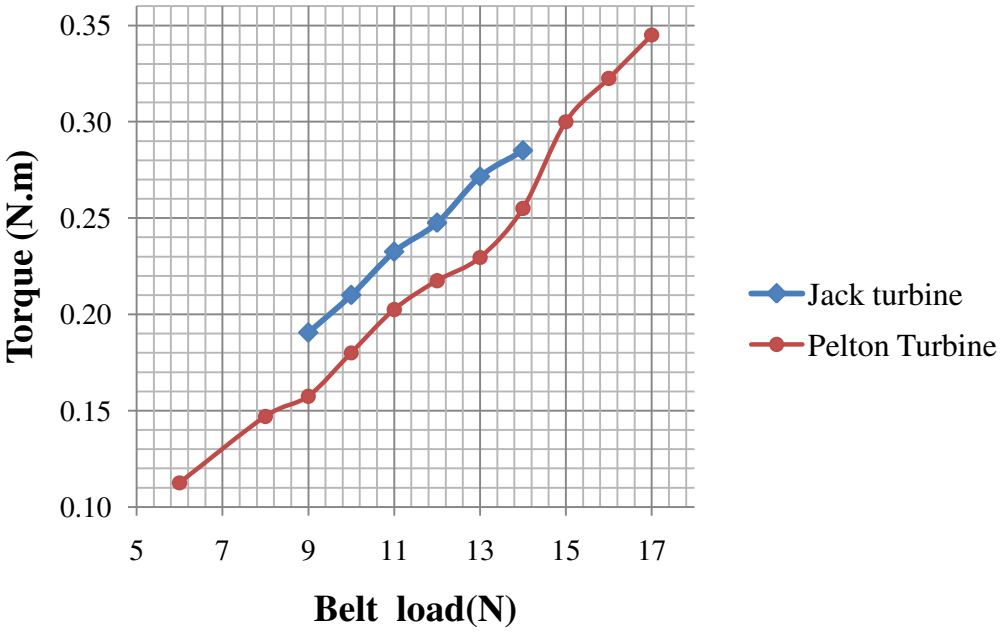

Figure 16.7. **Torque (N.m) vs Belt Load (N).** Shows the turbines torque (T) being compared to the varying belt force (N). We can see that The Jack Turbine is consistently producing more torque than The Pelton Turbine.

Let us now have a look at how these turbines compare in efficiency for the specified belt loads.

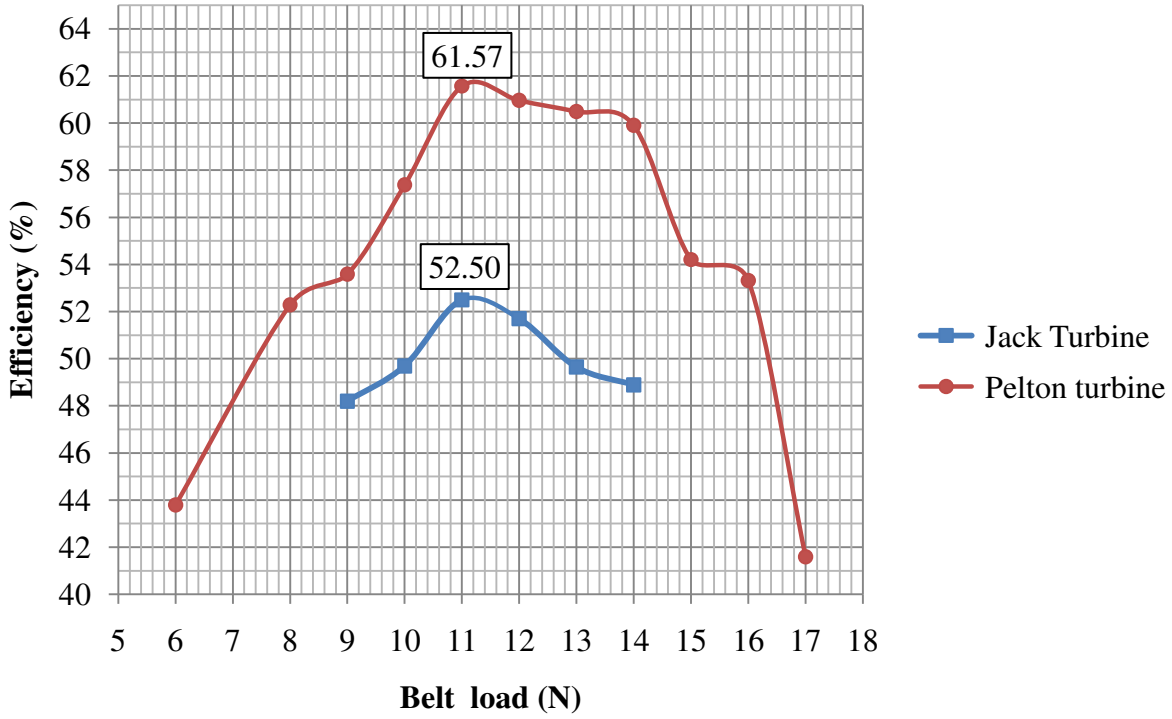

Figure 16.8. Efficiency (%) vs Belt Load (N). Here we see the efficiency`s on the y-axis against the varying belt load on the x-axis. The Pelton Turbine has reached a maximum efficiency of about 62 % whilst The Jack Turbine has reached maximum efficiency of 53 % for the given conditions. This is a 9 % difference.

Figure 16.8 above shows the turbines efficiency (ω) against belt load (N). We see that The Pelton Turbine reaches a maximum efficiency of 62 % for a 11 N belt load. At the same belt load The Jack Turbine reaches a maximum efficiency of 53 %. An average efficiency difference of about 9 % is evident.

Let us now have a look at an error analysis in section16.5 below. Discussions of these results are found in chapter 17 under discussions.

16.5. Error Analysis

There are two types of errors that have occurred during testing. The first type is with regard to human error.

16.5.1. Human error

The most common form of human error that could have occurred during testing was in the form of misread data. This involves all the data that is presented in appendix V.

With regards to the flow (Q) values one had to stop a timer at a specified water height of 25 liters. It was important that the tank filled at least 5 liters before one started the timer. This was such that the water mark would stabilize. One also had to get down and have ones line of site level with the water mark.

As mentioned earlier the tachometer also had to be held in for at least 5 seconds before an accurate angular velocity was measured.

The spring forces had a tendency to vibrate. Thus it was especially important to try find where the force stabilized between max and min forces.

16.5.2. Faulty Equipment

- The **tachometer** is a very accurate piece of equipment and I therefore do not think there is much error with our angular velocity readings. Thus the mechanical power of the turbine has received most if not all of its errors from the faulty torque values. These values are in turn a result of a bad belt/pulley arrangement.
- The **hydraulic bench** and its flow (Q) readings should be rather accurate because I chose a large volume (25 liters) over a relatively large time period. The hydraulic bench itself had no leaks and thus was working optimally. I therefore do not consider our flow values to contain much fault at all.
- Our **water head (h)** values give reason for suspicion due to its design. If we look at figure 3.2 again we notice that our test rig does not have the same setup before our water nozzle as that shown. Equation 3.8 assumes that there is near standstill conditions of the water before the water jet exits. The test rigs pressure gauge has a pipe connected to a much larger cross-sectional diameter before the water jet. The water here is moving at a pressure that is proportional to Bernouli`s equation. I know that moving water has a lower pressure than stationary water.

  Our test rig should ideally have had its pressure gauges piping end at a point that was in stationary water. It is true that water moves slowest at the walls of the piping but is it stationary? That depends on the flow(Q) and the cross-sectional area at which the pressure gauge is taking readings. Let us now consider the moving water into equation 3.8, thus:

  $$E_{hyd} = \left(\frac{1}{2}\rho v^2 + \rho g h\right) Q \qquad \text{eq 16.1}$$

  After opening the turbine and measuring this internal cross-sectional area. I found an outer diameter of 5 cm and a inner diameter of 1 cm (where an axel connects the nozzle point and nozzle handle). Let us now use the same data as in chapter 16.4 for head height (h=9m) and Flow (Q = 0.5 L/s). These values combined with the continuity equation (eq. 3.2) gives rise to a water velocity of 0.26 m/s. Thus the velocity part of equation 16.1 results in 35 N/m^2 whilst the water head pressure part resolves to 88025 N/m^2.

  I can therefore conclude that even though water is moving before the nozzle it has a negligible effect on the pressure gauge readings.

- One area of the test rig was especially faulty. This was the use of a **pulley/belt system** on our test rig. The belt became exceptionally warm due to friction as the belt slipped over the pulley. I even received angular velocities that decreased when the belt load increased (shown in figure 16.2 in yellow). It seemed that the warmer the belt and pulley become the more slip occurred and subsequent friction was produced. The more one operated the belts and pulleys the more inconsistent the results became. I quickly learnt that one had to wait a few minutes between every reading cycle in order to gain consistent results. This is why section 16.4 shows more consistency`s in its data than section 16.3.

17. Discussions

One needs to remember that the Jack Turbine blades used for testing did not have the best flow characteristics that were found during simulating. The best flow characteristic were found in simulation number 30. I therefore could not use this blade because The Water Nozzle in our boundary conditions was clashing with the blade. I therefore had to shrink the size of the blade enough for it to fit into the housing used in testing. This lead to the blade design of simulation number 37. The result was a water flow over the blade that was not as optimal as before but acceptable. There was a slight out swing of the exiting water jet which testing confirmed visually.

The construction process that I chose both disrupted and improved the surface of The Jack Turbine. The use of layering Epoxy over the blade made surface area smooth and did reduce surface friction but the end result was rather inferior compared to The Pelton Turbine Blades. One could feel the difference. In addition the very sensitive surface design where water travelled from one blade to the next was covered in layers of Epoxy too. This most likely worsened the flow behaviour in this region slightly although I cannot know for sure because I did not witness any water flow in the region during testing. What I do know for sure is that, because of the construction method the blades were most definitely not properly aligned. This was because I had to sandpaper at the blades basses to make them fit into the turbine housing. This created a slight deviation from the alignment of the water jet. Some of the blades were leaning a little upwards and others a little downwards. This produced obvious disadvantages to our Pelton turbine blades that had near perfect alignment to the water jet.

During testing I could not measure the diameter of the water jet hitting the turbine. This meant that I could not create an efficiency verses velocity-ratio graph, similar to the one shown in figure 3.17. All the graphs were compared to The Belt Load. This seemed appropriate because this was what was changing all the values whilst the hydraulic energy was held constant.

During single blade testing (section 16.1), I confirmed flow behaviour that was simulated in simulation number 36 and 37. I did not manage to receive single force reading from each type of blade. I found that an extra belt/pulley system was needed in order for the attempted method to work correctly. The absence of any force readings whether it was from simulations or testing, puts us in a difficult situation.

During multi-blade testing we are actually testing two things. The first is how well the water flow is being absorbed by the blades and the other is how well the blade allows the water flow to move from one blade to the next. For example, if I knew that both blade types absorbed the same amount of force from the single blade simulation testing. Then I could conclude that during multi-blade testing which ever blade performed better was also most likely to have a better flow behaviour form one blade to the next.

Before multi blade testing, I expected The Jack Turbine to produce more torque than The Pelton Turbine because it was designed to eject water at a larger radius. Our testing results seemed to agree with this too (figure 16.7 and 16.4). Figure 16.7 values were more consistent than those of figure 16.4 because during the second hydraulic power scenario I waited between each reading for the belt/pulley system to cool down. This reduced slip.

The other factor influencing mechanical power out is the rotational velocity of each turbine. As expected The Pelton Turbine produce consistently higher rotational velocities than The Jack Turbine.

The plan was that The Jack Turbine would compensate for a lower rotational velocity by having a much higher torque than The Pelton Turbine. We found out to our disappointment that the test rig that we were using was not very good at recording torque. The rigs belt/pulley system created a lot of heat, thus increasing slip and therefore faulty torque readings. I knew that the Tachometer

recorded angular velocity was very accurate. It was therefore very clear to me that The Test Rig recorded more accurate Power readings from The Pelton Turbine than that from The Jack turbine. A generator instead of the Belt/pulley system would have solved this dilemma.

As mentioned earlier; multi-blade testing, tested two things. I can therefore not use the results found in testing to make any detailed conclusions about blade energy absorption or water flow from one blade to the next.

Testing revealed a maximum efficiency for The Pelton Turbine to be on average 64 % whilst the Jack turbine was 54 %. Thus the average maximum efficiency difference between the two turbines was approximately10 %. The average efficiency difference between the two turbine types for all of the results was found to be approximately 11.5 %.

These values, in my eyes, are rather positive considering all the difficulties The Jack Turbine blades had to go through in order to fit and use this The Pelton Turbine test rig.

18. Conclusion

In chapter 9 I managed to design a blade that could absorb water as optimally as possible in a single blade setup.

After a single blade design was selected I managed to improve the design to allow water to move effectively from one blade to the next. This was done, whilst retaining the desired water flow that resulted in, maximum force absorption over the blades. The general flow behaviour for this setup was confirmed visually but not numerically in testing.

The Jack Turbine blade design had to be slightly downgraded in order to fit into The Pelton Turbines test rig. Testing proved that the designed blade abided to our boundary conditions by functioning during testing.

Testing confirmed the work done in simulations. I found that our test rig favoured The Pelton Turbine in that it was better suited for recording accurate angular velocities and not torque. A generator instead of a belt/pulley system on the test rig would have solved this problem.

The chosen construction material proved to function if one avoided maximum rotational velocities and/or harmonic frequencies. I better material is advised for any future testing.

Testing revealed that out of all the readings taken, The Pelton Turbine had an average of 11.5 % better efficiency than The Jack Turbine. The Pelton Turbine reached a maximum efficiency of 64 % whilst The Jack Turbine reached a maximum of 54 %.

Considering the circumstances, the results found in this thesis are positive for future investigation of The Jack Turbine Blade.

19. Further work

In this section I will explain what I would have done if I had enough time or what I am going to be working with in the future.

- Start over from chapter 9. Learn Fluid Surface Interaction (F.S.I) on Ansys Workbench (CFX). We know the general flow behaviour of The Jack Turbine Blade. We just need to optimize the design. With F.S.I we can measure exactly how much force the single blade or multiple blades are absorbing. This brings forth an incredible advantage; an analysis of the behaviour of the fluid over the blades presents concrete results instead of theories and speculation based on observations. In this way we can also make simulations of The Pelton Turbines blades and compare forces to The Jack Turbines Blade. This could really bring out some truths regarding which blade is better.

  By using F.S.I we can gain critical information regarding the relationship between the blades size and the water jets size. We can also check the blades for fatigue and harmonic frequency`s. This was not possible before. Long story short we can find out a lot more before any testing occurs. We know now from this thesis that Ansys Workbench (CFX) and its simulations are rather reliable and thus the more work that is done here in simulations the less work is necessary during testing. Thus a lot of time and money can be saved.

- Multi-jet simulating and testing. We only worked with a single water jet. The reality is that most commercial impulse water turbines have between 4 and 6 water jets, as it is shown in figure 19.1. below:

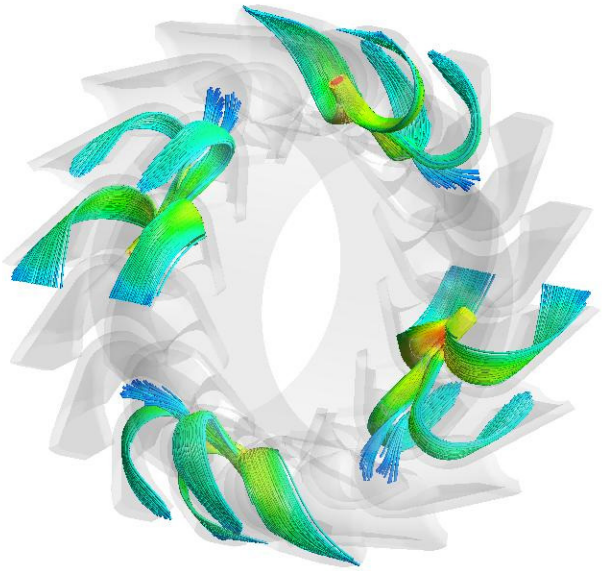

Figure 19.1. A blade configuration with 4 water jets being applied to simulation number 30.

  By increasing the number of water jets one also increases the turbines efficiency and power. A big advantage is that as a result of having more water jets the blades receive less force from each water jet, than if the total flow (Q) came from a single water jet. Thus the turbine becomes more stable.

- When all is done that can be done on CFX. Confirm it through testing. To do this correctly one will need a test setup that has a generator and not a belt/pulley system. Preferably more than one water jet and far better viewing windows. Thus one may consider an entirely new test setup than the one used in this thesis. Use better materials for the blades such as steel. In this way casting should be a more appropriate construction method.

- In order to fully verify that a blades design can survive the test of time. One will at some stage have to test the blades design in a real operating turbine setup over many years. Unfortunately this is the only real way to guarantee a robust and commercially viable product. Once this is achieved in a micro-power setup consider if it is worth starting over again, and designing for large scale Hydro-electrical Power.

20. References

Written references:

[1] **J. F. Douglas, J. M. Gasiorek, J. A. Swaffield**, Fluid mechanics, fourth edition, Pearson Prentice hall, England, 2001, ISBN 0-582-41476-8, pages 708 to 795

[2] **IOP Science,** Numerical prediction of Pelton Turbine efficiency http://www.turboinstitut.si/files/Articles/ENG/2010_012080.pdf

[3] **J.L. Meriam, L.G. Kraige**, Engineering Mechanics Dynamics, Fourth Edition, John Wiley & Sons,Inc., USA, 2003, ISBN: 0-471-26606-x

Internet sources:

http://www.microhydropower.net/casestudies/

http://www.alternative-energy-news.info/micro-hydro-power-pros-and-cons/

http://en.wikipedia.org/wiki/Micro_hydro

http://geosci.uchicago.edu/~moyer/GEOS24705/Assignments/EthiopiaPeltons.pdf

Programs:

1. **ANSYS Workbench 2010 , edition 12.1**
2. **Solid Works explorer 2010, Student version**

Appendix I

Design category 1 simulations

Sim num	Design num	L1 (mm)	L2 (mm)	L3 (mm)	Ø1 (deg)	Ø2 (deg)	Attack angle	Jet D (mm)	Sim type	Gap (mm)	Flow Results	Blade contact	a (mm)
1	**1**	47	20	20	45	90	0	10	F.S.F	0	Vout=0	Clash	0
2	**2**	47	47	24	45	90	0	10	F.S.F	0	Fail	Clash	0
3	**3**	47	20	16	25	90	0	10	F.S.F	0	Fail	Clash	0

Design category 2 simulations (single blade)

Sim num	Design num	L1 (mm)	L2 (mm)	L3 (mm)	Ø1 (deg)	Ø2 (deg)	Attack angle	Jet D (mm)	Sim type	Gap (mm)	Flow Results	Blade collision	a (mm)
4	**4**	20	15	16	15	80	0 deg	8	F.S.F	-	Fail	Clashes	0
5	**5**	20	15	16	25	80	0 deg	8	F.S.F	-	Fail	Clashes	0
6	**6**	20	15	16	35	80	0 deg	8	F.S.F	-	Fail	Clashes	0
7	**7**	40	20	28	45	90	0 deg	8	F.S.F	-	semi-pass	Clashes	0
8	**8**	25	15	28	45	90	0 deg	8	F.S.F	-	Fail	Clashes	8
9	**8**	25	15	28	45	90	22,5 deg	8	F.S.F	-	Fail	Clashes	8
10	9	25	15	28	45	90	0 deg	8	F.S.F	-	Fail	Clashes	8
11	**10**	30	12	28	45	90	0 deg	8	F.S.F	-	semi-pass	Clashes	5
12	**10**	30	12	34	45	90	22,5 deg	8	F.S.F	-	Fail	Clashes	5
13	**11**	30	15	28	45	90	0 deg	8	F.S.F	-	Fail	Clashes	5
14	**12**	45	12	34	45	90	0 deg	8	F.S.F	-	Pass	Clashes	5
15	**12**	45	12	34	45	90	22,5 deg	8	F.S.F	-	Pass	Clashes	5

Design category 2 simulations (multiple blade)

Sim num	Design num	L1 (mm)	L2 (mm)	L3 (mm)	Ø1 (deg)	Ø2 (deg)	Attack angle	Jet D (mm)	Sim type	Gap (mm)	Flow Results	Blade contact	a (mm)
16	**14**	30	20	34	45	90	≈ 10 deg	6	F.S.F	10	Over-flow	Clash	3
17	**15**	40	12	34	45	90	≈ 10 deg	6	F.S.F	10	Over-flow	Clash	3
18	**15**	40	12	34	45	90	≈ 10 deg	6	S.F	10	semi-pass	Nozzle	3
19	**16**	25	15	24	45	90	≈ 10 deg	6	F.S.F	10	Fail	Nozzle	3
20	16	25	15	24	45	90	≈ 10 deg	6	S.F	12	semi-pass	Nozzle	3
21	16	25	15	24	45	90	≈ 10 deg	6	S.F	14	semi-pass	Nozzle	3

22	16	25	15	24	45	90	≈ 20 deg	6	S.F	14	Fail	Nozzle	3
23	16	25	15	24	45	90	≈ 10 deg	6	S.F	13	Pass	Nozzle	3
24	16	25	15	24	45	90	≈ 20 deg	6	S.F	13	Fail	Nozzle	3
25	17	25	15	24	45	90	≈ 10 deg	6	F.S.F	13	Incon	Nozzle	3
26	17	25	15	24	45	90	≈ 10 deg	6	S.F	13	Incon	Nozzle	3
27	17	25	15	24	45	90	≈ 20 deg	6	F.S.F	13	Fail	Nozzle	2
28	17	25	15	24	45	90	≈ 10 deg	6	F.S.F	13	Pass	Nozzle	1
29	17	25	15	24	45	90	≈ 15 deg	6	F.S.F	13	Pass	Nozzle	1
30	17	25	15	24	45	90	≈ 20 deg	6	F.S.F	13	Pass	Nozzle	1
31	18	25	15	24	45	90	≈ 10 deg	6	F.S.F	13	Pass	Nozzle	1
32	19	25	15	24	45	90	≈ 10 deg	6	F.S.F	13	Pass	Nozzle	1
33	20	25	15	20	45	90	≈ 10 deg	6	F.S.F	13	Pass	Nozzle	1
34	21	25	15	16	45	80	≈ 10 deg	6	F.S.F	13	Fail	Pass	1
35	22	25	15	17	45	80	≈ 10 deg	6	F.S.F	13	Fail	Pass	1
36	23	25	15	18	45	90	≈ 10 deg	6	F.S.F	13	Pass	Pass	1
37	24	25	15	18	45	90	≈ 20 deg	6	F.S.F	13	Pass	Pass	1

Appendix II

This is an automated print out of simulations number 30 from Ansys Workbench Report.

Date

2011/04/28 15:11:14

1. File Report

Table 1. File Information for CFX

Case	CFX
File Path	F:\Master_thesis_static_huge4545_18march_file dp0\CFX\CFX\Fluid Flow 001.re
File Date	mars 2011
File Time	04:44:30
File Type	CFX5
File Version	12.1

2. Mesh Report

Table 2. Mesh Information for CFX

Domain	Nodes	Elements
Default Domain	275012	1455177

3. Physics Report

Table 3. Domain Physics for CFX

Domain - Default Domain	
Type	Fluid
Location	B1317
Materials	
Air at 25 C	
Fluid Definition	Material Library
Morphology	Continuous Fluid
Water	
Fluid Definition	Material Library
Morphology	Dispersed Fluid
Mean Diameter	1.0000e-02 [mm]
Settings	
Buoyancy Model	Buoyant
Buoyancy Reference Density	1.1800e+00 [kg m^-3]
Gravity X Component	0.0000e+00 [m s^-2]
Gravity Y Component	9.8100e+00 [m s^-2]
Gravity Z Component	0.0000e+00 [m s^-2]
Buoyancy Reference Location	Automatic
Domain Motion	Stationary
Reference Pressure	1.0000e+00 [atm]
Heat Transfer Model	Isothermal
Fluid Temperature	2.5000e+01 [C]
Homogeneous Model	True
Turbulence Model	k epsilon
Turbulent Wall Functions	Scalable

Table 4. Boundary Physics for CFX

Domain	Boundaries	
Default Domain	**Boundary - inlet**	
	Type	INLET
	Location	F964.1317
	Settings	
	Flow Regime	Subsonic
	Mass And Momentum	Normal Speed
	Normal Speed	1.2000e+01 [m s^-1]
	Turbulence	Medium Intensity and Eddy Viscosity Ratio
	Fluid	air
	Volume Fraction	Value
	Volume Fraction	0.0000e+00
	Fluid	water
	Volume Fraction	Value
	Volume Fraction	1.0000e+00
	Boundary - opening	
	Type	OPENING
	Location	F1316.1317, F965.1317, F966.1317, F967.1317, F968.1317, F970.1317
	Settings	
	Flow Direction	Normal to Boundary Condition
	Flow Regime	Subsonic
	Mass And Momentum	Opening Pressure and Direction
	Relative Pressure	1.0000e+00 [atm]
	Turbulence	Medium Intensity and Eddy Viscosity Ratio
	Fluid	air
	Volume Fraction	Value
	Volume Fraction	1.0000e-01
	Fluid	water
	Volume Fraction	Value
	Volume Fraction	9.0000e-01
	Boundary - Default Domain Default	
	Type	WALL
	Location	Over 600 faces
	Settings	
	Mass And Momentum	Free Slip Wall
	Fluid Pair	air | water

Appendix III

2-D drawing (only available in A3)

Appendix IV

Stresses due to bending on test rods

Practical experiment for our rods shown in the figure below. The rods managed to tolerate a minimum of 150 grams during testing.

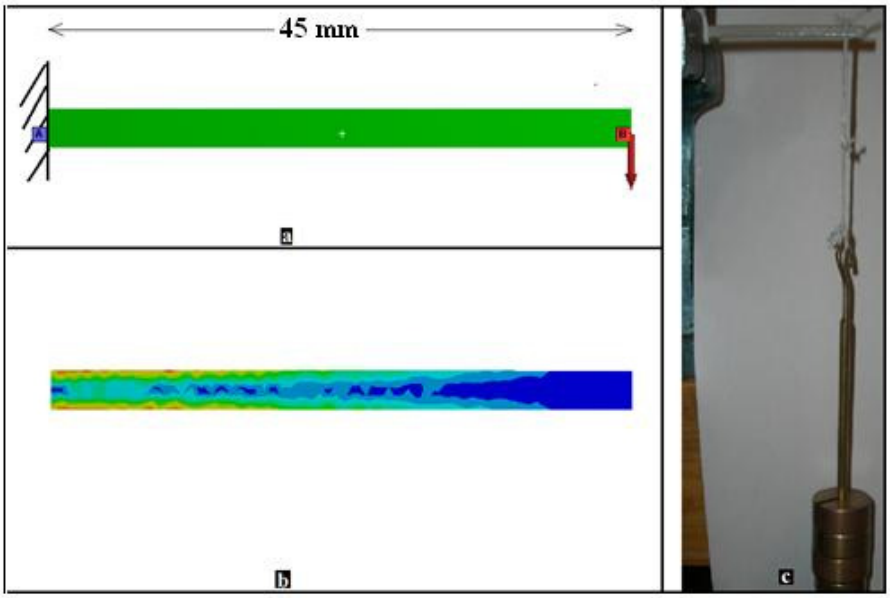

Figure IV . **a.)** The same scenario that was done during testing in figure c. Here we see the length of 45 mm, a force of 150 grams was placed at the side in red and the other side was held stationary. **b.)** In b we obtained a maximum of 18.5 MN/m^2. Tension on the top and compression on the underside. **c.)** A picture of the actual test being done.

Hand calculations:

At the top of the beam (at the wall fastener to the left) there are max tensile stresses and at the bottom max compressive stresses. The maximum tensile and compressive loads at these points are as follows:

$$\sigma = \frac{Mc}{I} = \frac{6Fx}{d^3} = \frac{6(1.5N)(0.045m)}{(0.003m)^3} = 15\ MN/m^2$$

The hand calculations seem to agree with the Workbench simulations in the figure above (3,5 MN/m^2). One must remember that Ansys Workbench takes changes in deflection when calculating solutions, hand calculations cannot do this.

Stress caused by plain shearing.

Plain shear proved to be the materials strongest characteristic. I therefore did not bother making any simulations because I did not manage to receive a force under 30 kg which means the test rod could manage shearing stresses in excess of 20 MPa.

Torsion and compression

Experiments involving only torsion are slightly more challenging to setup. If we look at the force distribution over The Jack Turbine blade in previous simulations we notice that there is very little torsion occurring anywhere and I will therefore ignore torsional effects as the biggest threat to our blade design. Compression seems difficult to test too and not much of a threat.

Appendix V

The Jack turbine (data from laboratory)

Test	Belt force (N)	Volume (L)	Time (s)	Force 1 (N)	Force 2 (N)	Angular velocity (rev/min)	Pressure (m)
1	9	25,00	56,00	8,00	2,75	1153,00	12,00
2	10	25,00	56,00	8,75	2,00	1114,00	12,05
3	11	25,00	57,00	10,25	2,00	1051,00	12,00
4	12	25,00	57,00	11,75	2,00	917,00	12,05
5	13	25,00	56,00	12,00	2,00	866,00	12,00
6	14	25,00	57,00	12,50	2,10	793,00	12,00
7	15	25,00	58,00	13,00	3,00	733,00	12,10

The Pelton Turbine (data from laboratory)

Test	Belt force (N)	Volume (L)	Time (s)	Force 1 (N)	Force 2 (N)	Angular velocity (rev/min)	Pressure (m)
1	4	25,00	56,00	4,00	1,00	1941,00	12,10
2	6	25,00	56,50	5,50	1,25	1816,00	12,10
3	8	25,00	56,40	7,00	1,50	1640,00	12,00
4	9	25,00	57,00	8,00	1,75	1516,00	12,00
5	10	25,00	57,00	8,25	1,75	1566,00	12,00
6	11	25,00	55,70	9,50	2,00	1433,00	12,00
7	12	25,00	56,60	11,20	2,00	1158,00	12,00
8	13	25,00	57,00	12,00	2,20	1075,00	12,00
9	14	25,00	57,40	13,00	2,50	947,00	12,00
10	15	25,00	57,00	13,20	2,70	945,00	12,00
11	16	25,00	58,00	14,10	3,00	786,00	12,00
12	17	25,00	61,00	15,50	3,00	425,00	12,00

The Jack turbine (data from laboratory)

Test	Belt force (N)	Volume (L)	Time (s)	Force 1 (N)	Force 2 (N)	Angular velocity (rev/min)	Pressure (m)
1	9	25,00	49,00	8,10	1,75	1085,00	9,00
2	10	25,00	48,00	9,00	2,00	1036,00	9,00
3	11	25,00	50,00	9,75	2,00	949,00	9,00
4	12	25,00	50,00	10,50	2,25	878,00	9,00
5	13	25,00	48,00	11,25	2,20	805,00	9,05
6	14	25,00	48,00	12,00	2,50	751,00	9,00

The Pelton Turbine (data from laboratory)

Test	Belt force (N)	Volume (L)	Time (s)	Force 1 (N)	Force 2 (N)	Angular velocity (rev/min)	Pressure (m)
1	6	25,00	51,00	5,00	1,25	1604,00	9,00
2	8	25,00	50,30	6,50	1,60	1486,00	9,00
3	9	25,00	50,31	7,25	2,00	1437,00	9,10
4	10	25,00	49,40	8,00	2,00	1356,00	9,00
5	11	25,00	49,00	9,00	2,25	1304,00	9,00
6	12	25,00	48,80	9,75	2,50	1207,00	9,00
7	13	25,00	49,50	10,40	2,75	1119,00	9,00
8	14	25,00	51,30	11,25	2,75	973,00	9,10
9	15	25,00	48,25	12,75	2,75	787,00	9,00
10	16	25,00	49,00	13,75	3,00	709,00	9,00
11	17	25,00	47,80	14,50	3,00	530,00	9,00